Alma Mater Studiorum · Università di Bologna

Scuola di Scienze
Dipartimento di Fisica e Astronomia
Corso di Laurea Magistrale in Fisica

Topological phases in spin ladders

Relatore:
Prof. Elisa Ercolessi

Presentata da:
Greta Ghelli

Anno Accademico 2017/2018

Acknowledgements

I would like to thank my supervisor Prof. Elisa Ercolessi for having supported me and for her help and encouragement during my thesis.

I also would like to thank PHD student Giuseppe Magnifico for his help in numerical analysis.

Abstract

Questa tesi si occupa di approfondire lo studio di possibili fasi topologiche in un sistema costituito da due catene di spin caratterizzate entrambe da un'interazione alternata forte e debole. Infatti è interessante capire se questo tipo di interazione può portare a termini topologici non nulli nella funzione di partizione, termini che invece sono assenti per due catene accoppiate quando l'interazione tra spin vicini è sempre la stessa.
Quello che si scopre dal punto di vista analitico è che, quando l'interazione su una catena è traslata di un sito rispetto a quella sull'altra catena, il nostro modello, nel limite del continuo, si può mappare nel modello sigma non lineare più un termine topologico diverso da zero. In corrispondenza di un certo valore critico del termine topologico si ha una transizione di fase tra due fasi isolanti differenti. Tale valore critico corrisponde a un certo valore critico del parametro che caratterizza l'interazione alternata sulle catene. L'analisi numerica, basata sul metodo DMRG, conferma questa previsione teorica. Inoltre, dal confronto tra i risultati numerici per i livelli energetici ottenuti con condizioni al contorno aperte e chiuse, si può già notare che una delle due fasi sembra avere proprietà topologiche non triviali.
$\grave{E}$ dunque molto interessante chiedersi se queste fasi siano caratterizzate da un qualche tipo di ordine topologico, rilevabile attraverso parametri d'ordine non locali. Le simulazioni numeriche confermano questa ipotesi: il parametro d'ordine non locale di stringa è non nullo nella fase caratterizzata da proprietà topologiche non triviali, che è dunque identificata come un isolante di Haldane, e il parametro d'ordine non locale di parità è non nullo nella fase topologicamente triviale, che è dunque identificata come un isolante di Mott. Si ha dunque una transizione di fase tra l'isolante di Mott e l'isolante di Haldane.

Contents

List of Figures

List of Tables

Introduction

An effective description of classical phase transitions has been completely achieved, in fact they are classified in two categories and they are described by the behavior of an order parameter, which is connected to the phenomenon of symmetry breaking. Symmetries play a crucial role in fact it has been understood that the critical behavior of a system surprisingly does not depend on microscopic details of interaction. On the contrary, it is shared by systems with the same symmetry group of the Hamiltonian and the same dimensionality of the lattice space. This charateristic is known as universality and we can summarize the phenomenology of critical phenomena in universality classes [23].
However this important framework is not sufficient to fully describe the new phases of matter that has been discovered. In particular, when we deal with one dimensional systems thermal and quantum fluctuations are much more important than they are in higher dimensions, therefore these fluctuations prevent most of the phenomena with a breaking of a symmetry as it happens in higher dimensions. In 1966 N.D.Mermin and H.Wagner underlined this peculiar characteristic in isotropic Heisenberg models [19] and in 1973 J.M.Kosterlizt and D.J.Thoulesse studied a phase transition [17] which concerns two-dimensional systems where topological features are crucial and it does not involve any continuous symmetry breaking. Furthermore, many other important works in 1960s and 1970s highlighted the features of both quantum and classical low dimensional systems. They can often be mapped into each other, in particular it is useful to map a system into the antiferromagnetic Heisenberg chain because it is exactly sovable using the Bethe ansazt technique. This solution shows that this model is gapless. Are Heisenberg chains of higher spins gapless too? In two papers F.D.M. Haldane [14, 15] mapped the Heisenberg antiferromagnetic chain, in the continuum limit, into the O(3) non linear sigma model, revealing a substantial difference between integer spin chains and half-integer spin chains. In fact, in half-integer spin chains, the presence of a topological term, in the path integral formulation of the partition function, implies a negative interference between spin configurations with non-zero winding number and this negative interference prevents the appearance of a mass gap. On the other hand, this topological term is absent in integer spin chains, which are therefore gapped. An important example of spin 1 model is known as AKLT chain [1] so called because of its inventors I.Affleck,

T.Kennedy, E.Lieb and H.Tasaki in 1987-1988. In this model we can think that each link in the chain hosts two auxiliary spin $\frac{1}{2}$ that are projected to a spin 1. In this way two "unpaired" spin $\frac{1}{2}$ degrees of freedom are present at the ends of the chain and they are an example of quantum number fractionalization, in fact the original degrees of freedom were spin 1. Furthermore, this model has an other important characteristic, i.e the presence of a Haldane gap [1]. This Haldane phase can be identified by a nonvanishing value of the non-local string order parameter [16]. Moreover, it is included among symmetry protected topological phases which have been deeply studied in many works, as for examples those of X.-G.Wen [34] and those of L.Fidkowski and A.Kitaev [11]. An other important model, where symmetry protected toplogical phases can be found, is the Hubbard model. In fact, in this model, there is a one-to-one correspondence between phases idenfied by non-local order parameters in the context of bonosization [4] and those obtained from group cohomology theory [20].
Spin ladders also represent models where toplogical properties are decisive to characterize the behavior of the system. Therefore we can ask if, in spin ladders, phases due to a non vanishing topological term in the partition function can also be characterized by some kind of topological order, detectable by non local order parameters. We try to answer to this intriguing question following previous works as [7, 18]. In particular, these works found a different behavior between standard spin ladders with an even number of legs and those with an odd number of legs [7] and the presence of a critical point mapping the ladder, in the continuum limit, into a non linear sigma model [18]. In this thesis we want to proceed in this direction, studying a ladder composed by two chains but with an interaction which is staggered along each chain and alternated between them. This kind of interaction implies a non vanishing topological term in the partition function, unlike what happens in two legs standard spin ladders. Furthermore, numerical analysis confirms the presence of a phase transitions between a topological trivial phase and a topological non trivial phase, which can be also characterized in the first case by non vanishing parity operator and in the second case by non vanishing string operator.

In order to develop this study, the thesis is organized as follows:

- In the first chapter we describe the theory of classical phase transitions, then we focus on the new framework used to explain topologically phase transitions. In particular we deepen the study of non local order parameters applied to Sine-Gordon model and Hubbard model. In the first chapter we also introduce the concepts of edge states, winding numbers and Berry phases.

- The second chapter deals with the analysis of topological terms in the path integral formulation of the partition function and of their consequences in spin chains and standard spin ladders.

- In the third chapter we report our original contribution which concerns the study

of staggered spin ladders. Our analytical and numerical analysis show that actually the two gapped phases, characterized by the presence or the absence of a topological term in the partition function, can also be identified by two non local order parameters. Therefore the chapter is divided into two parts: our analytical mapping of the model into the non linear sigma model and our numerical analysis of energy levels and of non local order parameters.

- Finally in chapter 4 we explain what kind of questions our analysis opens, in particular it would be interesting to extend our study to ladders with more than two legs. In this way we would like to proceed towards the study of topological properties of two-dimensional systems.

Chapter 1

Phase Transitions

1.1 Classical Phase Transitions

A phase transition is a change of the physical properties of a system due to a change of its equilibrium state. The equilibrium state of a system depends on the competition between two principles [23]:

- principle of energy minimization;
- principle of entropy maximization.

If we had only the first principle then we would obtain completely ordered systems and so we would observe big magnetic fields in many substances.
If we had only the second principle then we could never observe a system with a spontaneous magnetization.
Actually we know that these two situations do not occur, but we have always a balance between the two principles [23].

To take into account the competition between these two tendencies we must consider the temperature. It enters the free energy formula $F = U - TS$ and when it changes we have a different balance in the free energy between the entropy and the energy. The phase transition occurs at $T = T_C$ when this balance becomes perfect [23].

Classical phase transitions can not occur at $T = 0$ since they depend on thermal fluctuations which vanish at $T = 0$ [29].

1.1.1 First and second order phase transitions

First-order phase transitions are characterized by [23]:

1. a singularity in the first derivative of the free energy (Ehrenfest classification). This discontinuity implies a jump in the entropy. So it also means that a certain amount of latent heat is absorbed or released by the system at the transition point, while temperature stays constant;

2. absorption or release of latent heat can not occur istantaneously, so we have the presence of a mixed-phase regime where some parts of the system have completed the transition and others have not;

3. a finite correlation length ξ.

Second-order phase transitions are characterized by [23]:

1. a singularity in the second derivative of the free energy (Ehrenfest classification) and the absence of latent heat at the critical point;

2. different phases do not coexist;

3. an infinite correlation length ξ at the critical point. It gives rise to critical phenomena.

1.1.2 Order parameter and spontaneous symmetry breaking

An order parameter is a quantity that characterizes a phase transition because its thermal average is different in different phases. It is usually vanishing at $T > T_C$ and non vanishing at $T < T_C$.
First-order phase transitions are characterized by a discontinuous change of the order parameter, while second-order phase transitions are characterized by a continuous change of it from zero to a non zero value [9, 23].

Symmetry breaking can often be associated to a phase transition. For example in first order liquid-solid transition the continuous translational symmetry is broken, while in the liquid-vapor first order transition it is not. Second ordered phase transitions typically involve a breaking of symmetry [9, 23].
When the system is in an ordered phase which has less symmetry than the Hamiltonian of the system, we call this phenomenon a spontaneous symmetry breaking. On the contrary the symmetry is explicity broken when some terms in the Hamiltonian do not respect the symmetries of the theory [9, 23].
In order to better understand this difference, we can consider the Ising model [23]:

$$H = -\sum_{<i,j>} J_{i,j}\sigma_i\sigma_j - \Sigma_j B_j\sigma_j \tag{1.1}$$

The external magnetic field B_j and the coupling coefficients $J_{i,j}$ are usually considered to be constant J and B $\forall i, j$. In particular J is taken positive. The variables σ_i are discrete and they can be ± 1.

- Whitout the magnetic field the magnetization changes from 0 for $T > T_C$ (this is known as paramagnetic phase) to a finite value for $T < T_C$ (this is known as ferromagnetic phase). This change occurs in a continuous way so the transition is of second order [23].
  - Under T_C the equilibrium state of the system can be one of the two degenerate ground states ($\sigma_i = +1$ $\forall$i and $\sigma_i = -1$ $\forall$i). The system spontaneosly goes into one of them. The chosen configuration breaks the Z_2 symmetry.
  - In this situation, i.e. in the absence of a magnetic field, the Hamiltonian respects a Z_2 symmetry.

  So since the Z_2 symmetry is broken in the choice of one of the two ground states but it is respected in the Hamiltonian, this phenomenon is a spontaneous symmetry breaking [23].
- The presence of a magnetic field implies that the Hamiltonian is no longer invariant under Z_2 symmetry which is therefore explicity broken [23].

1.1.3 Correlation function, scale invariance and universality

The two point correlation function $C(i, j)$ between two spins at sites i and j is defined as $C(i, j) =< \vec{S_i} \cdot \vec{S_j} >$, when translation invariance is present this function depends only on the distance difference $r = |\vec{i} - \vec{j}|$, i.e we have $C(r)$. It gives a measurement of the degree of the relative alignement between two spins separated by a distance r [23].
Furthermore to evaluate spin fluctuations it is convenient to subtract from $C(r)$ their mean value $\vec{S_0}$, in this way we define the two point connected correlation function $C_c(r) =< (\vec{S_i} - \vec{S_0}) \cdot (\vec{S_j} - \vec{S_0}) >=< \vec{S_i} \cdot \vec{S_j} > -|\vec{S_0}|^2$. Its behavior is as follows [23]:

$$C_c(r) \simeq \begin{cases} \frac{1}{r^{D-2+\eta}} & T = T_C \\ e^{-r/\xi} & T \neq T_C \end{cases} \tag{1.2}$$

where D refers to a D-dimensional system, ξ is the correlation length and η is the anomalous dimension of the order parameter [23]. ξ diverges if $T \to T_C$, in fact if we define $\varepsilon_T = \frac{|T-T_C|}{T_C}$ then the behavior of ξ is [9]:

$$\xi \simeq |\varepsilon_T|^{-\nu} \tag{1.3}$$

where ν is a critical exponent [9].

At $T = T_C$ the effective interaction extends to the entire system and it involves all spins, it is a collective phenomenon. The correlation length ξ is infinite and since it measures the effective degrees of freedom of the system it may seem very difficult to study a phase transition. Fortunately two concepts help us [23]:

- **Scale invariance**
  The divergence of ξ implies scale invariance of the system. It means that it looks similar indipendently of the length scale. Therefore physical properties of it do not change if all lengths are rescaled by a common factor.

- **Universality**
  Critical behavior of a system does not depend on microscopic details of interaction. On the contrary it is shared by systems with the same symmetry group of the Hamiltonian and the same dimensionality of the lattice space. This charateristic is known as universality and we can summarize the phenomenology of critical phenomena in universality classes.

The link between them can be understood in renormalization group context [23]: hamiltonians that differ only for irrilevant operators share the same critical behavior, this is the origin of universality classes.

1.1.4 Landau theory

We focus on symmetry breaking transitions, they are described by Landau theory [22] which was developed in 1937. It is a phenomenological theory so it is not interested in the description of the microscopic details of the interactions but it considers the symmetries of the problem.

The basic ideas of the theory are (for simplicity we use a scalar and real order parameter):

1) in the continuum limit and if $m(x)$ and $h(x)$ represent the order parameter and the external field, then the partition function is given by a functional integral [22]:

$$Z\{h,T\} \propto \int \mathcal{D}m(x) e^{-\beta S\{h,m\}} \tag{1.4}$$

$$S\{h,m\} = S_0\{m\} - \int dx h(x) m(x) \tag{1.5}$$

The zero-field effective action $S_0\{m\}$ is invariant under the symmetry group of the Hamiltonian and it can be represented by the integral of a local density called Landau

function.
The Landau function $\mathcal{L}$ is also invariant under the symmetry group of the Hamiltonian and it depends on $m(x)$ and its derivatives $\partial m(x)$ [22].

2) If we fix the order parameter configuration [22]:

$$m(x) \propto \frac{\delta}{\delta h(x)} S\left\{h, m\right\} \tag{1.6}$$

then for that configuration we can consider $S\left\{h, m\right\}$ as the free energy associated with it and $\mathcal{L}$ as the corresponding free energy density.
Therefore the partition function $Z\left\{h, T\right\}$ is a functional average computed over all possible configurations of the order parameter [22].

3) Neglecting cubic terms and considering terms up to fourth-order then we have the following expansion of the effective action [22]:

$$S'\left\{h, m\right\} = \beta S\left\{h, m\right\} = \int dx \psi(m(x), \partial m(x), h(x)) \tag{1.7}$$

where

$$\psi(m(x), \partial m(x), h(x)) = \frac{1}{2}|\nabla m(x)|^2 + \frac{1}{2}a(T)m^2(x) + \frac{b}{4}m^4(x) - h(x)m(x) + ... \tag{1.8}$$

We assume that $b > 0$ and $a(T) \sim A(T - T_c)$ if $T \to T_c$ and $A > 0$. We also consider the case $h(x) = 0$ and $m(x)$ constant. The free energy density ψ is represented in Fig. 1.1. For $T > T_c$ ψ has a minimum in 0, whereas for $T < T_c$ ψ has two degenerate minima. The system chooses one of them and this breaks the symmetry, which is Z_2 in our case. Therefore the phase transition from $T > T_c$ to $T < T_c$ implies a symmetry breaking [22].

This theory assumes that the order parameter is uniform in space [22]. Therefore it means that we neglet its fluctuations [23] but in low dimensions fluctuations become increasingly important [23] and therefore this approach is not exact in low dimensions.

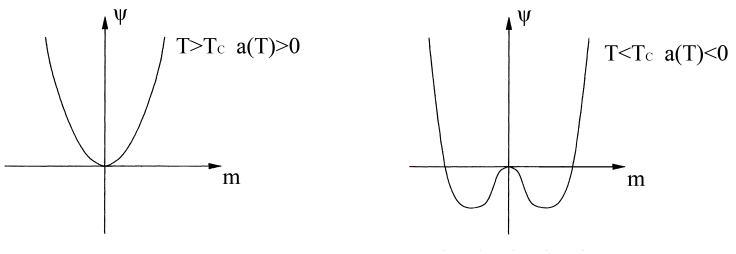

Figure 1.1: Behavior of free energy density ψ for $T > T_c$ on the left and for $T < T_c$ on the right.

1.2 Quantum Phase Transitions

Classical phase transitions occur because of thermal fluctuations and they do not happen at $T = 0$. On the other hand quantum phase transitions are due to quantum fluctuations (they are driven by Heisenberg uncertainty principle) and they occur at zero temperature. At finite temperature there is a competition between thermal and quantum fluctuations of the order parameter. If we call ω_{typ} the typical frequency at which degress of freedom at long distance fluctuate, then the energy of quantum fluctuations is $\hbar\omega_{typ}$. The energy of thermal fluctuations is $k_B T$. So fluctuations of the order parameter are [29]:

- predominantly quantum when $k_B T < \hbar\omega_{typ}$;
- predominantly classical when $k_B T > \hbar\omega_{typ}$.

In order to understand what a quantum phase transition is [29], we consider a Hamiltonian $H(g)$ where g is a dimensionless parameter, we vary g and we study the corresponding evolution of the ground state energy $E_{GS}(g)$.
For a **finite** lattice [29]:

- in general $E_{GS}(g)$ is an analytic function of g, this avoids level crossing;
- it may happen that $E_{GS}(g)$ is not an analytiv function of g, this implies the possibility of a level crossing between the ground state and an excited state.

The second case happens when g in $H(g)$ couples only to a conserved quantity, i.e. $H(g) = H_0 + gH_1$ such that $[H_0,H_1]=0$. In fact because of $[H_0,H_1]=0$ there exist a common set of eigenfunctions $|\psi_n>$ for H_0, H_1, $H(g)$ and they have eigenvalues $\{E_{n,(0)}\}$,

$\{E_{n,(1)}\}$, $\{E_n(g) = E_{n,(0)} + gE_{n,(1)}\}$. So eigenvalues of $H(g)$ depend on g, but its eigenfunctions do not depend on g. It means that at some critical point g_c there may be a level crossing between the ground state $E_0(g)$ and the excited state $E_1(g)$. In fact we can consider two phases A and B:
- in phase A we suppose that the minimum of energy eigenvalues coincides with $E_0(g)$;
- in phase B we suppose that the minimum of energy eigenvalues coincides with $E_1(g)$.
In this way the point $g = g_c$ is of non analyticity for $E_{GS}(g)$ because:
- $E^A_{GS}(g)$=$E_0(g)$ for $g < g_c$;
- $E^B_{GS}(g)$=$E_1(g)$ for $g > g_c$;
- $E_0(g) = E_1(g)$ for $g = g_c$.
A phase transition is defined as a point of non-analyticity in the ground state energy of the system in the limit of an **infinte** lattice and this can emerge from [29]:

- avoided level crossing for **finite** systems, in this case the energy gap between the ground state and the first excited state goes to zero when $L \to \infty$;
- level crossing for **finite** systems, as described above.

Quantum phase transitions happen at $T = 0$, but all experiments are obviously at some finite temperature, although as small as possible. So we would like to understand how the singularity at $T = 0$ in the ground state of the system influences the $T > 0$ regime. There are two possible cases [29]:

1. the thermodynamic singularity occurs only at $T = 0$, while all properties are analytic functions of g at $T > 0$;
2. the singularity at $T = 0$ is the end point of a line which describes a second order phase transition. Since the line is characterized by $k_B T \gg \hbar\omega_{typ}$ we can use a classical approach to study it.

Concluding this introduction, we note that quantum phase transitions in D dimensions are related to classical phase transitions in $D + z$ dimensions, this map is exact when the lattice spacing goes to zero. Since z is the dynamic critical exponent, see (1.11) in the next paragraph, it means that critical dimensions in quantum models are reduced by z respect to those in the corresponding classical models [9, 29].

1.2.1 Second order phase transitions

Second order quantum phase transitions [29] are described by the following property: the characteristic energy scale of fluctuations above the ground state (the energy gap Δ)

vanishes when $g \to g_c$. This also implies an other feature: the characteristic lenght scale (ξ) diverges when when $g \to g_c$. The behavior of Δ and ξ are [29]:

$$\Delta \sim J|g - g_c|^{z\nu} \tag{1.9}$$

$$\xi^{-1} \sim \Lambda|g - g_c|^{\nu} \tag{1.10}$$

$$\Delta \sim \xi^{-z} \tag{1.11}$$

where J is the energy scale describing a characteristic microscopic coupling, $z\nu$ is a critical exponent which is usually indipendent of microscopic features of the Hamiltonian, Λ is a momentum cutoff.

1.2.2 Mermin Wagner theorem and KT transition

Mermin-Wagner theorem prevents a spontaneous breaking of a continuous symmetry, and the resulting appearance of a true long-range ordered phase, at any finite temperature in systems with sufficiently short-range interactions in $D \leq 2$ [19]. It is explained by the fact that fluctuations become more important in low dimensions and they hinder the appearance of a potential order. A demonstration of absence of spontaneously broken spin symmetry in quantum Heisenberg model can be found in [3].

Anyway we can have phase transitions that do not break any continuous symmetry so they can not be classified according to Landau theory. We can ask how the system is ordered in these phase transitions. The answer is the appareance of non-local ordering. These new phases of matter usually deal with topological order, which does not entail a change of symmetry and it does not concern local real order parameters [9].

An example of phase transition, which does not involve any continuous symmetry breaking, is the Kosterlitz-Thouless (KT) transition [33, 17]. It concerns two-dimensional systems where topological features are crucial, such as superconducting and superfluid compounds and certain kinds of magnets. These systems can be described by the same effective theory because they belong to the same universality class and this happens because their order parameters are both described by a single angle θ as explained below.

- In two-dimensional magnets spins must lie on a plane, that we can call XY plane, on which they are free to rotate around the z axis. For this reason the direction of the magnetization is determined by the rotation angle θ [33, 17].
  As we will see, these spins can assume configurations (for example an individual votex or on the contrary a pair of vortex-antivortex) that are topologically distinct and that can be classified according to their vorticity, a topological invariant described below.

- Superconductors and superfluids are described by the complex order parameter $\psi = \sqrt{\rho_s} e^{i\theta}$, where the superfluid density is given by ρ_s and the phase of ψ is θ [33, 17].

In two dimensions the Hamiltonian that describes both these systems is [33, 17]:

$$H = -J \sum_{<ij>} \cos(\theta_i - \theta_j) \tag{1.12}$$

where $0 \leq \theta_i < 2\pi$. Taking the continuum limit, it becomes [33, 17]:

$$H = \frac{J}{2} \int d^2 r (\nabla \theta(r))^2 \tag{1.13}$$

where we can consider θ between $-\infty$ and $+\infty$ for simplicity.
In this case, if we consider a short-distance cutoff a, we achieve the following behavior for spin-spin connected correlation function [33, 17]:

$$\left\langle e^{i(\theta(r)-\theta(0))} \right\rangle \sim \left(\frac{a}{r}\right)^{\frac{K_B T}{2\pi J}} . \tag{1.14}$$

It is a power law decay even at high temperatures, whereas it is usually an exponential decay as we know from (1.2).

Kosterlitz, Thouless and Berezinskii understood this apparent paradox: a new kind of phase transition occurs that involves vortex configurations.
A vortex is characterized by a non-zero quantity know as vorticity [33, 17]:

$$v = \frac{1}{2\pi} \oint_{\mathcal{C}} dr \nabla \theta(r) \tag{1.15}$$

where the curve $\mathcal{C}$ encloses the center of the vortex. This integral gives the total rotation of the spin vector along the curve. If we divided it by 2π we achieve the number of full turns that the spin vector makes around the vortex.
If $v = \pm 1$ then $|\nabla \theta(r)| = \frac{1}{r}$ for (1.15). It means that the energy of the vortex for (1.13) is: $E = \frac{J}{2} \int d^2 r \left(\frac{1}{r}\right)^2 = J\pi \ln(\frac{L}{a})$. This energy increases with the size of the system L, therefore if we have a large system thermal fluctuations can not excite a single vortex because it would cost too much energy [33].
On the contrary if there is a vortex-antivortex pair it has a total zero vorticity and the energy required to create it is $E = J2\pi \ln\left(\frac{r}{a}\right)$ where r is the distance between the vortices. So thermal fluctuations are able to excite these pairs [33].
Therefore for $T < T_{KT}$ there exist such pairs, while at $T > T_{KT}$ pairs break up into individual vortices, which have high energy.

Furthermore the free energy of a single vortex is [33]:

$$F = E - TS = J\pi \ln\left(\frac{L}{a}\right) - K_B T \ln\left(\frac{L^2}{a^2}\right) \tag{1.16}$$

where we suppose that there are $\frac{L^2}{a^2}$ possible positions for a vortex with area a^2. At $T_{KT} = \frac{J\pi}{2K_B}$ there is a balance between energy and entropy and the transition to a phase of free vorteces happens.

1.2.3 Topological phases

We have already said that the concept of topological quantum phases has been developed to described phases which do not break any symmetry and where topological features are crucial.

Two kinds of topological phases can be identified [9]:

- phases characterized by an "intrinsic" topological order;
- phases characterized by the respect of a certain symmetry, they are called symmetry protected topological phases (SPT).

For free fermionic systems SPT have been classified in [34] to achieve a table for topological insulators and superconductors: noninteracting fermion systems characterized by time reversal, charge conjugation and/or $U(1)$ may have not simply $Z_2^T \times Z_2^C \times U(1)$ as total symmetry group ($\hat{T}$, $\hat{C}$ and $\hat{N}$ are generators of time reversal, charge conjugation and $U(1)$ symmetry), but their total group can have different forms. These different forms depend on relations between generators $\hat{T}$, $\hat{C}$ and $\hat{N}$. In reference [34] for some electron systems their total symmetry groups are listed. Therefore free fermion protected phases, protected by those symmetry groups, can be classified. This can be based on the assumption that fermions form an irreducible representation of the full symmetry group, but it may happen that this is not the case. Reference [34] considers both these situations.

For interacting fermions systems SPT have been studied for example in reference [11].
In fact it may happen that topological invariants of certain systems are stable with respect to interactions, for instance this occurs in the integer quantum Hall effect [11]. But this is not always the case and [11] takes the so-called Majorana chain, with an unusual time reversal symmetry, as an example to study the effect of interactions. In this system some phases which are distinct without interaction are actually connected in the interacting case.

1.3 Non-Local Order Parameters

We have already said that one dimensional quantum phases are not characterized by a local order parameter, on the contrary they can be identify using non-local string-like operators.

To better understand the difference between the two types of order parameter, we first remember what a local order parameter can be. Considering the Ising model (1.1) the local order parameter, i.e. the magnetization, is defined as [23]:

$$m = \frac{1}{N}\langle \sum_{i=1}^{N} \sigma_i \rangle. \tag{1.17}$$

An other example of local order parameter are correlators as those defined in paragraph 1.1.3, in fact the two-point correlator is [23]:

$$C(i,j) = \langle \sigma_i \sigma_j \rangle. \tag{1.18}$$

In the context of one dimensional fermionic systems these non-local string-like operators were introduced [8, 21] in both charge and spin channels ($\nu = c, s$):

$$O_P^{\nu}(j) = \prod_{k=0}^{j-1} e^{i2\pi S_k^{(\nu),z}} \tag{1.19}$$

$$O_S^{\nu}(j) = 2S_j^{(\nu),z} \prod_{k=0}^{j-1} e^{i2\pi S_k^{(\nu),z}} \tag{1.20}$$

where $S_k^{(s),z} = \frac{1}{2}(n_{k,\uparrow} - n_{k,\downarrow})$ and $S_k^{(c),z} = \frac{1}{2}(n_{k,\uparrow} + n_{k,\downarrow} - 1)$. They are known as parity and Haldane string.

The corresponding correlators are $C_A^{(\nu)}(r) = \left\langle O_A^{(\nu)\dagger}(j) O_A^{(\nu)}(j+r) \right\rangle$ with A=P,S, so they can be written as [8, 21]:

$$C_P^{(\nu)}(r) = \left\langle \prod_{k=j}^{j+r-1} e^{i2\pi S_k^{(\nu),z}} \right\rangle \tag{1.21}$$

$$C_S^{(\nu)}(r) = \left\langle 2S_j^{(\nu),z} \prod_{k=j}^{j+r-1} e^{i2\pi S_k^{(\nu),z}} 2S_{j+r}^{(\nu),z} \right\rangle \tag{1.22}$$

where $S_k^{(s),z} = \frac{1}{2}(n_{k,\uparrow} - n_{k,\downarrow})$ and $S_k^{(c),z} = \frac{1}{2}(n_{k,\uparrow} + n_{k,\downarrow} - 1)$ as before.

In the asympotic limit $r \to \infty$ these correlators can be considered order parameters because [8, 21]:

- each partly gapped phase is identified by $C_A^{(\nu)} \neq 0$ for a specif combination of A and ν, whereas the other three correlators are zero in that phase;

- each fully gapped phase is characterized by the coexistence of two non-local orders.

In the corresponding gapped phase in strong coupling limit $C_A^{(\nu)} = 1$, but fluctuations can reduce this value $C_A^{(\nu)} < 1$.
In particular fluctuations in the parity order imply [5]:
-in charge sector the formation of holon/doublon pairs in a background with a single particle for each site with up/down spin ("holon" means an empty site and "doublon" means a doubly occupied site), this is known as Mott insulator (MI);
-in spin sector the formation of up/down pairs in a background of holons and doublons, this is known as Luther Emery (LE).
On the contrary Haldane string order is represented by alternated and diluted holons and doublons, Haldane insulator (HI), or alternated and diluted up and down spins, not been observed yet.
A more detailed physical description of these phases will be present in next paragraphs.

In the remaining part of this paragraph we describe how these non-local order parameters can be studied in 1D lattice systems using the analytical technique known as bosonization.

1.3.1 Bosonization

Introduction: noninteracting fermion system

Bosonization is an analytical technique that we can use in order to establish a one-to-one correspondence between a fermionic theory and the corresponding bosonic theory. In fact its basic idea is as follows: there are some quantities which can be computed either in a fermionic theory or in a bosonic theory giving the same outcome, but they may be very difficult to calculate in one theory and quite simple to compute in the other one.
A detailed description of bosonization tecnique is present in [9, 28, 30].

We can start by considering the simple case of a system of noninteracting electrons on a lattice [30], it is described by the following microscopic Hamiltonian:

$$H_F = \sum_k \varepsilon(k) c^\dagger(k) c(k) \tag{1.23}$$

where $c(k)$ and $c^\dagger(k)$ are the electron annihilation and creation operators at wavevector k. We ignore the spin in this simple example.
In order to define the corresponding low-energy field theory, firstly we remember that

a field theory is a physical model defined on the continuum as opposed to a lattice. However, a purely continuum theory makes no sense because of quantum fluctuations. In order to make it meaningful, it is necessary to introduce a momentum cutoff Λ. This regularization introduces a length scale Λ^{-1}, which defines the theory together with its parameters. When Λ changes (through a trace over high-momentum degrees of freedom) it implies a modification of all other parameters of the theory. For this reason a field theory is characterized by a Renormalization Group trajectory, which traces the changing of parameters as the cutoff is lowered, rather than by some fixed parameters. If Renormalization procedure starts at arbitrary high energy it implies that an arbitrary number of irrilevant parameters can be added to the theory without measurable consequences, so in modern view it is usually to start at Λ_0. In condensed matter physics Λ_0^{-1} corresponds to the lattice spacing $\sim 10^{-8} cm$ [30].
So returning to our case, if we want to write the corresponding field theory for free particles (bosons or fermions) this poses no problem because their degrees of freedom at different momentum scales are decoupled, it means that a partial trace in a momentum shell has no consequence on the remaining degrees of freedom. The low-energy field theory can be achieved by defining creation and annihilation operators in the vicinity of the two Fermi points [30] represented in Fig.1.2:

$$c^\dagger(k_F + k) = \alpha^\dagger(k) \tag{1.24}$$

$$c^\dagger(-k_F - k) = \alpha^\dagger(-k) \tag{1.25}$$

$$c(k_F - k) = \beta^\dagger(k) \tag{1.26}$$

$$c(-k_F + k) = \beta^\dagger(-k) \tag{1.27}$$

where $\alpha^\dagger(k)$ creates an electron at $k_F + k$ and $\beta^\dagger(k)$ creates an hole at $k_F - k$ for the right Fermi point; the same concept is true for the left Fermi point too. In Fig. 1.2 the red lenght can be approximated to be linear near the two Fermi points, Fermi level is represented by a green line and momentum are represented in blue.

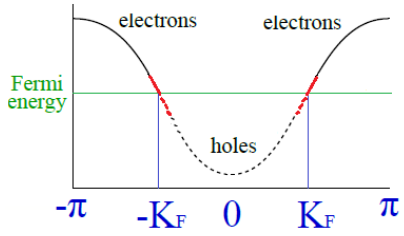

Figure 1.2: Dispersion relation of the system described by (1.23).

The Hamiltonian then becomes [30]:

$$H_F = \int \frac{dk}{2\pi} v|k|[\alpha^\dagger(k)\alpha(k) + \beta^\dagger(k)\beta(k)] \tag{1.28}$$

where v is the only remaining parameter from the lattice theory and it is the Fermi velocity. The integration is carried between $-\Lambda$ and Λ and this momentum cutoff implies a corresponding energy cutoff $v\Lambda$.
The basic idea is that these particle-hole excitations are bosonic in character [30].
The continuum limit is indeed a low-energy limit, in which the linear approximation to the dispersion relation is acceptable and for this reason particle-hole excitations enjoy Lorentz invariance. Interactions may violate Lorentz invariance when they imply the appearance of two non indipendent characteristic velocities, which are v_s the spin one and v_c the charge one. However in low-energy limit these two sectors are disjoint and each of them enjoy Lorentz invariance. So in this limit interactions that leave the spectrum similar to Fig. 1.2 with two Fermi points are allowed [30].

Right and left separation: fermion fields ψ_R and ψ_L

This procedure also implies that we can express the annihilation operator at a site **n** in terms of slow fields ψ_R and ψ_L [30]:

$$\frac{c_x}{\sqrt{a}} = \psi(x) = \psi_R(x)e^{ik_F x} + \psi_L(x)e^{-ik_F x} \tag{1.29}$$

where $\sqrt{a}$ reflects the engineering dimensions of the fields and it gives the proper delta-function anticommutator.
We can write the mode expansion of the continuum fields [30]:

$$\psi_R(x) = \int_{k>0} \frac{dk}{2\pi}[e^{ikx}\alpha(k) + e^{-ikx}\beta^\dagger(k)] \tag{1.30}$$

$$\psi_L(x) = \int_{k<0} \frac{dk}{2\pi}[e^{ikx}\alpha(k) + e^{-ikx}\beta^\dagger(k)] \tag{1.31}$$

and we can obtain the time dependence of these operators by the multiplicative phase $e^{-iv|k|t}$:

$$\psi_R(z) = \int_{k>0} \frac{dk}{2\pi}[e^{-kz}\alpha(k) + e^{kz}\beta^\dagger(k)] \tag{1.32}$$

$$\psi_L(\bar{z}) = \int_{k<0} \frac{dk}{2\pi}[e^{k\bar{z}}\alpha(k) + e^{-k\bar{z}}\beta^\dagger(k)] \tag{1.33}$$

where we use the complex variables $z = -i(x - vt)$ and $\bar{z} = i(x + vt)$.
The right-moving field ψ_R is expressed only in terms of the right-moving coordinate z

and the left-moving field ψ_L is written only in terms of the left-moving coordinate $\bar{z}$. The continuum Hamiltonian (1.28) becomes exactly the Dirac Hamiltonian when we use ψ_R and ψ_L [30]:

$$H_F = -iv \int dx[\psi_R^\dagger \partial_x \psi_R - \psi_L^\dagger \partial_x \psi_L]. \tag{1.34}$$

Particle-hole excitations in 1D and 2D

Why bosonisation is possible only in one dimension? We can understand it by a comparison between particle-hole excitations in one and two dimensions.
In one dimension the linear one particle dispersion, near the two Fermi points, implies that the particle and the hole have nearly the same group velocity. This means that they propagate together coherently in a new entity [30].
In two dimensions for a given momentum k the particle-hole pair has a corresponding continuous spectrum of energies. So it is very difficult to form coherent particle-hole pairs [30].

Right and left separation: boson fields ϕ_R and ϕ_L

Bose particles in one dimension can move to the left or to the right as fermions do. So the bosonic field can be written separating left and right moving parts [30]:

$$\phi(x,t) = -(\phi_R(x - vt) + \phi_L(x + vt)). \tag{1.35}$$

We can consider the momentum Π conjugate to field ϕ and we can introduce the so-called dual boson field θ, it is defined as [30]:

$$\begin{aligned} \partial_x \theta = -\Pi = -\frac{1}{v}\partial_t \phi = -i(\partial_z + \partial_{\bar{z}})(-\phi_R - \phi_L) \\ = -i(\partial_z - \partial_{\bar{z}})(-\phi_R + \phi_L) = \partial_x(-\phi_R + \phi_L). \end{aligned} \tag{1.36}$$

Therefore we have (up to an additive constant that can be put to zero):

$$\theta = -\phi_R + \phi_L. \tag{1.37}$$

From these relations we obtain that:

$$\phi_R = -\frac{1}{2}(\phi + \theta) \tag{1.38}$$

and

$$\phi_L = \frac{1}{2}(-\phi + \theta). \tag{1.39}$$

Bose representation without considering the spin

We can now try to write a first (although incomplete because for example we ignore the spin) representation of fermion fields in terms of bosons.

- We can consider the electron density as a bilinear in the electron fields. This implies that it has Bose statistics and so it may be written as the derivative of a boson field [30]:
$$\phi(x) = \lambda \int_x^\infty n_{total}(y)dy \quad n_{total}(x) = -\frac{1}{\lambda}\partial_x \phi(x) \tag{1.40}$$
where λ is a constant.

- The creation of a fermion at a certain position x' between x and ∞ implies that ϕ increases by λ because of equation (1.40).

- The operator $\exp(-i\lambda \int_{-\infty}^{x'} \Pi(y)dy)$ also implies that ϕ increases by λ beacuse Π is the coniugate momentum of ϕ.

- So a creation operator $\psi_R^\dagger(x')$ and $\psi_L^\dagger(x')$ can be represented by the operator $\exp(-i\lambda \int_{-\infty}^{x'} \Pi(y)dy)$ multiplied by an operator that commutes with ϕ such as $\exp(\pm i\lambda\phi(x'))$. This extra factor must imply that $\psi_R^\dagger$ has a dependence on $x - vt$ only and that $\psi_L^\dagger$ has a dependence on $x + vt$ only.

- We now remember that $\Pi = \frac{1}{v}\partial_t \phi = -\partial_x \theta$ so $-i\lambda \int_{-\infty}^{x'} \Pi(y)dy = i\lambda\theta(x')$.

- Therefore, because of the last two equations in the previous point and because of the expressions of ϕ_R and ϕ_L in terms of ϕ and θ written before (1.38) and (1.39), we can obtain the following Ansaz [30]:
$$\psi_R^\dagger(x) = Ae^{2i\lambda\phi_R(x)} \quad \psi_L^\dagger(x) = Ae^{-2i\lambda\phi_L(x)} \tag{1.41}$$
$$\psi_R(x) = Ae^{-2i\lambda\phi_R(x)} \quad \psi_L(x) = Ae^{2i\lambda\phi_L(x)} \tag{1.42}$$
where A and λ are constant to be determined.

- $\psi^\dagger|0>$ represents one-electron states and they are also coherent states of the boson field ϕ because $\psi^\dagger$ is given in terms of exponentials of the boson creation operators. On the other hand Bose excitations are electron-hole excitations, as said before [30].

After the determination of the two constants, see reference [9, 30], we can sum up relations (1.41) and (1.42) in this way:

$$\psi_\chi(x) = \frac{\eta_\chi}{\sqrt{2\pi\alpha}} e^{-i\sqrt{4\pi}\chi\phi_\chi(x)} \tag{1.43}$$

χ=R,L where in the first case χ is 1 and in the second case χ is -1, $\alpha \sim$a where a is the lattice spacing and the meaning of the Klein factor η_χ will be clear later.

We have already seen that $\theta = -\phi_R + \phi_L$ and $\phi = -(\phi_R + \phi_L)$ so we can also write:

$$\psi_\chi(x) = \frac{\eta_\chi}{\sqrt{2\pi\alpha}} e^{i\sqrt{\pi}(\chi\phi(x)+\theta(x))}. \tag{1.44}$$

The zero mode is not well defined in the previous expressions and we can neglect it when we consider the thermodynamic limit $L \to \infty$ because it goes as $\frac{1}{L}$. If we want to include it we can add an extra factor to (1.43) and (1.44). We obtain [9, 28]

$$\psi_\chi(x) = \frac{\eta_\chi}{\sqrt{2\pi\alpha}} e^{-i\sqrt{4\pi}\chi\phi_\chi(x)} e^{i\chi\frac{2\pi N_\chi}{L}x}, \tag{1.45}$$

$$\psi_\chi(x) = \frac{\eta_\chi}{\sqrt{2\pi\alpha}} e^{i\sqrt{\pi}(\chi\phi(x)+\theta(x))} e^{i\chi\frac{2\pi N_\chi}{L}x}. \tag{1.46}$$

N_χ represents the number of right particles $\chi = R$ or left particles $\chi = L$ added to the system or removed from it, when it is in the excited state. This operator N_χ does not commute with Klein factors [9, 28] but it commutes with bosonic fields [9, 28] and so it can be neglected when we compute their commutation rules.

Commutation Rules

Some usefull relations concern commutators between $\phi(x)$ and $\theta(x)$. They enable us to get commutators between chiral fields ϕ_R and ϕ_L too.

Between $\phi(x)$ and $\theta(x)$ we have these following commutation rules [9, 28]:

$$[\phi(x), \phi(y)] = 0; \tag{1.47}$$

$$[\theta(x), \theta(y)] = 0; \tag{1.48}$$

$$[\phi(x), \theta(y)] = \frac{i}{2} sgn(x-y). \tag{1.49}$$

If we remember that $\phi_R = -\frac{\phi+\theta}{2}$ and $\phi_L = -\frac{\phi-\theta}{2}$ we can deduce the commutators between them from (1.47), (1.48), and (1.49) in particular [9, 28]:

- for the same chirality we have:

$$[\phi_\chi(x), \phi_\chi(y)] = \frac{1}{4}[\phi(x) + \chi\theta(x), \phi(y) + \chi\theta(y)] =$$

$$= \frac{\chi}{4}([\phi(x),\theta(y)] - [\phi(y),\theta(x)]) = \frac{\chi}{4}(\frac{i}{2}sgn(x-y) - \frac{i}{2}sgn(y-x)) =$$

$$= \chi\frac{i}{4}sgn(x-y); \tag{1.50}$$

- for different chiralities:

$$[\phi_R(x),\phi_L(y)] = -\frac{1}{4}([\phi(x),\theta(y)] + [\phi(y),\theta(x)]) =$$

$$= \frac{1}{4}(\frac{i}{2}sgn(x-y) + \frac{i}{2}sgn(y-x)) = 0. \tag{1.51}$$

Derivatives of the bosonic fields appear when we bosonize the Hamiltonian at first order in a, so we can consider commutation rules between them too [9]:

$$[\nabla\phi(x),\nabla\phi(y)] = [\nabla\theta(x),\nabla\theta(y)] = 0 \tag{1.52}$$

$$[\phi(x),\nabla\phi(y)] = [\theta(x),\nabla\theta(y)] = 0 \tag{1.53}$$

$$[\nabla\phi(x),\nabla\theta(y)] = \nabla_x\nabla_y[\phi(x),\theta(y)] = -\frac{i}{2}\nabla_x\nabla_y sgn(y-x) = -i \tag{1.54}$$

$$[\nabla\phi(x),\theta(y)] = \nabla_x[\phi(x),\theta(y)] = \frac{i}{2}\nabla_x sgn(x-y) = i\delta(x-y) \tag{1.55}$$

$$[\phi(x),\nabla\theta(y)] = \nabla_y[\phi(x),\theta(y)] = \frac{i}{2}\nabla_y sgn(x-y) = -i\delta(x-y). \tag{1.56}$$

Normal Ordering

The Hamiltonian usually contains an even number of fermion operators (1.43), so it is necessary to know how to deal with products of exponential operators of bosonic field. Since ϕ is a fluctuating field, any function of it requires a careful definition to avoid divergent average values [30].

We adopt the prescription known as normal ordering that consists in putting all the creation operators on the left of all annihilation operators. We denote it as :: and we have [9, 30]:

$$e^{i\sqrt{4\pi}\phi(x)} = e^{i\sqrt{4\pi}(\varphi(x)+\varphi^\dagger(x))} = e^{i\sqrt{4\pi}\varphi^\dagger(x)}e^{i\sqrt{4\pi}\varphi(x)}e^{2\pi[\varphi^\dagger(x),\varphi(x)]} =$$

$$=: e^{i\sqrt{4\pi}\phi(x)} : e^{-2\pi[\varphi(x),\varphi^\dagger(x)]} =: e^{i\sqrt{4\pi}\phi(x)} : \frac{2\pi\alpha}{L}, \tag{1.57}$$

where the real field $\phi(x)$ can be written as the sum $\varphi(x) + \varphi^\dagger(x)$ of two hermitian coniugate fields. If we compute the exponential of a difference between the same field in two different points we obtain [9, 30]:

$$e^{i\sqrt{4\pi}[\phi(x+r)-\phi(x)]} =: e^{i\sqrt{4\pi}[\phi(x+r)-\phi(x)]} : \left(\frac{\alpha}{r}\right)^2. \tag{1.58}$$

We can replace $\phi(x+r) = \phi(x)+r\nabla\phi(x)$ in the last expression. A consequence of normal ordering can be seen in the Taylor expansion of the exponential [9, 30]:

$$: e^{i\sqrt{4\pi}r\nabla\phi(x)} :\sim 1 + i\sqrt{4\pi}r\nabla\phi(x). \tag{1.59}$$

Bose representation for spinfull fermions

Up to this point we have dealt with spinless fermions, but now we can generalize the previous expressions to the case of spinfull fermions by adding a spin index. In this way we have two different fermionic species, explicitly they are $(\phi_\uparrow, \theta_\uparrow)$ and $(\phi_\downarrow, \theta_\downarrow)$. They are characterized by commutators (1.47), (1.48), (1.49) but with spin index too [9]:

$$[\phi_\sigma(x), \phi_{\sigma'}(y)] = [\theta_\sigma(x), \theta_{\sigma'}(y)] = 0 \tag{1.60}$$

$$[\phi_\sigma(x), \theta_{\sigma'}(y)] = \delta_{\sigma,\sigma'}\frac{i}{2}sgn(x-y). \tag{1.61}$$

We can rewrite the Bose representation of a fermion field (1.43) and (1.44) with the addition of the spin index [9]:

$$\psi_{\chi\sigma}(x) = \frac{\eta_{\chi\sigma}}{\sqrt{2\pi\alpha}}e^{-i\sqrt{4\pi}\chi\phi_{\chi\sigma}(x)} \tag{1.62}$$

$$\psi_{\chi\sigma}(x) = \frac{\eta_{\chi\sigma}}{\sqrt{2\pi\alpha}}e^{i\sqrt{\pi}(\chi\phi_\sigma(x)+\theta_\sigma(x))}. \tag{1.63}$$

As we will see, the Hamiltonian can often be written as the sum of two indipendent Hamiltonians, which concern separately charge and spin degrees of freedom. For this reason we introduce spin and charge bosonic fields in terms of $(\phi_\uparrow, \theta_\uparrow)$ and $(\phi_\downarrow, \theta_\downarrow)$. They are defined as [9]:

$$\phi_s(x) = \frac{\phi_\uparrow - \phi_\downarrow}{\sqrt{2}} \quad \theta_s(x) = \frac{\theta_\uparrow - \theta_\downarrow}{\sqrt{2}} \quad \phi_c(x) = \frac{\phi_\uparrow + \phi_\downarrow}{\sqrt{2}} \quad \theta_c(x) = \frac{\theta_\uparrow + \theta_\downarrow}{\sqrt{2}}. \tag{1.64}$$

They are characterized by these commutators [9]:

$$[\phi_c(x), \phi_s(y)] = [\theta_c(x), \theta_s(y)] = 0 \tag{1.65}$$

$$[\phi_c(x), \theta_s(y)] = \frac{1}{2}([\phi_\uparrow(x), \theta_\uparrow(y)] - [\phi_\downarrow(x), \theta_\downarrow(y)] + [\phi_\downarrow(x), \theta_\uparrow(y)] - [\phi_\uparrow(x), \theta_\downarrow(y)]) = 0 \tag{1.66}$$

$$[\phi_c(x), \theta_c(y)] = \frac{1}{2}([\phi_\uparrow(x), \theta_\uparrow(y)] + [\phi_\downarrow(x), \theta_\downarrow(y)] + [\phi_\downarrow(x), \theta_\uparrow(y)] + [\phi_\uparrow(x), \theta_\downarrow(y)]) =$$

$$= \frac{1}{2} 2[\phi(x), \theta(y)] = \frac{i}{2} sgn(x - y) \tag{1.67}$$

$$[\phi_s(x), \theta_s(y)] = \frac{1}{2}([\phi_\uparrow(x), \theta_\uparrow(y)] + [\phi_\downarrow(x), \theta_\downarrow(y)] - [\phi_\downarrow(x), \theta_\uparrow(y)] - [\phi_\uparrow(x), \theta_\downarrow(y)]) =$$

$$= \frac{1}{2} 2[\phi(x), \theta(y)] = \frac{i}{2} sgn(x - y). \tag{1.68}$$

If we want to express the fermionic field in terms of $(\phi_\uparrow, \theta_\uparrow)$ and $(\phi_\downarrow, \theta_\downarrow)$, we can rewrite (1.63) in this way [9]:

$$\psi_{\chi\sigma}(x) = \frac{\eta_{\chi\sigma}}{\sqrt{2\pi\alpha}} e^{i\sqrt{\frac{\pi}{2}}[\chi\phi_c(x) + \theta_c(x) + \sigma(\chi\phi_s(x) + \theta_s(x))]}. \tag{1.69}$$

Klein factors

Klein factors $\eta_{\chi\sigma}$ and $\eta_{\chi\sigma}$ are introduced in (1.43), (1.44), (1.45), (1.46), (1.62), (1.63) and (1.69) to ensure anticommutation of different fermion species. In fact fermions with different chiralities and (or) different spin must anticommute, whereas boson fields of different chiralities (1.51) and of different spin (1.60) commute, so Klein factors are necessary [9, 30, 28].

These factors satisfy the following anticommutating rules, where $\lambda = (\chi, \sigma)$ [9, 30, 28]:

$$\eta_\lambda^\dagger \eta_\lambda = \eta_\lambda \eta_\lambda^\dagger = 1 \tag{1.70}$$

$$\left\{\eta_\lambda, \eta_{\lambda'}^\dagger\right\} = 2\delta_{\lambda,\lambda'} \tag{1.71}$$

$$\left\{\eta_\lambda^\dagger, \eta_{\lambda'}^\dagger\right\} = 0 \quad \lambda \neq \lambda' \tag{1.72}$$

$$\{\eta_\lambda, \eta_{\lambda'}\} = 0 \quad \lambda \neq \lambda'. \tag{1.73}$$

They commute with bosonic fields [9, 28] but they do not commute with the number operator [9, 28] becuase thay change the total number of fermions by one. This fact

guarantees the correct anticommutation rules as said before. The change by one is negligible in the thermodynamic limit, and we can concentrate only on the change of sign due to them.

Klein factors act on a different Hilbert space than that of bosonic operators. This Hilbert space expansion must be compensated by choosing a "gauge" and we will see what it means. The Klein Hilbert space is the representation space of the Clifford algebra and it is chararcterized by a minimal dimension. This dimension is determined by the number of fermions species, in our case we have 4 species (left and right, up and down) and it is 4. Therefore a representation in terms of tensor products of Pauli matrices is possible [30]:

$$\eta_{R\uparrow} = \sigma^x \otimes \sigma^x \quad \eta_{R\downarrow} = \sigma^z \otimes \sigma^x \quad \eta_{L\uparrow} = \sigma^y \otimes \sigma^x \quad \eta_{L\downarrow} = I \otimes \sigma^y. \tag{1.74}$$

In the Hamiltonian products of four Klein factors appear and they are diagonal with eigenvalues ± 1. The choice of one of them is the "gauge fixing" said before. For example we can choose: $\eta_{L\downarrow}\eta_{L\uparrow}\eta_{R\downarrow}\eta_{R\uparrow} = 1$ [30].

Fermion densities ρ_χ

We can use (1.43), (1.44), (1.45), (1.46), (1.62), (1.63) and (1.69) as a basis to translate various operators in terms of bosons, but we must pay attention to normal ordering, which is always required.

Among these operators we introduce fermion densities defined as $\rho_\chi =: \psi^\dagger_\chi(x)\psi_\chi(\mathrm{x}):$. Normal ordering can be achieved by point spitting, i.e., by the following definition [9, 30, 28]:

$$\rho_\chi =: \psi^\dagger_\chi(x)\psi_\chi(x) := \lim_{a\longrightarrow 0} [\psi^\dagger_\chi(x+a)\psi_\chi(x) - < \psi^\dagger_\chi(x+a)\psi_\chi(x) >] =$$

$$= \lim_{a\longrightarrow 0} [\frac{\eta^\dagger_\chi \eta_\chi}{2\pi\alpha} e^{i\chi\sqrt{4\pi}\phi_\chi(x+a)} e^{-i\chi\sqrt{4\pi}\phi_\chi(x)} - < ... >] \simeq$$

$$\simeq -\frac{1}{\sqrt{\pi}}\nabla\phi_\chi(x) = \frac{1}{2\sqrt{\pi}}(\nabla\phi(x) + \chi\nabla\theta(x)). \tag{1.75}$$

This expression means that:

$$\rho_R = -\frac{1}{\sqrt{\pi}}\nabla\phi_R = \frac{1}{2\sqrt{\pi}}(\nabla\phi + \nabla\theta) \tag{1.76}$$

$$\rho_L = -\frac{1}{\sqrt{\pi}}\nabla\phi_L = \frac{1}{2\sqrt{\pi}}(\nabla\phi - \nabla\theta). \tag{1.77}$$

We can sum or subtract these expression in order to achieve the total density ρ and the renormalized current $\overline{j}=\frac{j}{v_F}$ [9, 30, 28]:

$$\rho = \rho_R + \rho_L = \frac{1}{\sqrt{\pi}}\nabla\phi \tag{1.78}$$

$$\overline{j} = \rho_R - \rho_L = \frac{1}{\sqrt{\pi}}\nabla\theta. \tag{1.79}$$

Expression (1.75) have not a spin index, but it is straightforward its addition and we rewrite it as [9]:

$$\rho_{\chi\sigma} = -\frac{1}{\sqrt{\pi}}\nabla\phi_{\chi\sigma}(x) = \frac{1}{2\sqrt{\pi}}(\nabla\phi_\sigma(x) + \chi\nabla\theta_\sigma(x)) \tag{1.80}$$

We can also separate spin and charge degrees of freedom in the expressions of density and current [9]:

$$\rho_s = \frac{\rho_\uparrow - \rho_\downarrow}{\sqrt{2}} = \frac{1}{\sqrt{\pi}}\nabla\phi_s \quad \overline{j}_s = \frac{\overline{j}_\uparrow - \overline{j}_\downarrow}{\sqrt{2}} = \frac{1}{\sqrt{\pi}}\nabla\theta_s \tag{1.81}$$

$$\rho_c = \frac{\rho_\uparrow + \rho_\downarrow}{\sqrt{2}} = \frac{1}{\sqrt{\pi}}\nabla\phi_c \quad \overline{j}_c = \frac{\overline{j}_\uparrow + \overline{j}_\downarrow}{\sqrt{2}} = \frac{1}{\sqrt{\pi}}\nabla\theta_c. \tag{1.82}$$

1.3.2 Sine-Gordon model

We can apply bosonization tecnique to the Hamiltonian of an interacting fermion model [9, 20]. First of all we note that we can approximate it as the sum of two contribution H_0 and H_{int}:

$$H \simeq H_0 + H_{int} \tag{1.83}$$

where we have [9]:

$$H_0 = v_F \sum_{k,\chi,\sigma} \chi k : c^\dagger_{k,\chi,\sigma} c_{k,\chi,\sigma} : \tag{1.84}$$

and

$$H_{int} = \frac{1}{2L} \sum_{k,k',q} \sum_{\chi} \sum_{\sigma,\sigma'} (g_{1,\sigma,\sigma'} c^\dagger_{k+q,\chi,\sigma} c_{k,\bar{\chi},\sigma} c^\dagger_{k'-q,\bar{\chi},\sigma'} c_{k',\chi,\sigma'} + g_{2,\sigma,\sigma'} c^\dagger_{k+q,\chi,\sigma} c_{k,\chi,\sigma} c^\dagger_{k'-q,\bar{\chi},\sigma'} c_{k',\bar{\chi},\sigma'} +$$

$$+ g_{3,\sigma,\sigma'} c^\dagger_{k+q,\chi,\sigma} c_{k,\bar{\chi},\sigma} c^\dagger_{k'-q,\chi,\sigma'} c_{k',\bar{\chi},\sigma'} + g_{4,\sigma,\sigma'} c^\dagger_{k+q,\chi,\sigma} c_{k,\chi,\sigma} c^\dagger_{k'-q,\chi,\sigma'} c_{k',\chi,\sigma'}) \tag{1.85}$$

we use $\bar{\chi}$ to indicate the opposite moving branch with respect to χ and q is sufficiently small so that $k \pm q$ and k are around the same Fermi point.

Interactions are represented in Fig. 1.3 below.

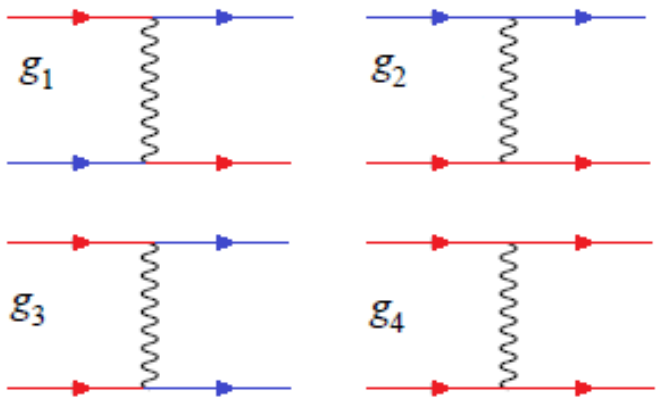

Figure 1.3: The four possible interactions, right-moving electrons are represented by red lines and left-moving electrons by blue lines.

These interactions are described below.

- g_1 describes the backward scattering: each electron changes branch, but it keeps its spin.
- g_2 and g_4 represent dispersion, i.e. scattering of left onto right electrons, and forward scattering, i.e. scattering of left onto left electrons or right onto right electrons.
- g_3 is called Umklapp interaction: two left electrons become right electrons or viceversa. This process implies a change in the total momentum which has to be absorbed by the lattice because of crystal momentum conservation. But momentum takes its value in the Brioullin zone, it means that the total momentum change must be a multiple of $\frac{2\pi}{a}$, so this process is possible only at some particular filling. We can consider a, the lattice spacing, equal to 1 and the filling is so half-filling.

By the transformation $c_{k,\chi,\sigma} = \frac{1}{\sqrt{L}} \int dx e^{-ikx} \psi_{\chi,\sigma}(x)$ we can rewrite (1.84) and (1.85) [9]:

$$H_0 = v_F \sum_{\chi,\sigma} \int dx : \psi^\dagger_{\chi\sigma}(x)(-i\chi\partial_x)\psi_{\chi\sigma} : \tag{1.86}$$

and

$$\begin{aligned} H_{int} = \frac{1}{2} \sum_{\chi} \sum_{\sigma,\sigma'} (& g_{1,\sigma,\sigma'} \psi^\dagger_{\chi,\sigma} \psi_{\bar{\chi},\sigma} \psi^\dagger_{\bar{\chi},\sigma'} \psi_{\chi,\sigma'} + g_{2,\sigma,\sigma'} \psi^\dagger_{\chi,\sigma} \psi_{\chi,\sigma} \psi^\dagger_{\bar{\chi},\sigma'} \psi_{\bar{\chi},\sigma'} + \\ & + g_{3,\sigma,\sigma'} \psi^\dagger_{\chi,\sigma} \psi_{\bar{\chi},\sigma} \psi^\dagger_{\chi,\sigma'} \psi_{\bar{\chi},\sigma'} + g_{4,\sigma,\sigma'} \psi^\dagger_{\chi,\sigma} \psi_{\chi,\sigma} \psi^\dagger_{\chi,\sigma'} \psi_{\chi,\sigma'}). \end{aligned} \tag{1.87}$$

By applying the bosonisation mapping, the Hamiltonian (1.83) becomes [9, 20]:

$$H = \sum_{\nu=c,s} H_\nu + H_{cs} \tag{1.88}$$

where we have:

$$H_\nu = \frac{1}{2} \int dx [v_\nu K_\nu (\nabla\theta_\nu(x))^2 + \frac{v_\nu}{K_\nu} (\nabla\phi_\nu(x))^2] + \frac{2g_\nu}{(2\pi a)^2} \int dx \cos(\sqrt{8\pi}\phi_\nu(x)) \tag{1.89}$$

and:

$$H_{cs} = \frac{2g_{cs}}{(2\pi a)^2} \int dx \cos(\sqrt{8\pi}\phi_c(x)) \cos(\sqrt{8\pi}\phi_s(x)). \tag{1.90}$$

We can consider that interactions depend only on the relative orientation of spins since the system is not polarized and we can adopt the following notation:

$$g_{i\uparrow\uparrow} = g_{i\downarrow\downarrow} = g_{i\parallel} \quad i = 1, 2, 3, 4 \tag{1.91}$$

$$g_{i\uparrow\downarrow} = g_{i\downarrow\uparrow} = g_{i\perp} \quad i = 1, 2, 3, 4. \tag{1.92}$$

With this notation coefficients in (1.89) and (1.90) [9]:

$$v_\nu K_\nu = v_F \left[1 + \frac{g_{4\parallel} - g_{4\perp} - c_\nu(g_{2\parallel} - g_{1\parallel} - g_{2\perp})}{2\pi v_F}\right] \tag{1.93}$$

$$\frac{v_\nu}{K_\nu} = v_F \left[1 + \frac{g_{4\parallel} + g_{4\perp} - c_\nu(g_{2\parallel} - g_{1\parallel} + g_{2\perp})}{2\pi v_F}\right] \tag{1.94}$$

$$g_c = -g_{3\perp} \quad g_s = g_{1\perp} \quad g_{cs} = -g_{3\parallel}. \tag{1.95}$$

We also have $c_c = +1$ and $c_s = -1$. Equations (1.93) and (1.94) can be solved in order to obtain the velocities v_ν and the Luttinger parameters K_ν. They are [9]:

$$v_\nu = v_F[(1 + y_{-,\nu})(1 + y_{+,\nu})]^{\frac{1}{2}} \simeq v_F \left[1 + \frac{y_{-,\nu}}{2} + \frac{y_{+,\nu}}{2}\right] \tag{1.96}$$

$$K_\nu = \left[\frac{1 + y_{-,\nu}}{1 + y_{+,\nu}}\right]^{\frac{1}{2}} \simeq \left[1 + \frac{y_{-,\nu}}{2} - \frac{y_{+,\nu}}{2}\right] \tag{1.97}$$

$$y_{\pm,\nu} = \frac{g_{4\parallel} \pm g_{4\perp} - c_\nu(g_{2\parallel} - g_{1\parallel} \pm g_{2\perp})}{2\pi v_F}. \tag{1.98}$$

The Hamiltonian (1.90) couples charge and spin degrees of freedom and, as written in [9], it is often negligible using a renormalisation group analysis. So, at first order in the lattice parameter a, the model reduces to two decoupled Hamiltonians where charge and spin degrees of freedom are separated [9, 20]:

$$H_{SG} = \frac{1}{2}\int dx[vK(\nabla\theta(x))^2 + \frac{v}{K}(\nabla\phi(x))^2] + \frac{2g}{(2\pi a)^2}\int dx \cos(\sqrt{8\pi}\phi(x)). \tag{1.99}$$

This Hamiltonian is known as the sine-Gordon Hamiltonian.
The quadratic terms favors the fluctuations of the field ϕ, whereas the cosine term is a massive contribution and it tries to pin the field ϕ in one of its minima.
If we want to know which term wins the competition we have to apply the renormalisation group procedure. The original field can be decomposed into short-wavelenght and long-wavelength, then we integrate over the first to obtain an effective action for the low-energy physical properties of the model.
Renormalisation group equations link the original couplings to the renormalized ones and so it implies that we can get the phase diagram for low energies.
The result of RG procedure in both charge and spin sectors is [9, 30]:

- the system flows to $g = 0$ if $|g| < 2\pi v(K-1)$, it means that g decreases algebraically under renormalisation, i.e. it is irrelevant. In this case the theory is massless $\Delta = 0$;
- the system flows towards strong coupling if $|g| > 2\pi v(K-1)$, it means that g increases algebraically under renormalisation, i.e. it is relevant. In this case the theory is massive $\Delta \neq 0$ with two phases which depend on the sign of g;
- $K = 1$ the cosine term is marginal.

So if $|g| > 2\pi v(K-1)$ the theory is massive ($\Delta \neq 0$) and it means that ϕ is pinned in one of the minima of the cosine term. In this case we have two possibilitie [9, 20]:

- $g > 0$ $\phi = \sqrt{\frac{\pi}{8}}$;
- $g < 0$ $\phi = 0$.

1.3.3 Non-Local Order Parameters in Sine-Gordon model

As said before, the theory is in gapped phase ($\Delta_\nu \neq 0$) if [9, 20]:

- $\phi_\nu = \sqrt{\frac{\pi}{8}}$ and for this value of ϕ $\sin(\sqrt{2\pi}\phi_\nu) = 1$;
- $\phi_\nu = 0$ and for this value of ϕ $\cos(\sqrt{2\pi}\phi_\nu) = 1$.

So these operators $\sin(\sqrt{2\pi}\phi_\nu)$ and $\cos(\sqrt{2\pi}\phi_\nu)$ can be use as detectors to identify the corresponding gapped phases.

They are the continuum version of the parity and Haldane operators previously introduced [9, 20]:

$$O_P^\nu(x) \sim \cos(\sqrt{2\pi}\phi_\nu(x)) \quad O_S^\nu(x) \sim \sin(\sqrt{2\pi}\phi_\nu(x)). \tag{1.100}$$

$$O_S^\nu(x) \sim \sin(\sqrt{2\pi}\phi_\nu(x)). \tag{1.101}$$

Their corresponding correlators act as order parameters in the asymptotic limit [9, 20]:

$$C_P^\nu(R) \sim < \cos(\sqrt{2\pi}\phi_\nu(x)) \cos(\sqrt{2\pi}\phi_\nu(x+R)) >, \tag{1.102}$$

$$C_S^\nu(R) \sim < \sin(\sqrt{2\pi}\phi_\nu(x)) \sin(\sqrt{2\pi}\phi_\nu(x+R)) > . \tag{1.103}$$

We sum up all possibile cases in Table 1.1 [9, 20]. Bosonization enable us to identify all these phases using the pinning values of the filed ϕ, in fact in both charge and spin channels the values $\phi = 0$ and $\phi = \sqrt{\frac{\pi}{8}}$ correspond to parity and Haldane order.

	Δ_c	Δ_s	ϕ_c	ϕ_s	NLOP
LL	0	0	u	u	none
MI	$\neq 0$	0	0	u	C_P^c
LE	0	$\neq 0$	u	0	C_P^s
HI	$\neq 0$	0	$\sqrt{\frac{\pi}{8}}$	u	C_S^c
HLE	0	$\neq 0$	u	$\sqrt{\frac{\pi}{8}}$	C_S^s
CDW	$\neq 0$	$\neq 0$	$\sqrt{\frac{\pi}{8}}$	0	C_S^c,C_P^s
SDW	$\neq 0$	$\neq 0$	0	$\sqrt{\frac{\pi}{8}}$	C_P^c,C_S^s
BOW	$\neq 0$	$\neq 0$	0	0	C_P^c,C_P^s
BSDW	$\neq 0$	$\neq 0$	$\sqrt{\frac{\pi}{8}}$	$\sqrt{\frac{\pi}{8}}$	C_S^c,C_S^s

Table 1.1: Classification of 1D quantum phases with corresponding non-local order parameters NLOP. Letter u is used to identify unpinned fields [9, 20].

There are four fully gapped and four partly gapped phases. We want to underline that:

- partly gapped phases can be detected only by a non-vanishing non-local order parameter;
- fully gapped phases can be detected by two non-vanishing non-local order parameters but it is always possible to find a local order parameter for a fully gapped phase, where charge and spin degrees of freedom are recombined.

A schematic representation of some of these phases is reported in Fig. 1.4 below, taken from [5].

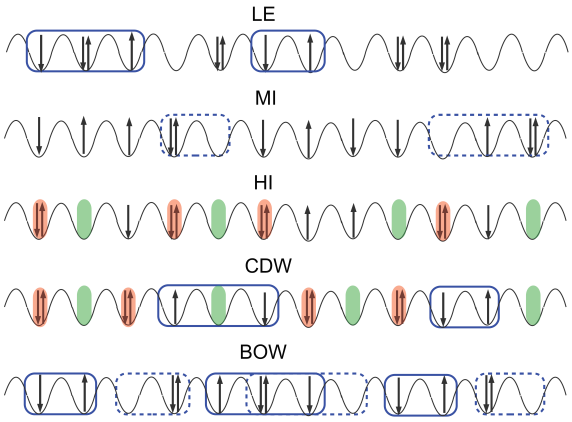

Figure 1.4: Representation taken from reference [5] of LE, MI, HI, CDW, BOW phases. The blue continuos (dashed) lines represent the correlated pairs of up-down spin or holon-doublon such that the mean value of C_P^s and C_P^c are different from zero, whereas green and red circles show the alternation of sites occupied by holons and doublons implying a nonvanishing mean value for C_S^c.

1.3.4 Hubbard model

Origin of the model

The study of characteristics of many materials can begin with a simple case, i.e. a single electron moving in a periodic potential and then we generalize it to $N_{electrons}$ electrons. In reference [3] there is a complete treatment, here we report only a few points.

If we deal with a single electron its band structure equation incorporates two contributions, i.e. the kinetic term and the ionic potential [3]:

$$H_0\phi_{k,s}(x) = (-\frac{\vec{p}^2}{2m} + V_{ion}(x))\phi_{k,s}(x) = \varepsilon_k\phi_{k,s}(x) \tag{1.104}$$

where k and s are its lattice momentum and its spin. $\phi_{k,s}(x)$ represents a Bloch wave function and ε_k is the band energy.
If we deal with $N_{electrons}$ electrons and if the Hamiltonian is a separable sum of single particle Hamiltonians then we have [3]:

$$H_{0,N_{electrons}} = \sum_{i=1}^{N_{electrons}} H_0(\vec{p}_i, x_i) \tag{1.105}$$

and the Schrödinger equation is simply a set of band structure equations as (1.104).
The eigenstates of $H_{0,N_{electrons}}$ are Fock states given by Slater determinants [3]:

$$\psi_{k,s}(x_1, ..., x_{N_{electrons}}) = det_{i,j}[\phi_{k_i,s_i}(x_j)] \tag{1.106}$$

and eigenenergies of $H_{0,N_{electrons}}$ are [3]:

$$E_k = \sum_{i=1}^{N_{electrons}} \varepsilon_{k_i}. \tag{1.107}$$

Of course the Fermi surface in k space is identified by $\max(\varepsilon_k)$=ε_F.
If we want to include Coulomb repulsion between electrons then the total Hamiltonian becomes [3]:

$$H_{total} = H_{0,N_{electrons}} + \frac{1}{2}\sum_{i\neq j} V_{Coulomb}(x_i, x_j). \tag{1.108}$$

$V_{Coulomb}(x_i, x_j)$ implies that H_{total}, unlike $H_{0,N_{electrons}}$, is no longer separable and so H_{total} is more difficult to diagonalize. But a first simplification concerns this possibility: part of the Coulomb interaction can be considered inside the single particle part of H_{total} so that we can replace [3]:

$$H_{0,N_{electrons}} \to \tilde{H}_{0,N_{electrons}} = \sum_{i=1}^{N_{electrons}} (H_0(\vec{p}_i, x_i) + V^{eff}_{Coulomb}(x_i, \rho)). \tag{1.109}$$

- The single particle part is [3]:

$$V^{eff}_{Coulomb}(x_i, \rho). \tag{1.110}$$

  It is a mean field contribution and $\rho(x)$ is the ground state density.
  There are different approximation schemes for $V^{eff}_{Coulomb}(x_i, \rho)$, it usually depends on ρ at x but we do not deepen this point.

- The residual interactions are [3]:

$$V^{residual}_{Coulomb}(x_i, x_j) = V_{Coulomb}(x_i, x_j) - \frac{V^{eff}_{Coulomb}(x_i) + V^{eff}_{Coulomb}(x_j)}{N_{electrons}}. \tag{1.111}$$

  These residual interactions are negligible in many materials, but when we deal with magnetism and superconductivity we can not ignore them.

In order to study this many electron Hilbert space, we can introduce second quantized operators [3].
The field operator $\psi^\dagger_s(x)$ creates a particle localized at x with spin s:

$$< x's'|\psi^\dagger_s(x)|0 >= \delta_{s,s'}\delta(x - x'). \tag{1.112}$$

We can use an orthonormal single particle basis $\{\phi\}$:

$$\psi^\dagger_s(x) = \sum_i \phi^*_i(x) c^\dagger_{is}. \tag{1.113}$$

The local density operator $\hat{\rho}(x)$ gives the possibility of finding a particle of either spin localized at x [3]:

$$\hat{\rho}(x) = \sum_s \psi^\dagger_s(x)\psi_s(x) = \sum_{s,ii'} \phi^*_i(x)\phi_{i'}(x) c^\dagger_{is} c_{i's}. \tag{1.114}$$

The expectation value of $\hat{\rho}(x)$ in coordinate space is [3]:

$$\rho(x) = \sum_i \delta(x - x_i). \tag{1.115}$$

Now we can use these operators to write the single particle and the residual interaction parts of the Hamiltonian [3]:

$$H_{total} = \tilde{H}_{0,N_{electrons}} + V^{residual}_{Coulomb} \tag{1.116}$$

$$\tilde{H}_{0,N_{electrons}} = \sum_s \int d^3x \psi^\dagger_s(x)(H_0 + V^{eff}_{Coulomb}(x))\psi_s(x), \tag{1.117}$$

$$V_{Coulomb}^{residual} = \frac{1}{2}\int d^3x d^3y \tilde{V}(x,y)(\hat{\rho}(x)\hat{\rho}(y) - \delta(x-y)\hat{\rho}(x)) =$$
$$= \frac{1}{2}\int d^3x d^3y \tilde{V}(x,y)\sum_{s,s'}\psi_s^\dagger(x)\psi_{s'}^\dagger(y)\psi_{s'}(y)\psi_s(x). \tag{1.118}$$

These quartic interaction $V_{Coulomb}^{residual}$ represent a truly many-particle problem and it is very difficult to deal with it because its Hilbert space size grows exponentially when the number of electrons and the size of single-particle basis set increase [3].

We can replace H_{total} with an effective Hamiltonian H_{eff} which concerns the lower energies subspace. This procedure is called renormalisation and in a path integral formulation it means that high-frequency modes are integrated out (as said in paragraph 1.3.1). Under renormalisation irrilevant interactions are negligible and they are suppresed. Therefore many of the microscopic details of the real interaction and band structure are not present in the effective Hamiltonian which concerns only the most relevant interactions. One of the minimal models of interacting electrons is the Hubbard model. It was introduced in 1963 for a description of collective phenomena in transition and rare-earth metal [3].

$\tilde{H}_{0,N_{electrons}}$ has band energies and Bloch wave functions given by $\varepsilon_{k,\alpha}$ and $\phi_{k,\alpha}$, where α is the band index. We can obtain a single-particle basis from $\phi_{k,\alpha}$, these states are called Wannier states and they are labelled by two indexes: i the site index and α the band index as before. The Wannier states are [3]:

$$\phi_{i,\alpha}(x) = \frac{1}{\sqrt{N_{sites}}}\sum_k e^{-ikx_i}\phi_{k,\alpha}(x) \tag{1.119}$$

and the Wannier operators [3]:

$$c_{i,s,\alpha}^\dagger \equiv \int d^3x \phi_{i,\alpha}(x)\psi_s^\dagger(x) \tag{1.120}$$

and inverting [3]:

$$\psi_s^\dagger(x) = \sum_{i,\alpha}\phi_{i,\alpha}(x)^* c_{i,s,\alpha}^\dagger. \tag{1.121}$$

The interecting Hamiltonian (1.116) sum of (1.117) and (1.118) can now be written in this way [3]:

$$H = -\sum_{s,ij,\alpha} t_{i,j,\alpha}c_{i,s,\alpha}^\dagger c_{j,s,\alpha} + \sum_{ss',ijkl,\alpha\beta\gamma\delta} U_{i,j,k,l}^{\alpha,\beta,\gamma,\delta}c_{i,s,\alpha}^\dagger c_{j,s',\beta}^\dagger c_{k,s',\gamma}c_{l,s,\delta} \tag{1.122}$$

where:

$$t_{i,j,\alpha} = -<\phi_{i,s,\alpha}|\tilde{H}_{0,N_{electrons}}|\phi_{j,s,\alpha}> \tag{1.123}$$

and:

$$U_{i,j,k,l}^{\alpha,\beta,\gamma,\delta} = \frac{1}{2}\int d^3x d^3y \tilde{V}(x,y)\phi_{i,\alpha}^*(x)\phi_{j,\beta}^*(y)\phi_{k,\gamma}\phi_{l,\delta}. \tag{1.124}$$

The first term $t_{i,j,\alpha}$ is called hopping term while the second term $U_{i,j,k,l}^{\alpha,\beta,\gamma,\delta}$ are interaction parameters.
In absence of an external gauge field $t_{i,j}$ can be choosen to be real and the range and the magnitude of $U_{i,j,k,l}^{\alpha,\beta,\gamma,\delta}$ can be minimized by an optimal choice of Wannier states. It is a consequence of an optimal choice of the mean field potential $V_{Coulomb}^{eff}(x_i,\rho)$ (1.110). When $U_{i,j,k,l}^{\alpha,\beta,\gamma,\delta}$ are small compared to $t_{i,j,\alpha}$ we can consider them equal to zero in a first approximation. Then we deal with them by perturbation theory [3].

In order to simplify our model we pay attention to the some possible approximations [3].

- In the Hubbard model $U_{i,j,k,l}^{\alpha,\beta,\gamma,\delta}$ are not negligible but their range is very small since only intra-atomic contribution are considered, i.e. $U_{i,i,i,i}^{\alpha,\beta,\gamma,\delta}$.

- When the Fermi surface lies within a single conduction band $\alpha = 1$ we can ignore matrix elements that concern other bands if these bands are well separated from the Fermi energy. We call this model one-band Hubbard model.
  This approximation is not always correct, in fact for f-electron metals (rare earth compounds) the interaction parameters $U_{i,j,k,l}^{\alpha,\beta,\gamma,\delta}$ are larger than the interband splittings, as a consequence there are charge fluctuations that link localized f levels with delocalized s and p levels. They are described by Anderson and Kondo Hamiltonians. Anyway, here we suppose that this approximation can be done.

  The Hamiltonian then becomes [3]:

$$H = -\sum_{s,ij} t_{i,j} c_{i,s}^\dagger c_{j,s} + \sum_{ss',i} U c_{i,s}^\dagger c_{i,s'}^\dagger c_{i,s'} c_{i,s} \tag{1.125}$$

  where $U_{i,i,i,i} = U$.

- If tight binding approximation is considered then hopping processes are relevant only between neighboring sites.

- If isotropic hopping is considered then $t_{i,j} = t$.

  The Hamiltonian then becomes [3]:

$$H = -t\sum_{s,<ij>} c_{i,s}^\dagger c_{j,s} + U\sum_i n_{i,\uparrow} n_{i,\downarrow} \tag{1.126}$$

  where $< ij >$ means nearest neighboring sites and $n_{i,s} = c_{i,s}^\dagger c_{i,s}$.

Properties of the model

If we assume periodic boundary condition (PBC) $c_{L+1,s} = c_{1,s}$ and we restric to 1D case then the Hubbard Hamiltonian becomes [4, 9]:

$$H = -t \sum_{j=1}^{L} \sum_{s=\uparrow,\downarrow} (c_{j,s}^{\dagger} c_{j+1,s} + c_{j+1,s}^{\dagger} c_{j,s}) + U \sum_{j=1}^{L} n_{j,\uparrow} n_{j,\downarrow}. \tag{1.127}$$

These fermionic operators satisfy anticommutation rules [9]:

$$\left\{ c_{i,s}, c_{j,s'}^{\dagger} \right\} = \delta_{i,j} \delta_{s,s'}, \tag{1.128}$$

$$[n_{i,s}, c_{i,s}] = -c_{i,s} \quad [n_{i,s}, c_{i,s}^{\dagger}] = c_{i,s}^{\dagger}. \tag{1.129}$$

The hopping term in (1.127) is diagonal in Bloch basis, whereas the interaction term in (1.127) is diagonal in Wannier basis, so they can not be concurrently diagonalized, i.e. they do not commute. As seen before these two basis are related by Fourier transform: Wannier wave functions are localized in real space and Bloch wave functions are localized in the reciprocal space [9].
The model is so characterized by a competition between the two terms: the hopping one tries to delocalized fermions, whereas interaction tries to localized them.
Parameters t and U characterize the behaviour of the system together with the dimension D of the lattice, the temperature T and the filling n [9].

The Hilbert space at each site is given by four states $|0>$, $|\uparrow>$, $|\downarrow>$, $|\uparrow\downarrow>$ so the total Hilbert space for L sites has dimension 4^L. However symmetries of the model can help in order to restrict to a smaller subspace.

The total particle number [9]:

$$\hat{N} = \hat{N}_{\uparrow} + \hat{N}_{\downarrow} = \sum_{j=1}^{L} (n_{j,\uparrow} + n_{j,\downarrow}) \tag{1.130}$$

and the total magnetization [9]:

$$S^{(s),z} = \frac{1}{2}(\hat{N}_{\uparrow} - \hat{N}_{\downarrow}) = \frac{1}{2} \sum_{j=1}^{L} (n_{j,\uparrow} - n_{j,\downarrow}) \tag{1.131}$$

are two important conserved quantities. In fact both $\hat{N}_{\uparrow}$ and $\hat{N}_{\downarrow}$ commute with the Hamiltonian $[\hat{N}_{\uparrow}, H] = 0$ and $[\hat{N}_{\downarrow}, H] = 0$, therefore they are conserved. As an obvious

consequence the total particle number and the total magnetization are conserved too, i.e. $[\hat{N}, H] = 0$ and $[S^{(s),z}, H] = 0$.

We can also introduce the total charge operator [9]:

$$S^{(c),z} = \frac{1}{2}(\hat{N} - L) = \frac{1}{2}\sum_{j=1}^{L}(n_j - 1). \tag{1.132}$$

At half-filling the mean value of the local particle number operator is 1 (a particle at each site) so $n_j - 1$ measures the deviation of the local particle number at site j n_j from the mean value. For this reason $n_j - 1$ coincides with the normal ordered operator $: n_j :$.

As we said, H commutes with $\hat{N}$, so if we add to H a term proportial to $\hat{N}$ this new hamiltonian still commutes with $\hat{N}$, it means that its spectrum does not change. So we can write the Hamiltonian modified as [9]:

$$H = -t\sum_{j=1}^{L}\Sigma_{s=\uparrow,\downarrow}(c^{\dagger}_{j,s}c_{j+1,s} + c^{\dagger}_{j+1,s}c_{j,s}) + U\sum_{j=1}^{L}(n_{j,\uparrow} - \frac{1}{2})(n_{j,\downarrow} - \frac{1}{2}). \tag{1.133}$$

This Hamiltonian has some continuos symmetries [9]:

- U(1) symmetry linked to the conservation of $S^{(s),z}$ and $S^{(c),z}$;
- SU(2) symmetry because H commutes with $S^{(s),z}$, $S^{(s),y}$, $S^{(s),x}$ and they are a representation of the Lie algrabra su(2) that generates the group SU(2). This is the group of rotations in spin space and the Hamiltonian is so completely rotation invariant;
- H does not commute with the local spin components $S^{(s),z}_j$, $S^{(s),y}_j$, $S^{(s),x}_j$;
- an other SU(2) symmetry because H commutes with $S^{(c),z}$, $S^{(c),y}$, $S^{(c),x}$ but only when L is even.

We can write both $S^{(c),\alpha}$ and $S^{(s),\alpha}$ in terms of fermionic creation and annihilation operators:

$$S^{(c),\alpha} = \frac{1}{2}\sum_{j=1}^{L}(c^{\dagger}_{j,\uparrow} \quad (-)^j c_{j,\downarrow}) \begin{pmatrix} (\sigma^{\alpha})_{\uparrow\uparrow} & (\sigma^{\alpha})_{\uparrow\downarrow} \\ (\sigma^{\alpha})_{\downarrow\uparrow} & (\sigma^{\alpha})_{\downarrow\downarrow} \end{pmatrix} \begin{pmatrix} c_{j,\uparrow} \\ (-)^j c^{\dagger}_{j,\downarrow} \end{pmatrix} \tag{1.134}$$

and

$$S^{(s),\alpha} = \frac{1}{2}\sum_{j=1}^{L}(c^{\dagger}_{j,\uparrow} \quad c^{\dagger}_{j,\downarrow}) \begin{pmatrix} (\sigma^{\alpha})_{\uparrow\uparrow} & (\sigma^{\alpha})_{\uparrow\downarrow} \\ (\sigma^{\alpha})_{\downarrow\uparrow} & (\sigma^{\alpha})_{\downarrow\downarrow} \end{pmatrix} \begin{pmatrix} c_{j,\uparrow} \\ c_{j,\downarrow} \end{pmatrix} \tag{1.135}$$

where $\alpha = x, y, z$.
Charge operators (1.134) can be obtained from spin operators (1.135) by this transformation: $c_{j,\uparrow} \to c_{j,\uparrow} \quad c_{j,\downarrow} \to (-)^j c^{\dagger}_{j,\downarrow}$. This transformation also maps the repulsive U

regime into the attractive U regime. It means $H(t,U) \to H(t,-U)$.

The Hamiltonian (1.133) has also some discrete simmetries [9]:

- translation invariance if there are PBC $c_{j,s} \to c_{j+r,s}$;
- reflection symmetry $c_{j,s} \to c_{-j+L+1,s}$;
- the symmetry $c_{j,\uparrow} \to c_{j,\uparrow} \quad c_{j,\downarrow} \to (-)^j c^\dagger_{j,\downarrow}$;
- spin-flip symmetry;
- time-reversal symmetry $c_{j,\sigma} \to s c_{j,\bar{\sigma}}$ where s is a plus sign if it is up and a minus sign if it is down.

Bosonization of the model

The Hubbard model can be enriched by the addition of a nearest-neighbor interaction. In this case the Hamiltonian becomes [4, 9]:

$$H = -t \sum_{j=1}^{L} \sum_{\sigma=\uparrow,\downarrow} (c^\dagger_{j,\sigma} c_{j+1,\sigma} + c^\dagger_{j+1,\sigma} c_{j,\sigma}) + U \sum_{j=1}^{L} n_{j,\uparrow} n_{j,\downarrow} + V \sum_{j=1}^{L} n_j n_{j+1}. \tag{1.136}$$

It is known as extended Hubbard model. It is characterized by the same symmetries described in the previous paragraph, except for $SU(2)$ symmetry due to $S^{(c),z}$, $S^{(c),y}$, $S^{(c),x}$ which here is reduced to $U(1)$.

This model has a rich phase diagram which is a consequence of the competition between V and U interactions. In fact depending on different values of the Hamiltonian parameters, charge or spin gap opens [4, 9]:

$$\Delta_c = \frac{E(N = L+2, S^{(s),z} = 0) + E(N = L-2, S^{(s),z} = 0) - 2E(N = L, S^{(s),z} = 0)}{2} \tag{1.137}$$

$$\Delta_s = E(N = L, S^{(s),z} = 1) - E(N = L, S^{(s),z} = 0). \tag{1.138}$$

We can apply the bosonization technique to (1.136) and in the weak coupling limit this model is mapped into two decoupled sine-Gordon models, which concern separately charge ($\nu = c$) and spin ($\nu = s$) degrees of freedom [4, 9]:

$$H = H_c + H_s \tag{1.139}$$

$$H_\nu = \frac{1}{2}\int dx[v_\nu K_\nu(\nabla\theta_\nu(x))^2 + \frac{v_\nu}{K_\nu}(\nabla\phi_\nu(x))^2] + \frac{2g_\nu}{(2\pi a)^2}\int dx\cos(\sqrt{8\pi}\phi_\nu(x)). \quad (1.140)$$

Of course g_ν,v_ν and K_ν are functions of the parameters of the extended Hubbard model t,U and V [4, 9]:

$$g_\nu = -ac_\nu(U-2V) \quad (1.141)$$

$$v_\nu K_\nu = 2ta \quad (1.142)$$

$$\frac{v_c}{K_c} = 2ta\left[1 + \frac{1}{2t\pi}(U+6V)\right] \quad (1.143)$$

$$\frac{v_s}{K_s} = 2ta\left[1 - \frac{1}{2t\pi}(U-2V)\right]. \quad (1.144)$$

We know from the introduction of pargraph 1.3 that gapped phases ($\Delta_\nu \neq 0$) are classifiable by the pinning values of the field ϕ_ν i.e. 0 or $\sqrt{\frac{\pi}{8}}$. In this model due to SU(2) symmetry for spin channel the value $\phi_s = \sqrt{\frac{\pi}{8}}$ is not allowed and we have six different phases overall [4, 9].
Here we report only some steps from reference [4, 9, 10] useful to bosonize (1.136).

Focus on hopping term

The hopping term in (1.136) is $: Q_{j,j+1,\sigma} :=: c^\dagger_{j,\sigma}c_{j+1,\sigma} + h.c. :$ where normal ordering is considered. We replace lattice operator $c^\dagger_{j,\sigma}$ and its hermitian conjugate with fields $\psi_{R,\sigma}(x)$, $\psi^\dagger_{R,\sigma}(x)$, $\psi_{L,\sigma}(x)$ and $\psi^\dagger_{L,\sigma}(x)$ defined on a continuum, using (1.29). These fields $\psi_{R,\sigma}(x)$, $\psi^\dagger_{R,\sigma}(x)$, $\psi_{L,\sigma}(x)$ and $\psi^\dagger_{L,\sigma}(x)$ are given in (1.63). Therefore the hopping term becomes [4, 9, 10]:

$$\begin{aligned} &: Q_{j,j+1,\sigma} :=: c^\dagger_{j,\sigma}c_{j+1,\sigma} + h.c. := \\ &= a : \left[(-i)^j\psi^\dagger_{R,\sigma}(x) + (i)^j\psi^\dagger_{L,\sigma}(x)\right]\left[(i)^{j+1}\psi_{R,\sigma}(x+a) + (-i)^{j+1}\psi_{L,\sigma}(x+a)\right] := \\ &= ai\left[:\psi^\dagger_{R,\sigma}(x)\psi_{R,\sigma}(x+a): - :\psi^\dagger_{L,\sigma}(x)\psi_{L,\sigma}(x+a):\right] + h.c. + \\ &-ai(-1)^j\left[\psi^\dagger_{R,\sigma}(x)\psi_{L,\sigma}(x+a) - \psi^\dagger_{L,\sigma}(x)\psi_{R,\sigma}(x+a)\right] + h.c. \end{aligned} \quad (1.145)$$

Now we can develop the first line of expression (1.145) remembering (1.62), (1.63), (1.75), (1.76), (1.77), (1.78) and (1.80). Furthermore, we can use these properties [4, 9, 10]:

- $\phi_\sigma(x+a) - \phi_\sigma(x) = a\nabla\phi_\sigma(x)$;
- $\theta_\sigma(x+a) - \theta_\sigma(x) = a\nabla\theta_\sigma(x)$;
- a first order Taylor expansion for exponentials and the fact that α is equal to a.

We achieve for $:\psi^{\dagger}_{R,\sigma}(x)\psi_{R,\sigma}(x+a):$ the following result [4, 9, 10]:

$$:\psi^{\dagger}_{R,\sigma}(x)\psi_{R,\sigma}(x+a):=\frac{\eta^{\dagger}_{R,\sigma}\eta_{R,\sigma}}{2\pi\alpha}e^{-i\sqrt{\pi}[\phi_{\sigma}(x)+\theta_{\sigma}(x)]}e^{i\sqrt{\pi}[\phi_{\sigma}(x+a)+\theta_{\sigma}(x+a)]}-<...>=$$

$$=\frac{1}{2\pi\alpha}e^{i\sqrt{\pi}((\phi_{\sigma}(x+a)-\phi_{\sigma}(x))+(\theta_{\sigma}(x+a)-\theta_{\sigma}(x)))}e^{\frac{\pi}{2}[\phi_{\sigma}(x)+\theta_{\sigma}(x),\phi_{\sigma}(x+a)+\theta_{\sigma}(x+a)]}-<...>=$$

$$=\frac{1}{2\pi\alpha}e^{i\sqrt{\pi}((\phi_{\sigma}(x+a)-\phi_{\sigma}(x))+(\theta_{\sigma}(x+a)-\theta_{\sigma}(x)))}e^{\frac{\pi}{2}(-i)}-<...>=$$

$$=\frac{-i}{2\pi\alpha}[1+i\sqrt{\pi}a\nabla\phi_{\sigma}(x)+i\sqrt{\pi}a\nabla\theta_{\sigma}(x)]-<...>=$$

$$=\frac{1}{2\sqrt{\pi}}[\nabla\phi_{\sigma}(x)+\nabla\theta_{\sigma}(x)]=\rho_{R,\sigma}(x). \tag{1.146}$$

Since steps in the computation of $:\psi^{\dagger}_{L,\sigma}(x)\psi_{L,\sigma}(x+a):$ are the same, we report only the final expression for it [4, 9, 10]:

$$:\psi^{\dagger}_{L,\sigma}(x)\psi_{L,\sigma}(x+a):=\frac{1}{2\sqrt{\pi}}[\nabla\phi_{\sigma}(x)-\nabla\theta_{\sigma}(x)]=\rho_{L,\sigma}(x). \tag{1.147}$$

So combining (1.146) and (1.147) we can compute their difference which is substantially the first line of (1.145) and it is [4, 9, 10]:

$$:\psi^{\dagger}_{R,\sigma}(x)\psi_{R,\sigma}(x+a):-:\psi^{\dagger}_{L,\sigma}(x)\psi_{L,\sigma}(x+a):=\rho_{R,\sigma}(x)-\rho_{L,\sigma}(x)=\frac{1}{\sqrt{\pi}}\nabla\theta_{\sigma}(x). \tag{1.148}$$

Now we can compute the oscillating part of expression (1.145) which is given by terms $\psi^{\dagger}_{R,\sigma}(x)\psi_{L,\sigma}(x+a)$ and $\psi^{\dagger}_{L,\sigma}(x)\psi_{R,\sigma}(x+a)$. We replace these operators with (1.63) and we proceed with straightforward calculations [4, 9, 10]:

$$\psi^{\dagger}_{R,\sigma}(x)\psi_{L,\sigma}(x+a)=\frac{\eta^{\dagger}_{R,\sigma}\eta_{L,\sigma}}{2\pi\alpha}e^{-i\sqrt{\pi}(\phi_{\sigma}(x)+\theta_{\sigma}(x))}e^{i\sqrt{\pi}(-\phi_{\sigma}(x+a)+\theta_{\sigma}(x+a))}=$$

$$=\frac{-i}{2\pi\alpha}e^{-i\sqrt{\pi}(\phi_{\sigma}(x)+\phi_{\sigma}(x+a))}e^{+i\sqrt{\pi}(-\theta_{\sigma}(x)+\theta_{\sigma}(x+a))}e^{\frac{\pi}{2}[\phi_{\sigma}(x)+\theta_{\sigma}(x),-\phi_{\sigma}(x+a)+\theta_{\sigma}(x+a)]}=$$

$$=\frac{-i}{2\pi\alpha}e^{-i2\sqrt{\pi}\phi_{\sigma}(x)}=$$

$$=\frac{1}{\pi\alpha}\frac{e^{-i2\sqrt{\pi}\phi_{\sigma}(x)}}{2i} \tag{1.149}$$

and we also obtain [4, 9, 10]:

$$\psi^{\dagger}_{L,\sigma}(x)\psi_{R,\sigma}(x+a)=-\frac{1}{\pi\alpha}\frac{e^{i2\sqrt{\pi}\phi_{\sigma}(x)}}{2i}. \tag{1.150}$$

So the previous expressions (1.149) and (1.150) give the oscillating part of (1.145) which is as follows [4, 9, 10]:

$$\psi^{\dagger}_{R,\sigma}(x)\psi_{L,\sigma}(x+a) - \psi^{\dagger}_{L,\sigma}(x)\psi_{R,\sigma}(x+a) = \frac{1}{\pi\alpha i}\cos(2\sqrt{\pi}\phi_{\sigma}(x)). \tag{1.151}$$

If we also compute in this way h.c. terms in (1.145) and we sum all contributions then we achieve [4, 9, 10]:

$$: Q_{j,j+1,\sigma} := -\frac{2}{\pi}(-1)^{j}\cos(2\sqrt{\pi}\phi_{\sigma}(x)) - a^{2}[(\nabla\phi_{\sigma}(x))^{2} + (\nabla\theta_{\sigma}(x))^{2}]. \tag{1.152}$$

We also remember that normal order implies this relation [4, 9, 10]:

$$Q_{j,j+1,\sigma} =: Q_{j,j+1,\sigma} : + < Q_{j,j+1,\sigma} >=: Q_{j,j+1,\sigma} : + \frac{2}{\pi}. \tag{1.153}$$

Focus on U and V interactions

Now we want to compute U and V contribution. In order to obtain these terms, firstly we focus on the computation of $n_{j,\sigma} =: c^{\dagger}_{j,\sigma}c_{j,\sigma} :=$, which can be expressed using (1.29) as follows [4, 9, 10]:

$$= a : \left[(-i)^{j}\psi^{\dagger}_{R,\sigma}(x) + (+i)^{j}\psi^{\dagger}_{L,\sigma}(x)\right]\left[(+i)^{j}\psi_{R,\sigma}(x) + (-i)^{j}\psi_{L,\sigma}(x)\right] :=$$

$$= a\left[: \psi^{\dagger}_{R,\sigma}(x)\psi_{R,\sigma}(x) : + : \psi^{\dagger}_{L,\sigma}(x)\psi_{L,\sigma}(x) : +(-)^{j}\left(\psi^{\dagger}_{R,\sigma}(x)\psi_{L,\sigma}(x) + \psi^{\dagger}_{L,\sigma}(x)\psi_{R,\sigma}(x)\right)\right] =$$

$$= a\left[\rho_{R,\sigma}(x) + \rho_{L,\sigma}(x) + (-)^{j}\left(\psi^{\dagger}_{R,\sigma}(x)\psi_{L,\sigma}(x) + \psi^{\dagger}_{L,\sigma}(x)\psi_{R,\sigma}(x)\right)\right]. \tag{1.154}$$

Therefore we are interested to know $\psi^{\dagger}_{R,\sigma}(x)\psi_{L,\sigma}(x)+\psi^{\dagger}_{L,\sigma}(x)\psi_{R,\sigma}(x)$. We always consider (1.63) and we compute $\psi^{\dagger}_{R,\sigma}(x)\psi_{L,\sigma}(x) + \psi^{\dagger}_{L,\sigma}(x)\psi_{R,\sigma}(x)$ in the following way [4, 9, 10]:

$$\psi^{\dagger}_{R,\sigma}(x)\psi_{L,\sigma}(x) = \frac{\eta^{\dagger}_{R,\sigma}\eta_{L,\sigma}}{2\pi\alpha}e^{-i\sqrt{\pi}(\phi_{\sigma}(x)+\theta_{\sigma}(x))}e^{+i\sqrt{\pi}(-\phi_{\sigma}(x)+\theta_{\sigma}(x))} = \frac{-i}{2\sqrt{\pi}\alpha}e^{-i2\sqrt{\pi}\phi_{\sigma}(x)} \tag{1.155}$$

$$\psi^{\dagger}_{L,\sigma}(x)\psi_{R,\sigma}(x) = \frac{i}{2\sqrt{\pi}\alpha}e^{i2\sqrt{\pi}\phi_{\sigma}(x)} \tag{1.156}$$

So we can calculate their sum $\psi^{\dagger}_{R,\sigma}(x)\psi_{L,\sigma}(x) + \psi^{\dagger}_{L,\sigma}(x)\psi_{R,\sigma}(x)$:

$$\psi^{\dagger}_{R,\sigma}(x)\psi_{L,\sigma}(x) + \psi^{\dagger}_{L,\sigma}(x)\psi_{R,\sigma}(x) = -\frac{1}{\pi\alpha}\sin(2\sqrt{\pi}\phi_{\sigma}(x)). \tag{1.157}$$

Therefore (1.154) becomes [4, 9, 10]:

$$: n_{j,\sigma} := a\left[\frac{1}{\sqrt{\pi}}\nabla\phi_\sigma(x) - \frac{(-1)^j}{\pi\alpha}\sin(2\sqrt{\pi}\phi_\sigma(x))\right]. \tag{1.158}$$

We also remember that, as before, normal ordering implies this relation [4, 9, 10]:

$$n_{j,\sigma} =: n_{j,\sigma} : +\frac{1}{2}. \tag{1.159}$$

For all the previous calculations we can rewrite **V interaction** as follows [4, 9, 10]:

$$: n_{j,\sigma} :: n_{j+1,\sigma} := a^2\left[\frac{1}{\pi}\nabla\phi_\sigma(x)\nabla\phi_\sigma(x+a) - \frac{1}{(\pi\alpha)^2}\sin(2\sqrt{\pi}\phi_\sigma(x))\sin(2\sqrt{\pi}\phi_\sigma(x+a))\right] +$$

$$+a^2\left[\frac{(-1)^j}{\pi\sqrt{\pi}\alpha}\Big(\nabla\phi_\sigma(x)\sin(2\sqrt{\pi}\phi_\sigma(x+a)) - \sin(2\sqrt{\pi}\phi_\sigma(x))\nabla\phi_\sigma(x+a)\Big)\right]. \tag{1.160}$$

In order to simplify (1.160) we can use these three approximations [4, 9, 10]:

$$\nabla\phi_\sigma(x)\nabla\phi_\sigma(x+a) = (\nabla\phi_\sigma(x))^2 \tag{1.161}$$

$$\sin(2\sqrt{\pi}\phi_\sigma(x))\sin(2\sqrt{\pi}\phi_\sigma(x+a)) = \frac{1}{2} - \frac{1}{2}\cos(4\sqrt{\pi}\phi_\sigma(x)) - \pi\alpha^2(\nabla\phi_\sigma(x))^2 \tag{1.162}$$

$$\nabla\phi_\sigma(x)\sin(2\sqrt{\pi}\phi_\sigma(x+a)) - \sin(2\sqrt{\pi}\phi_\sigma(x))\nabla\phi_\sigma(x+a) = \frac{2}{\sqrt{\pi}a}\cos(2\sqrt{\pi}\phi_\sigma(x)) \tag{1.163}$$

Therefore if we replace (1.161), (1.162) and (1.163) in (1.160) we achieve the final result for V interaction [4, 9, 10]:

$$: n_{j,\sigma} :: n_{j+1,\sigma} := a^2\frac{2}{\pi}(\nabla\phi_\sigma(x))^2 - \frac{1}{2\pi^2} + \frac{1}{2\pi^2}\cos(4\sqrt{\pi}\phi_\sigma(x)) + (-)^j\frac{2}{\pi^2}\cos(2\sqrt{\pi}\phi_\sigma(x)). \tag{1.164}$$

Since we know $: n_{j,\sigma} :$ from (1.158) then we also compute **U interaction**, which concerns the following term [4, 9, 10]:

$$: n_{j,\uparrow} :: n_{j,\downarrow} := a^2\left[\frac{1}{\pi}\nabla\phi_\uparrow(x)\nabla\phi_\downarrow(x) + \frac{1}{\pi^2\alpha^2}\sin(2\sqrt{\pi}\phi_\uparrow(x))\sin(2\sqrt{\pi}\phi_\downarrow(x)) + ...\right]. \tag{1.165}$$

We also remember that in the continuum limit sums become integrals: $\sum_j \to \frac{1}{a}\int dx$. Now we have all tools to bosonize Hamiltonian (1.136) and charge-spin separation will emerge.

We can consider the hopping term, as an example to know how to apply bosonization technique. If we neglect the oscillating part of (1.152) which gives a vanishing result after integration and we remember (1.64), then we achieve [4, 9, 10]:

$$-t\sum_j\sum_\sigma : Q_{j,j+1,\sigma} :=$$

$$= -t\frac{1}{a}\int dx \sum_\sigma \left[-a^2\left((\nabla\phi_\sigma(x))^2 + (\nabla\theta_\sigma(x))^2\right)\right] =$$

$$= ta\int dx \sum_\sigma [(\nabla\phi_\sigma(x))^2 + (\nabla\theta_\sigma(x))^2] =$$

$$= ta\int dx \left[(\nabla\phi_\uparrow(x))^2 + (\nabla\theta_\uparrow(x))^2 + (\nabla\phi_\downarrow(x))^2 + (\nabla\theta_\downarrow(x))^2\right] =$$

$$= ta\int dx \left[(\nabla\phi_c(x))^2 + (\nabla\theta_c(x))^2 + (\nabla\phi_s(x))^2 + (\nabla\theta_s(x))^2\right]. \tag{1.166}$$

In the same way it is straightforward to compute the contributions due to (1.164) and (1.165) and to achieve Hamiltonian (1.139) and (1.140), but details of these calculations are present in [4, 9, 10].

1.3.5 Non-Local Order Parameters in Hubbard model

We remember that parity and Haldane string non-local oreder operators are [4, 9]:

$$O_P^{(\nu)}(j) = \prod_{k=0}^{j-1} e^{i2\pi S_k^{(\nu),z}} \tag{1.167}$$

$$O_S^{(\nu)}(j) = (\prod_{k=0}^{j-1} e^{i2\pi S_k^{(\nu),z}}) 2S_j^{(\nu),z} \tag{1.168}$$

where $S_k^{(c),z} = \frac{n_k - 1}{2}$ and $S_k^{(s),z} = \frac{n_{k,\uparrow} - n_{klate,\downarrow}}{2}$.

The theory is in gapped phase ($\Delta_\nu \neq 0$) if [4, 9]:

- $\phi_c = \sqrt{\frac{\pi}{8}}$ (only charge channel) and for this value of ϕ $\sin(\sqrt{2\pi}\phi_c) = 1$;
- $\phi_\nu = 0$ and for this value of ϕ $\cos(\sqrt{2\pi}\phi_\nu) = 1$.

Therefore we already know that operators $\sin(\sqrt{2\pi}\phi_c)$ and $\cos(\sqrt{2\pi}\phi_\nu)$ can be use as detectors to classify fully gapped and partly gapped phases.

They are the continuum version [4, 9] of the parity and Haldane operators (1.167) and (1.168):

$$O_P^\nu(x) \sim \cos(\sqrt{2\pi}\phi_\nu(x)) \tag{1.169}$$

$$O_S^c(x) \sim \sin(\sqrt{2\pi}\phi_c(x)). \tag{1.170}$$

We have already said that their corresponding correlators act as order parameters in the asymptotic limit, because they stay finite in the presence of a specific gapped phase in ν channel. Correlators are [4, 9]:

$$C_P^\nu(R) \sim < \cos(\sqrt{2\pi}\phi_\nu(x)) \cos(\sqrt{2\pi}\phi_\nu(x+R)) >, \tag{1.171}$$

$$C_S^c(R) \sim < \sin(\sqrt{2\pi}\phi_c(x)) \sin(\sqrt{2\pi}\phi_c(x+R)) > . \tag{1.172}$$

Phases of extended Hubbard model are summarized in Table 1.2 and they are represented Fig. 1.5 and Fig. 1.6 from reference [4, 9].

	Δ_c	Δ_s	NLOP
LL	0	0	none
MI	$\neq 0$	0	C_P^c
LE	0	$\neq 0$	C_P^s
PS	0	$\neq 0$	C_P^s
CDW	$\neq 0$	$\neq 0$	C_S^c,C_P^s
BOW	$\neq 0$	$\neq 0$	C_P^c,C_P^s

Table 1.2: Classification, from references [4, 9], of 1D quantum phases with corresponding non-local order parameters NLOP for extended Hubbard model.

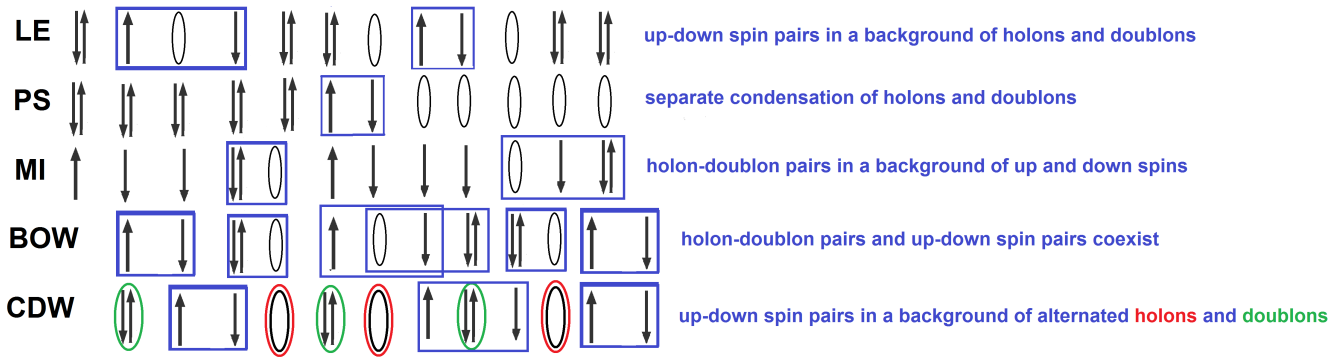

Figure 1.5: Schematic representation of the phases of the extended Hubbard model. This picture is taken from references [4, 9].

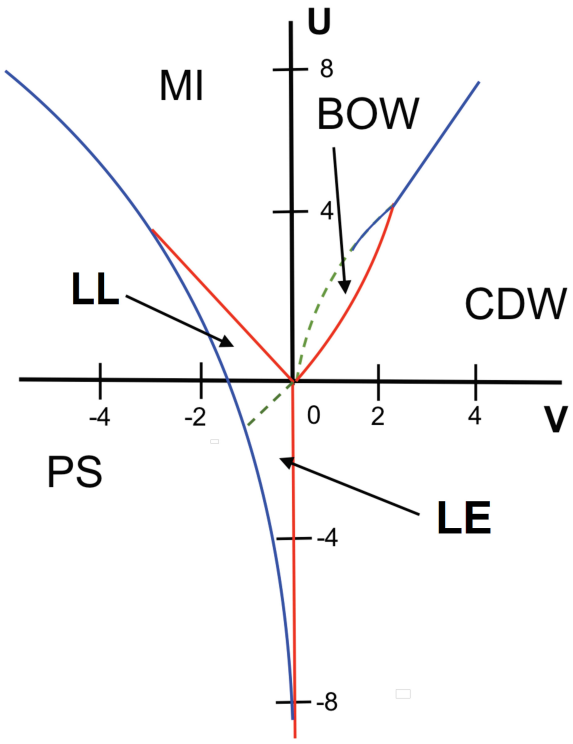

Figure 1.6: Phases and phase transitions of the extended Hubbard model, from references [4, 9]. The picture represents KT transitions with dashed green lines, first order transitions with blue lines and continuos Gaussian transitions with red lines.

Case $U > 0$ and $V > 0$

- In strong repulsive nearest-neighbor interaction ($V > 0$) we have an alternation of holons and doublons. It is known as CDW (charge density wave) and it is a fully gapped phase.
  When V is reduced this phase continues to exist but it is affected by fluctuations, which are the presence of pairs of singly occupied sites.
- In the strong repulsive on-site interaction ($U > 0$) we have the presence of one particle per site. It is known as MI (Mott insulator) and it is a charge gapped phase.
  When U is reduced this phase continues to exist but it is affected by fluctuations, which are the presence of pairs of holons and doublons.
- Between CDW and MI and at intermediate couplings, we have the BOW (bond ordered wave) phase where holon/doublon and up/down spin pairs localized on bonds are both present.

Case $U < 0$ and $V > 0$

- There is the CDW phase.

Case $V < 0$

- Mott insulator is still present for $U > 0$.
  The background is characterized by singly occupied sites and fluctuations are holon/doublon pairs, as said before.
- The PS phase at strong attractive $V < 0$ produces a separate condensation of holons and doublons with a non-zero spin gap.
- The spin gap remains finite at the transition with LE (Luther Emery) region.
  The background is characterized by holons and doublons and fluctuations are up/down spin pairs.
- The gap vanishes in LL (Luttinger Liquid) region. There is not a long range order.

Phase transistions are listed below.

- PS-LE first order transition: it is characterized by a sudden jump of $C_P^{(s)}$ as it is confirmed by DMRG analysis in reference [4, 9]. Fig. 1.7 is taken from that reference and it shows the behaviour of the non-local order parameter $C_P^{(s)}$.

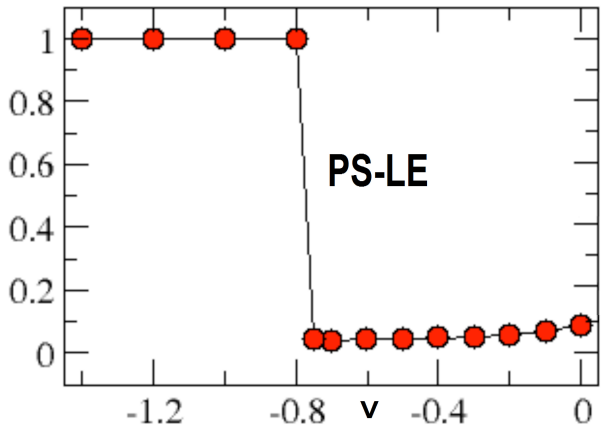

Figure 1.7: Behaviour of $C_P^{(s)}$ in PS-LE transition. This picture is taken from the DMRG analysis in reference [4, 9].

- PS-LL first order transition.

- LE-LL KT transition: it is characterized by a slow increase of $C_P^{(s)}$ from zero to non-zero values as it is confirmed by DMRG analysis in reference [4, 9]. LE phase has a finite spin gap while LL phase has a zero spin gap, so at the same time the gap opens exponentially. Fig. 1.8 from reference [4, 9] represents the behaviour of the non-local order parameter $C_P^{(s)}$.

- PS-MI first order transition.

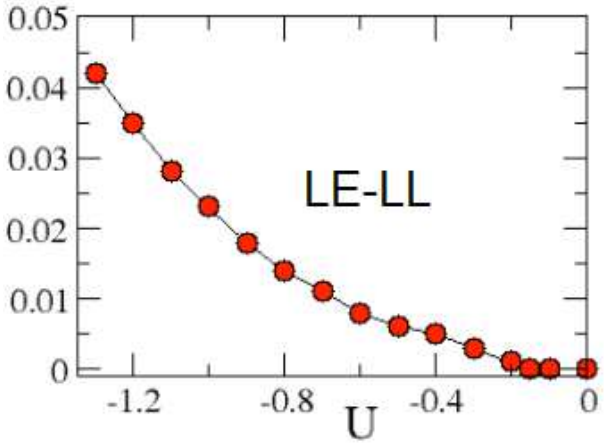

Figure 1.8: Behaviour of $C_P^{(s)}$ in LE-LL transition. This picture is taken from the DMRG analysis in reference [4, 9].

- LL-MI continuos Gaussian transition: the behavior of the non-local order parameter $C_P^{(c)}$ is represented in Fig. 1.9 and it is always achieved by a DMRG analysis in reference [4, 9].

- LE-CDW continuos Gaussian transition.

- MI-CDW first order transition.

- MI-BOW KT transition and first order transition depending on the strength of U with respect to V.

- BOW-CDW continuos Gaussian transition.

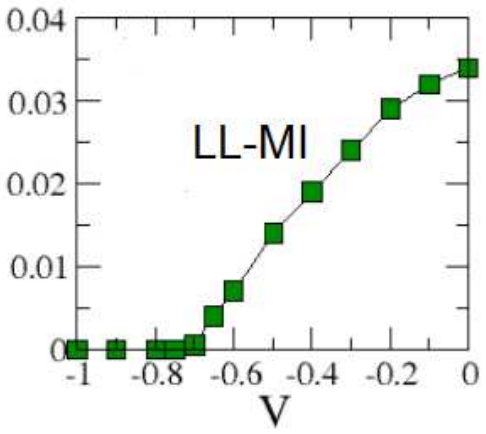

Figure 1.9: Behaviour of $C_P^{(c)}$ in LL-MI transition. This picture is taken from the DMRG analysis in reference [4, 9].

We have represented only same cases (one for each kind of transition) but DMRG analysis confirms the behaviour supposed for all C_A^ν parameters ($A = P, S$ and $\nu = c, s$), in order to have these kind of transitions. See reference [4, 9] for a detailed description of how DMRG analysis has been done.

1.3.6 Conclusion on non-local order parameters

Both non local order parameters and topological phases can not be described by Landau SB theory. This is not a simple coincidence but there is a connection between these two topics. In fact it is possible to find a one-to-one correspondence between phases idenfied by non-local order parameters in the context of bonosization and those obtained from group cohomology theory [20].

1.4 Edge States and Bulk Winding Number

According to band theory, an insulator is characterized by well separated completely filled bands and completely empty bands and a conductor is characterized by partially filled bands which allow electrons conduction across the bulk. However this description is not complete because there exist insulators which have conducting edge states [2]. In this paragraph we try to explain why these edge states are connected to the bulk winding number and why they are both non trivial topological properties. Therefore we try to understand some elements which can characterize a massive phase which is topologically non trivial.
In order to introduce these topological properties, we use the SSH model [2] as a guide example. The SSH model describes spinless fermions hopping on a chain with staggered hopping amplitudes ν and μ. To represent this model we use Fig. 1.10 based on [2]. Since we have staggered hopping amplitudes we can consider sites as if they belonged to two sublattices A and B and we can consider a unit cell as if it were composed of one site of A and the site of B next to it.

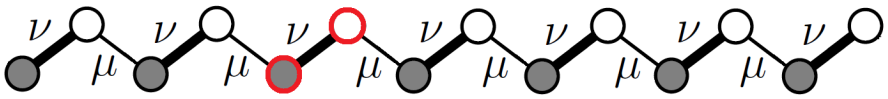

Figure 1.10: Representation of the ssh model. White sites belong to sublattice B and grey sites belong to sublattice A. We have also drawn an example of unit cell using red circles, therefore ν is the intracell hopping and μ is the intercell hopping. This picture is based on [2].

1.4.1 SSH model: topological invariants

The chain of the SSH model has a bulk and a boundary. The bulk constitutes the long central part of the chain while boundaries are the two ends or edges of the chain [2].

Firstly we focus on the bulk and, using periodic boundary conditions for simplicity, the Hamiltonian of it can be written in this way [2]:

$$H_{bulk} = \sum_{m=1}^{N} (\nu|m, B><m, A| + \mu|(m \, mod \, N) + 1, A><m, B|) + h.c. \qquad (1.173)$$

By performing a Fourier transformation, we can also write the bulk Hamiltonian in momentum space as [2]:

$$H_{bulk}(k) = \begin{pmatrix} 0 & \nu + e^{-ik}\mu \\ \nu + e^{ik}\mu & 0 \end{pmatrix}. \tag{1.174}$$

Then it can be shown that eigenvalues are [2]:

$$E(k) = \mid \nu + e^{\pm ik}\mu \mid = \pm\sqrt{\nu^2 + \mu^2 + 2\nu\mu\cos(k)}. \tag{1.175}$$

Furthermore, as long as $\nu \neq \mu$, the bulk is characterized by an energy gap of 2Δ between the lower filled band and the upper empty band (here, we consider the case with filling 1, i.e. one fermion per site). Therefore, as long as $\nu \neq \mu$, the bulk is an insulator. From [2] this gap is:

$$\Delta = \min_k E(k) = \mid \nu - \mu \mid . \tag{1.176}$$

The bulk Hamiltonian in momentum space, i.e. (1.174), can also be written as follows [2]:

$$H_{bulk}(k) = d_x(k)\sigma_x + d_y(k)\sigma_y + d_z(k)\sigma_z \tag{1.177}$$

where $d_x(k) = \nu + \mu\cos(k)$ and $d_y(k) = \mu\sin(k)$ and $d_z(k) = 0$. As the wavenumber changes in the Brioullin zone ($k = 0 \to 2\pi$), the endpoint of the vector $\mathbf{d}(k)$ traces out a closed path of radius μ on the d_x, d_y plane centred in (ν,0). For more general two-dimensional insulators this path is not necessarily a circle but it is always a closed loop. It always avoids the origin because if this were not the case then from (1.176) the bulk gap would close and the bulk would not be an insulator. The topology of this loop is characterized by an integer known as the bulk winding number which counts the number of times the loop winds around the origin of the d_x, d_y plane [2].
The winding number can be computed graphically by counting the number of times $\mathbf{d}(k)$ intersects a curve $\mathcal{L}$ that goes from the origin of the d_x, d_y plane to infinity. Since $\mathbf{d}(k)$ has a left side and a right side, we consider a +1 for each intersection of $\mathcal{L}$ with $\mathbf{d}(k)$ from the left side of $\mathbf{d}(k)$ and we consider a -1 for each intersection of $\mathcal{L}$ with $\mathbf{d}(k)$ from the right side of $\mathbf{d}(k)$. The winding number is a topological invariant: in fact under continuos deformations of $\mathcal{L}$ and $\mathbf{d}(k)$ intersections between them can move but the winding number does not change. Intersections between $\mathcal{L}$ and $\mathbf{d}(k)$ can also appear or disappear but they always appear or disappear pairwise. For the SSH model the winding number is 0 when the phase is trivial and it is 1 when the phase is topological [2]. Below we focus on these two situations.

Now we try to describe some properties of the edge states. We consider the fully dimerized limit which means two possible cases [2]:

- trivial case when $\nu = 1$ and $\mu = 0$;

- topological case when $\nu = 0$ and $\mu = 1$.

In the trivial case dimers are the unit cells described before, while in the topological case dimers are shared between two neighboring unit cells and there is one isolated site per edge. These two situations are drawn in Fig. 1.11 taken from reference [2].
In the trivial situation all energy eigenstates are those of the bulk. In the topological situation there are also other two eigenstates in fact each end of the chain hosts a single eigenstate at zero energy (zero mode). These states are also edge states, in the sense that their wavefunction is localized at the edges. Moving away from the fully dimerized limit the energy of the edge states are still very close to zero energy. Furthermore, the wavefunctions of almost-zero-energy-edge-states have to be exponentially localized at the left-right edges [2].
We want to underline a very important property of the number of edge states, but, before it, we have to introduce some concepts [2]:
- an insulating Hamiltonian is adiabatically deformed if its parameters are changed continuosly, the important symmetries of the system are maintained and the bulk gap remains open.
- two Hamiltonians are adiabatically connected or adiabatically equivalent if there is an adiabatic deformation connecting them. The Hamiltonian corresponding to the topological phase ($\nu = 0$ and $\mu = 1$) and that corresponding to the trivial phase ($\nu = 1$ and $\mu = 0$) are not adiabatically connected.
- An integer number which characterizes an insulating Hamiltonian and which does not change under adiabatic deformations is a topological inviariant.
- As a consequence of what has just been said, two Hamiltonians are not adiabatically equivalent if their topological invariants differ and they are adiabatically equivalent if their topological invariants are the same.
It is possible to demonstrate that the number of edge states is an integer which does not change under adiabatic deformation. In particular it is 0 in the trivial case ($\nu = 1$ and $\mu = 0$) and 1 in the topological phase ($\nu = 0$ and $\mu = 1$). For these reasons the number of edge states is a topological invariant [2].

1.4.2 SSH model: bulk boundary correspondence

The bulk winding number and the number of edge states which concern the bulk and the boundary of the chain are both topological invariants, in particular they are 1 in the topological phase and 0 in the trivial phase. This shows that we can use the bulk topological invariant to obtain simple and robust predictions about the low-energy physics at the edge. This is a simple example of the bulk-boundary correspondence [2].

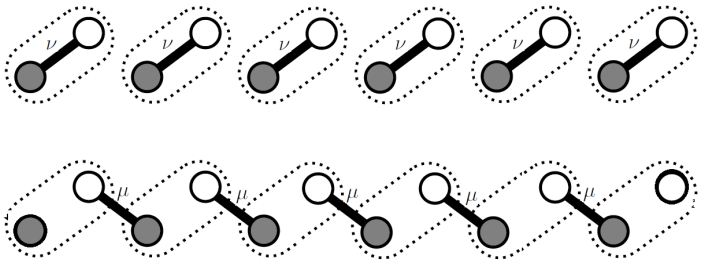

Figure 1.11: Representation of the two possible situations in the dimerized limit of the ssh model. The trivial situation $\nu = 1$ and $\mu = 0$ is above while the topological situation $\nu = 0$ and $\mu = 1$ is below. This picture is taken from [2].

1.5 Berry phases and Berry connection

In this paragraph we introduce the concept of Berry phases because it is connected to topologically invariant quantities. In particular, we will see in paragraph 2.7 that in the partition function, of one-dimensional quantum antiferromagnets, a term due to Berry phases will be directly present in the definition of the winding number of a given spin configuration.

We start by considering a continuum set of states $|\psi(\mathbf{R})>$ where $\mathbf{R}$'s are elements of some D dimensional parameter space $\mathcal{P}$. We now introduce a curve $\mathcal{C}$ in $\mathcal{P}$ and we define the relative phase between two neighbouring states on the curve $\mathcal{C}$ which correspond to $\mathbf{R}$ and $\mathbf{R} + d\mathbf{R}$ [2]:

$$e^{-i\Delta\gamma} = \frac{<\psi(\mathbf{R})|\psi(\mathbf{R}+d\mathbf{R})>}{|<\psi(\mathbf{R})|\psi(\mathbf{R}+d\mathbf{R})>|} \tag{1.178}$$

and

$$\Delta\gamma = i<\psi(\mathbf{R})|\nabla_{\mathbf{R}}|\psi(\mathbf{R})>\cdot d\mathbf{R} \tag{1.179}$$

at first order in $d\mathbf{R} \to 0$. The last expression contains the so called Berry connection [2]:

$$\mathbf{A}(\mathbf{R}) = i<\psi(\mathbf{R})|\nabla_{\mathbf{R}}|\psi(\mathbf{R})>. \tag{1.180}$$

Under a gauge transformation the relative phase of two states is not invariant in fact $|\psi(\mathbf{R})> \to e^{i\alpha(\mathbf{R})}|\psi(\mathbf{R})>$, therefore Berry connection also changes as $\mathbf{A}(\mathbf{R}) \to \mathbf{A}(\mathbf{R}) - \nabla_{\mathbf{R}}\alpha(\mathbf{R})$.
If we consider now a closed directed curve $\mathcal{C}$ in $\mathcal{P}$ the Berry phase along that curve is computed as follows [2]:

$$\gamma(\mathcal{C}) = -arg\exp\left(-i\oint_{\mathcal{C}}\mathbf{A}\cdot d\mathbf{R}\right) \tag{1.181}$$

where $arg(z)$ denotes the phase of the complex number z. When $\mathcal{C}$ is a a closed directed curve, it can be proved that the Berry phase is gauge invariant [2].
We would like to express this gauge invariant Berry phase as a surface integral of a gauge invariant quantity. The last is called Berry curvature. In order to define it, we can consider a two dimensional parameter space and a connected region $\mathcal{F}$ on it. We consider $\mathbf{R} = (x, y)$, therefore $\mathbf{A}_x(\mathbf{R}) = i < \psi(\mathbf{R})|\frac{\partial}{\partial_x}|\psi(\mathbf{R}) >$ and $\mathbf{A}_y(\mathbf{R}) = i < \psi(\mathbf{R})|\frac{\partial}{\partial_y}|\psi(\mathbf{R}) >$. We also suppose that $|\psi(\mathbf{R}) >$ is smooth in the neighborhood of $\mathcal{F}$, under these assumptions the Berry curvature is [2]:

$$\mathbf{F}(x, y) = \partial_x \mathbf{A}_y - \partial_y \mathbf{A}_x. \tag{1.182}$$

Then we consider the oriented curve $\partial\mathcal{F}$ which bounds $\mathcal{F}$ and we directly apply the two-dimensional Stokes theorem. The Berry phase becomes [2]:

$$\gamma(\partial\mathcal{F}) = -arg \exp\left(-i \oint_{\partial\mathcal{F}} \mathbf{A} \cdot d\mathbf{R}\right)$$

$$= -arg \exp\left(-i \int_{\mathcal{F}} (\partial_x \mathbf{A}_y - \partial_y \mathbf{A}_x)\, dxdy\right) = -arg \exp\left(-i \int_{\mathcal{F}} \mathbf{F}(x, y) dxdy\right). \tag{1.183}$$

We continue our short introduction by considering a set of states $|n(\mathbf{R}) >$ where $\mathbf{R}$'s are elements of some D dimensional parameter space $\mathcal{P}$ as before, but $|n(\mathbf{R}) >$ are also eigenvectors of a Hamiltonian H, which is a smooth function of the parameters at least in the region of interest. We want to show that the adiabatic phase picked up by a state during a cyclic adiabatic change of the Hamiltonian is equivalent to the Berry phase corresponding to the closed oriented curve representing the Hamiltonian's path in the parameter space [2].
In the eigenvalue problem $H(\mathbf{R})|n(\mathbf{R}) >= E_n(\mathbf{R}|n(\mathbf{R}) >$ we use the snapshot basis $|n(\mathbf{R}) >$ where "snapshot" means that otherwise arbitrary phase prefactor for every $|n(\mathbf{R}) >$ is specified. We suppose that at the beginning the system is initialized with $\mathbf{R} = \mathbf{R}_0$ and $|\psi(t = 0) >= |n(\mathbf{R}_0) >$. As time evolves $t = 0 \to T$ the parameters $\mathbf{R}$ are slowly changed, it means that they are t dependent and they define a continuous direct curve $\mathcal{C}$ in parameter space. The state of the system changes according to the time-dependent Schrödinger equation $i\frac{d}{dt}|\psi(t) >= H(\mathbf{R}(t))|\psi(t) >$.
If the evolution can be considered to be adiabatic, then $|n(\mathbf{R}(t)) >$ only picks up a phase. In order to find it we use the following Ansatz [2]:

$$|\psi(t) >= e^{i\gamma_n(t)} e^{-i\int_0^t dt'\, E_n(\mathbf{R}_{(t')})} |n(\mathbf{R}(t)) > . \tag{1.184}$$

The time derivative of (1.184) becomes:

$$i\frac{d}{dt}|\psi(t) >= e^{i\gamma_n(t)} e^{-i\int_0^t dt'\, E_n(\mathbf{R}_{(t')})} \left(-\frac{d\gamma_n}{dt}|n(\mathbf{R}(t)) > + E_n(\mathbf{R})|n(\mathbf{R}(t)) > + i|\frac{d}{dt} n(\mathbf{R}(t)) >\right). \tag{1.185}$$

In this expression the last term can be written in the following equivalent way [2]:

$$|\frac{d}{dt}n(\mathbf{R}(t)) >= \frac{d\mathbf{R}}{dt}|\nabla_R n(\mathbf{R}(t)) > . \tag{1.186}$$

If we replace (1.184) and (1.185) in the Schrödinger equation and we use $H(\mathbf{R})|n(\mathbf{R}) >= E_n(\mathbf{R}|n(\mathbf{R}) >$ we achieve [2]:

$$-\frac{d\gamma_n(t)}{dt}|n(\mathbf{R}(t)) > +i|\frac{d}{dt}n(\mathbf{R}(t)) >= 0. \tag{1.187}$$

If we multiply it by $< n(\mathbf{R}(t))|$ and we use (1.187) then we obtain:

$$\frac{d\gamma_n(t)}{dt} = i < n(\mathbf{R}(t))|\frac{d}{dt}n(\mathbf{R}(t)) >= \frac{d\mathbf{R}}{dt}i < n(\mathbf{R}(t))|\nabla_R n(\mathbf{R}(t)) > . \tag{1.188}$$

Therefore for the curve $\mathcal{C}$ traced out by $\mathbf{R}(t)$ in the parameter space there is an adiabatic phase [2]:

$$\gamma_n(\mathcal{C}) = \int_{\mathcal{C}} i < n(\mathbf{R})|\nabla_R n(\mathbf{R}) > d\mathbf{R} \tag{1.189}$$

If now we consider an adiabatic and cyclic change of the Hamiltonian, i.e. $\mathcal{C}$ is closed and therefore $\mathbf{R}(T) = \mathbf{R}_0$, then the adiabatic phase is [2]:

$$\gamma_n(\mathcal{C}) = \oint_{\mathcal{C}} i < n(\mathbf{R})|\nabla_R n(\mathbf{R}) > d\mathbf{R} \tag{1.190}$$

which is the Berry phase corresponding to the closed oriented curve given by the Hamiltonian's path in the parameter space, as we wanted to prove [2].

In paragraph 2.3, considering a single spin systems, we will introduce coherent states to have a path integral formulation of the partition function. The nonorthogonality of these coherent states will cause the presence of exponentials of Berry phases in their overlap, as it happens in (1.178). We will understand the geometric meaning of Berry phases and, as said at the beginning, we will find a deep link between them and the winding number.

To conclude this brief introduction we only want to underline that Berry phases are detectable by an interferometric setup [2]. This means that the wavefunction of a system must be coherently splitted into two parts. Then they are taken through two adiabatic trips in parameter space and at the end they meet again, their interference comes from the overlap between states i.e. from Berry phases.

Chapter 2

Toplogical terms in spin chains and standard spin ladders

2.1 Short review of the Heisenberg model

The Heisenberg model can be derived as a special limit of the Hubbard model [3]. In fact it is the Hubbard model in the large U/t regime and at half filling.

The model has been intensively studied [12], but here we focus only on its mapping to the sine-Gordon theory.

After applying Jordan-Wigner transformation Heisenberg Hamiltonian becomes [12]:

$$H = \frac{J}{2}\sum_{j=1}^{N}(c_j^\dagger c_{j+1} + h.c.) + \gamma J \sum_{j=1}^{N}(n_j - \frac{1}{2})(n_{j+1} - \frac{1}{2}) \tag{2.1}$$

where $n_j = c_j^\dagger c_j$ is the density of fermions. For γ=1 it is known as isotropic Heisenberg model and for γ=0 it is called the spin one-half XY model.

The non-interacting part $H_0 = \frac{J}{2}\sum_{j=1}^{N}(c_j^\dagger c_{j+1} + h.c.)$ can be rewritten using different changes of variable. All the precise steps are present in [12] but, as before, here there are only the main results:

- $a_j = i^{-j}c_j$ and H_0 becomes $H_0 = \frac{J}{2}\sum_{j=1}^{N} i a_j^\dagger[a_{j+1} - a_{j-1}]$, it can also be written separating the sum into even and odd sites [12]:

$$H_0 = \frac{J}{2}\sum_{s=1}^{N/2} i[a_{2s}^\dagger[a_{2s+1} - a_{2s-1}] + a_{2s+1}^\dagger[a_{2s+2} - a_{2s}]]. \tag{2.2}$$

- We can introduce the spinor field ϕ_α $\alpha = 1, 2$ which is $\phi_1(n) = a_{2s}$ on even sites and $\phi_2(n) = a_{2s+1}$ on odd sites. Therefore (2.2) becomes [12]:

$$H_0 = i\frac{J}{2}\sum_{s=1}^{N/2}(\phi_1^\dagger(2s)[\phi_2(2s+1)-\phi_2(2s-1)]+\phi_2^\dagger(2s+1)[\phi_1(2s+2)-\phi_1(2s)]). \quad (2.3)$$

- We can express $\phi_\alpha(n)$ defined on the lattice in terms of $\psi_\alpha(x)$ defined in the continuum $\psi_\alpha(x) = \frac{1}{\sqrt{2a_0}}\phi_\alpha(n)$ where a_0 is the lattice spacing. So we get the effective hamiltonian in the continuum limit [12]:

$$\tilde{H}_0 = \int dx\psi^\dagger(x)\sigma^x i\partial_x\psi(x) \quad (2.4)$$

  where $\tilde{H}_0 = \frac{H_0}{Ja_0}$ and it is just the Dirac Hamiltonian with $\hbar = 1$ and Fermi velocity $v_F = 1$ and σ^x is one of the Pauli matrices.

The interacting part $H_{int} = \gamma J\sum_{j=1}^{N}(n_j - \frac{1}{2})(n_{j+1} - \frac{1}{2})$ can be manipulated in the same way and it becomes [12]:

$$\tilde{H}_{int} = -2\gamma\int dx(\bar{\psi}(x)\psi(x))^2 \quad (2.5)$$

where we neglet an irrilevant constant and $\tilde{H}_{int} = \frac{H_{int}}{Ja_0}$. In expression (2.5) $\bar{\psi} = \psi^\dagger\sigma^x$ and (2.5) is usually known as Gross-Neveu interaction.

At this point the bosonization technique can be applied. Rescaling the field ϕ as $(1 + \frac{2\gamma}{\pi})^{\frac{1}{2}}\phi(x) = \varphi(x)$ the Lagrangian density of the model is [12]:

$$\mathcal{L}_B = \frac{1}{2}(\partial_\mu\varphi)^2 + g : \cos(\beta\varphi) : \quad (2.6)$$

this is the lagrangian written in sine-Gordon form. We also have that β is such that [12]:

$$\beta^2 = \frac{16\pi}{1+\frac{2\gamma}{\pi}} \quad g \sim \frac{\gamma}{\pi^2 a_0^2}. \quad (2.7)$$

Therefore the model is characterized by:

- for $\beta^2 > 8\pi$ the cosine term is irrilevant.
  Mermin Wagner theorem forbids the spontaneos symmetry breaking of the continuos symmetry of the model.
  The system is critical, i.e. there are no energy gaps, and correlation functions are characterized by a power law behaviour;

- for $\beta^2 < 8\pi$ the cosine term is relevant and a gap is developed.

2.2 Generalization of Heisenberg model

In general it is not possible to have gapless states without the spontaneous breaking of a continuos symmetry whereas this situation is possible in Heisenberg model. Therefore it is important to study generalizations of the this model too. Two approaches have been followed to this aim [12]:

- to keep $SU(2)$ symmetry group but to consider higher spin;
- to consider higher symmetry groups, $SU(N)$ for example.

The first approach was developed by Haldane: he studied the large spin limit, which is a semiclassical limit ($s \to \infty$). In this limit he obtained an effective lagrangian which is almost the lagrangian of the quantum non-linear sigma model [12].
The non-linear sigma model is characterized by a finite correlation lenght therefore it can not be critical, so how could it be a limit of the Heisenberg model? The answer is as follows [12]:
- for integer spin the system is not critical;
- for half-integer spin in addition to the sigma model there is an extra term. It is a topological term proportional to a topological invariant known as winding number or Pontryagin index of the spin configurations. It makes the behaviour of half-integer spin chains different from that of integer spin chains.

The second approach showed that it is possible for these systems to be critical when their parameters have some particular values but this critical behaviour is different from that in the Heisenberg case. In fact, at least in one dimensional case, they are either critical or without long range order. But here we do not deepen this important analysis.

2.3 A single spin systems: coherent states and path integral formulation

In order to achieve the same results as those obtained by Haldane, firstly we can consider a simpler case: a single spin s.

We will use a path integral approach to study the evolution operator between initial and final states and it will deal with coherent states so we have to introduce them.

Spin operators are generators of the $SU(2)$ transformations, so we can write group members in this way [3]:

$$\mathcal{R} = e^{i\phi S_x} e^{i\theta S_y} e^{i\chi S_z} \tag{2.8}$$

they are parametrized by the three Euler angles ϕ, θ, χ.

Now we can obtain the coherent state $|\hat{\Omega} >$ from the highest weight state $|S, S >$, applying to this maximally polarized state the rotation $\mathcal{R}$[3, 12]:

$$|\hat{\Omega} >= \mathcal{R}|S, S >= e^{i\phi S_x} e^{i\theta S_y} e^{i\chi S_z} |S, S > . \tag{2.9}$$

The rotation of an arbitrary angle around the z axis gives the same physical state except for an overall phase, so we fix this "gauge feeedom" neglecting the term $e^{i\chi S_z} = 1$.
Therefore $\hat{\Omega}$ is parametrized by $\theta \in [0, \pi]$ and $\phi \in [-\pi, \pi]$, θ is the "latitude" and ϕ is the "longitude". So we have [3, 12]:

$$\hat{\Omega} = (\sin\theta\cos\phi, \sin\theta\sin\phi, \cos\theta). \tag{2.10}$$

Our aim concerns path integral formulation so in order to write it other important relations are necessary [3, 12]:

$$< \hat{\Omega}_1|\hat{\Omega}_2 >= e^{i\varphi(\hat{\Omega}_1, \hat{\Omega}_2, \hat{\Omega}_3)s} \left(\frac{1 + \hat{\Omega}_1 \hat{\Omega}_2}{2} \right)^s \tag{2.11}$$

$$< \hat{\Omega}|\vec{S}|\hat{\Omega} >= s\hat{\Omega}, \tag{2.12}$$

as well as the integration measure:

$$d\mu(\hat{\Omega}) = \frac{2s+1}{4\pi} d^3\Omega \delta(\hat{\Omega}^2 - 1). \tag{2.13}$$

and the resolution of identity:

$$I = \int d\mu(\hat{\Omega}) |\hat{\Omega} >< \hat{\Omega}|. \tag{2.14}$$

Spin coherent states elucidate the correspondence between classical and quantum spins. The expectation values of spin operators (2.12) are functions of unit vectors, as it happens in classical case (of course $\hat{\Omega}$ are unit vectors) and the overlap of different coherent states (2.11) vanishes in the classical limit ($s \to \infty$), quantum effects are associated with the nonorthogonality of coherent states [3].
$\varphi(\hat{\Omega}_1, \hat{\Omega}_2, \hat{\Omega}_3)$ is the area of the spherical triangle bounded dy $\hat{\Omega}_1, \hat{\Omega}_2, \hat{\Omega}_3$. As it is evident from Fig. 2.1, there are two possibilities for this area (white and pink in Fig. 2.1). However, since their difference is 4π and since spin operator has integer or half integer eigenvalues m, this ambiguity has no physical consequences and $e^{i4\pi m} = 1$ [12].

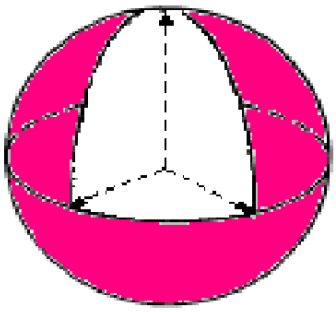

Figure 2.1: Representation, inspired from reference [12], of the two possible areas $\varphi(\hat{\Omega}_1, \hat{\Omega}_2, \hat{\Omega}_3)$ bounded by $\hat{\Omega}_1, \hat{\Omega}_2, \hat{\Omega}_3$. These vectors are the three dashed arrows.

Now we have all tools to write the path integral representation of the partiton function [12]:

$$Z = Tre^{-\beta H} \tag{2.15}$$

with PBC.

The imaginary time interval β can be divided into N_t steps each of lenght δt such that $N_t \delta t = \beta$ stays constant while $N_t \to \infty$ and $\delta t \to 0$. Using Trotter formula Z becomes [12]:

$$Z = \lim_{N_t \to \infty, \delta t \to 0} (e^{-\delta t H})^{N_t}. \tag{2.16}$$

We can now insert the resolution of identity (2.14) N_t times and write (2.16) as [12]:

$$Z = \lim_{N_t \to \infty, \delta t \to 0} \left(\prod_{j=1}^{N_t} \int d\mu(\hat{\Omega}_j) \right) \left(\prod_{j=1}^{N_t} < \hat{\Omega}(t_j) | e^{-\delta t H} | \hat{\Omega}(t_{j+1}) > \right). \tag{2.17}$$

We can approximate (2.17) because δt is very small [12]:

$$Z = \lim_{N_t \to \infty, \delta t \to 0} \left(\prod_{j=1}^{N_t} \int d\mu(\hat{\Omega}_j) \right) \left(\prod_{j=1}^{N_t} [< \hat{\Omega}(t_j) | \hat{\Omega}(t_{j+1}) > - \delta t < \hat{\Omega}(t_j) | H | \hat{\Omega}(t_{j+1}) >] \right). \tag{2.18}$$

If $\hat{\Omega}_0$ is along the quantization axis i.e. $\hat{\Omega} \cdot \hat{\Omega}_0 = \cos(\theta)$, from (2.11) we have [12]:

$$< \hat{\Omega}(t_j)|\hat{\Omega}(t_{j+1}) >= e^{i\varphi(\hat{\Omega}(t_j),\hat{\Omega}(t_{j+1}),\hat{\Omega}_0)s}\left(\frac{1+\hat{\Omega}(t_j)\hat{\Omega}(t_{j+1})}{2}\right)^s \tag{2.19}$$

and always because δt is very small we can write the following approximation [12]:

$$\frac{< \hat{\Omega}(t_j)|H|\hat{\Omega}(t_{j+1}) >}{< \hat{\Omega}(t_j)|\hat{\Omega}(t_{j+1}) >} \simeq < \hat{\Omega}(t_j)|H|\hat{\Omega}(t_j) > +\mathcal{O}(\delta t). \tag{2.20}$$

So from (2.18), (2.19) and (2.20) we have [12]:

$$Z = \lim_{N_t\to\infty,\delta t\to 0}\int \mathcal{D}\hat{\Omega}e^{-S_E[\hat{\Omega}]} \tag{2.21}$$

$$\mathcal{D}\hat{\Omega} = \prod_{j=1}^{N_t}\int d\mu(\hat{\Omega}(t_j)) \tag{2.22}$$

$$-S_E[\hat{\Omega}] = is\sum_{j=1}^{N_t}\varphi(\hat{\Omega}(t_j),\hat{\Omega}(t_{j+1}),\hat{\Omega}_0) + s\sum_{j=1}^{N_t}\ln\left(\frac{1+\hat{\Omega}(t_j)\hat{\Omega}(t_{j+1})}{2}\right)$$
$$-\sum_{j=1}^{N_t} < \hat{\Omega}(t_j)|H|\hat{\Omega}(t_j) > \tag{2.23}$$

2.4 A single spin systems: topological term

We focus on the first term of the Euclidean action (2.23). It implies a contribution $e^{is\mathcal{A}[\hat{\Omega}]}$ where [12]:

$$\mathcal{A}[\hat{\Omega}] = \lim_{N_t\to\infty,\delta t\to 0}\sum_{j=1}^{N_t}\varphi(\hat{\Omega}(t_j),\hat{\Omega}(t_{j+1}),\hat{\Omega}_0). \tag{2.24}$$

This contribution is represented in blu in Fig. 2.2. and explained after it and it represents a sum of areas of spherical triangles each bounded by $\hat{\Omega}(t_j)$, $\hat{\Omega}(t_{j+1})$, $\hat{\Omega}_0$. $\hat{\Omega}(t_0) = \hat{\Omega}(t_{N+1})$ so (2.24) is the total area of the cap Σ on S_2 sphere [12]. Σ is bounded by the trajectory Γ parametrized by $\hat{\Omega}(t)$. In Fig. 2.2 there is the representation of Σ in blue and Γ in red. Since S_2 has no boundaries there are two possibile caps: the blu area Σ and the white area complementary to Σ, but their difference is 4π and s is an integer or an half-integer so this ambiguity does not imply any physical consequences [12].

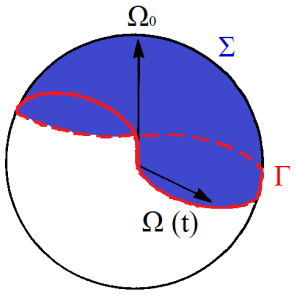

Figure 2.2: Representation, inspired from reference [12], of the total area Σ in blue bounded by Γ in red.

We can evaluate the contribution (2.24) in the limit $N_t \to \infty$ and $\delta t \to 0$ [12]:

$$\mathcal{A}[\hat{\Omega}] = \int_0^1 d\tau \int_0^\beta dt \hat{\Omega}(t,\tau) \cdot (\partial_\tau \hat{\Omega}(t,\tau) \times \partial_t \hat{\Omega}(t,\tau)). \tag{2.25}$$

In (2.25) we use $\hat{\Omega}(t,\tau)$ in order to parametrized the cup Σ where $t \in [0,\beta]$ and $\tau \in [0,1]$. $\hat{\Omega}(t,\tau)$ is smooth and arbitrary and it is subject to these boundary conditions [12]:

$$\hat{\Omega}(t,0) = \hat{\Omega}(t) \quad \hat{\Omega}(t,1) = \hat{\Omega}_0 \quad \hat{\Omega}(0,\tau) = \hat{\Omega}(\beta,\tau). \tag{2.26}$$

If now we replace the expression (2.10) i.e. we consider $\hat{\Omega}$ as function of θ and ϕ (2.24) is also equal to [3]:

$$\mathcal{A}[\hat{\Omega}] = -\int_0^\beta dt \dot{\phi} \cos\theta. \tag{2.27}$$

Now this geometric contribution is called:

- in reference [12] Wess-Zumino or Chern-Simons term

$$S_{WZ}[\hat{\Omega}] = \int_0^1 d\tau \int_0^\beta dt \hat{\Omega}(t,\tau) \cdot (\partial_\tau \hat{\Omega}(t,\tau) \times \partial_t \hat{\Omega}(t,\tau)); \tag{2.28}$$

- in reference [3] Berry phase

$$\omega[\hat{\Omega}] = -\int_0^\beta dt \dot{\phi} \cos\theta. \tag{2.29}$$

In the continumm limit $N_t \to \infty$ and $\delta t \to 0$ (2.23) becomes [12]:

$$S_E[\hat{\Omega}] = -isS_{WZ}[\hat{\Omega}] + \frac{s\delta t}{4}\int_0^\beta dt(\partial_t\hat{\Omega}(t))^2 + \int_0^\beta dtH[\hat{\Omega}]. \tag{2.30}$$

If we go back from Euclidean to real time, i.e. $t = ix_0$ and $\beta = iT$ the action (2.30) becomes [12]:

$$S_{\mathcal{M}}[\hat{\Omega}] = sS_{WZ}[\hat{\Omega}] + \frac{s\delta t}{4}\int_0^T dx_0(\partial_0\hat{\Omega}(x_0))^2 - \int_0^T dx_0 H[\hat{\Omega}] \tag{2.31}$$

and so (2.21) becomes [12]:

$$Z = \int \mathcal{D}\hat{\Omega}e^{is_{\mathcal{M}}[\hat{\Omega}]}. \tag{2.32}$$

2.5 Generalization to many spin systems

Now we can consider a system of many spins described by: $H = J\sum_{\mathbf{r},\mathbf{r'}} \mathbf{S}(\mathbf{r})\mathbf{S'}(\mathbf{r'})$ where $(\mathbf{r},\mathbf{r'})$ indicates pairs of sites on an arbitrary lattice. We can generalize expressions (2.30), (2.31) and (2.32) [12]:

$$S_E[\hat{\Omega}] = -is\sum_{\mathbf{r}} S_{WZ}[\hat{\Omega}(\mathbf{r})] + \frac{s\delta t}{4}\int_0^\beta dt\sum_{\mathbf{r}}(\partial_t\hat{\Omega}(\mathbf{r},t))^2 + \int_0^\beta dt\sum_{\mathbf{r},\mathbf{r'}} Js^2\hat{\Omega}(\mathbf{r},t)\hat{\Omega}(\mathbf{r'},t). \tag{2.33}$$

We suppose to take the limit for $\delta t \to 0$ so we can neglet the term with δt. As before, the first term in (2.33) represents the toplogical term. In real time the action (2.33) becomes [12]:

$$S_{\mathcal{M}}[\hat{\Omega}] = s\sum_{\mathbf{r}} S_{WZ}[\hat{\Omega}(\mathbf{r})] - \int_0^T dx_0\sum_{\mathbf{r},\mathbf{r'}} Js^2\hat{\Omega}(\mathbf{r},x_0)\hat{\Omega}(\mathbf{r'},x_0) \tag{2.34}$$

and the partition function [12]:

$$Z = \int \mathcal{D}\hat{\Omega}e^{iS_{\mathcal{M}}[\hat{\Omega}]}. \tag{2.35}$$

Up to now, we have not made use of the semiclassical limit to derive these expressions. However, if we consider it, the stationary points of the action $S_{\mathcal{M}}[\hat{\Omega}]$ will dominate the path integral Z in the semiclassical limit $s \to \infty$ since (2.34) scales with s [12].

2.6 Effective action: NLσM

If we focus on Heisenberg antiferromagnet case described by $H = s^2 \sum_{ij} J_{ij} \hat{\Omega}_i \hat{\Omega}_j$, following [3], we can generalize (2.30) for this case and write it in terms of Berry phase:

$$S_E[\hat{\Omega}] = -is \sum_i \omega[\hat{\Omega}_i] + \frac{s\delta\tau}{4} \int_0^\beta d\tau \sum_i \left(\partial_\tau \hat{\Omega}_i(\tau)\right)^2 + \int_0^\beta d\tau s^2 \sum_{ij} J_{ij} \hat{\Omega}_i \hat{\Omega}_j. \tag{2.36}$$

We suppose to take the limit for $\delta\tau \to 0$ so we can neglect the term $\frac{s\delta\tau}{4} \int_0^\beta d\tau \sum_i \left(\partial_\tau \hat{\Omega}_i(\tau)\right)^2$. We write the action (2.36) in a more compact way (it is usuful for next calculations) [3]:

$$S_E[\hat{\Omega}] = -is \sum_i \omega[\hat{\Omega}_i] + \int_0^\beta d\tau H(\tau). \tag{2.37}$$

We consider a cubic lattice of dimension D with lattice constant a and even number of sites in each dimension. The total number of sites is $\mathcal{N}$.

We suppose that J_{ij} are short range, i.e. $\frac{1}{2d} \sum_i |J_{ij}||x_i - x_j|^2 < \infty$, and that, for this system, the important configurations in the semiclassical limit (large s) have an antiferromagnetic order at least at short range, whereas at longer scales there could be a significant deviation from Néel state.
The first step is to rewrite the field $\hat{\Omega}$ in this way [3]:

$$\hat{\Omega}_i = \eta_i \hat{n}(x_i) \sqrt{1 - \left(\left| \frac{\mathbf{L}(x_i)}{s} \right| \right)^2} + \frac{\mathbf{L}(x_i)}{s} \tag{2.38}$$

where $\eta_i = e^{ix_i\pi}$, Néel field $\hat{n}$ and transverse canting field $\mathbf{L}$ are continuus and they are characterized by [3]:

$$|\hat{n}(x_i)| = 1 \quad \mathbf{L}(x_i) \cdot \hat{n}(x_i) = 0. \tag{2.39}$$

We have substituted $\hat{\Omega}$, which is characterized by two degrees of freedom θ and ϕ, with six variables (three components of $\hat{n}$ and three components of $\mathbf{L}$), but we have two constraints (2.39) and it is possible to fix an other relation. This third constraint is achieved by writen $\mathcal{D}\hat{\Omega}$ as a function of $\hat{n}_q$ and $\mathbf{L}_q$, Fourier transformed of $\hat{n}(x_i)$ and $\mathbf{L}(x_i)$, in this way [3]:

$$\mathcal{D}\hat{\Omega} = \prod_{|q|} d\hat{n}_q d\mathbf{L}_q \delta(\hat{n}\mathbf{L}) \mathcal{J}[\hat{n}, \mathbf{L}] \tag{2.40}$$

in this expression $\mathcal{J}[\hat{n}, \mathbf{L}]$ is the Jacobian of transformation (2.38) and the product is over Fourier components such that $|q| < \frac{2\pi}{R_J}$ where R_J is the characteristic range of antiferromagnetic interaction. If we compute the degrees of freedom for left and right sides of (2.40), we find that they are $2\mathcal{N}$ and in this way we fix the number of Fourier

components $\hat{n}_q$ and $\mathbf{L}_q$ in the measure (2.40), in other words we fix the third constraint.

Haldane mapped [3, 14, 15] the effective long-wavelength action of quantum Heisenberg antiferromagnet in D dimensions into a non linear sigma model NLσM in $D+1$ dimensions:

- since R_J is the characteristic range of antiferromagnetic interactions $J_{i,j}$ and ξ is the correlation length, we suppose that, in the large $\frac{\xi}{a}$ limit, there exist a cutoff Λ such that $\xi^{-1} \ll \Lambda \ll \frac{2\pi}{R_J}$;
- in order to obtain the effective long-wavelength action in the path integral expansion we will eliminate length scale fluctuations which are shorter with respect to Λ^{-1};
- or equivalently we neglet Fourier components of $\hat{n}$ if $|q| > \Lambda$ i.e. we consider $|\hat{n}_q| \ll 1$ if $|q| > \Lambda$;
- or this also means to consider the canting field small $|\frac{\mathbf{L}}{s}| \ll 1$.

Therefore Haldane's mapping is based on the distinction between short and long length scale fluctuations, which in turn is based on the existence of Λ such that $\xi^{-1} \ll \Lambda \ll \frac{2\pi}{R_J}$. This can be achieved in the semiclassical limit ($s \to \infty$), when, as said before, at least locally there is antiferromagnetic order [3].

In order to map quantum Heisenberg antiferromagnet in D dimensions into a non linear sigma model NLσM in $D+1$ dimensions, firstly we can rewrite the term $-is\sum_i \omega[\hat{\Omega}_i]$ in (2.37) as [3]:

$$\begin{aligned} -is\sum_i \omega_i &= -is\sum_i \eta_i \omega[\hat{n}_i + \eta_i(\mathbf{L}_i \setminus s)] = \\ &= -is\sum_i \left[\eta_i \omega[\hat{n}_i] + \frac{\delta\omega}{\delta\hat{n}_i}\cdot(\mathbf{L}_i \setminus s)\right] = \\ &= -i\Upsilon - i\int_0^\beta d\tau \sum_i (\hat{n}_i \times \partial_\tau \hat{n}_i \cdot \mathbf{L}_i). \end{aligned} \tag{2.41}$$

where here

$$\Upsilon[\hat{n}] = s\sum_i \eta_i \omega[\hat{n}(x_i)] \tag{2.42}$$

is the topological Berry phase.

Secondly we focus on $\int_0^\beta d\tau H(\tau)$, which is the second term in (2.37) and which becomes [3]:

$$\hat{\Omega}_i \cdot \hat{\Omega}_j \sim \eta_i\eta_j - \frac{1}{2}\eta_i\eta_j(\hat{n}_i - \hat{n}_j)^2 + \left(\frac{1}{s}\right)^2 \left[\mathbf{L}_i\mathbf{L}_j - \frac{1}{2}\eta_i\eta_j(\mathbf{L}_i^2 + \mathbf{L}_j^2)\right] + \\ + \frac{1}{s}(\eta_j\mathbf{L}_i\hat{n}_j + \eta_i\mathbf{L}_j\hat{n}_i) + \mathcal{O}(|\mathbf{L}|^2|\hat{n}_i - \hat{n}_j|). \tag{2.43}$$

The interaction $\hat{\Omega}_i \cdot \hat{\Omega}_j$ is expanded to quadratic order in $|\mathbf{L}/s|^2$ and now we can obtain the continuum limit of the Hamiltonian. Here we describe the main steps [3]:

- in the continuum limit lattice sums become integrals:

$$\sum_i A_i \quad \to \quad a^{-D}\int d^D x \sum_i \delta(x - x_i)A(x) \tag{2.44}$$

- the first term in (2.43) is:

$$s^2 \sum_{i,j} J_{i,j}\eta_i\eta_j = E_0^{classical} \tag{2.45}$$

- then we consider the derivatives of the vector fields $\hat{n}$:

$$\hat{n}_i - \hat{n}_j \sim \partial_l\hat{n}(x_i)x_{ij}^l + \frac{1}{2}(\partial_l\partial_k\hat{n})x_{ij}^l x_{ij}^k \tag{2.46}$$

  so replacing (2.44) and (2.46), the second term in (2.43) becomes:

$$\frac{1}{2}\int d^D x \rho_s \sum_l |\partial_l\hat{n}|^2$$

$$\rho_s = -\frac{s^2}{2D\mathcal{N}a^D}\sum_{ij} J_{ij}\eta_i\eta_j|x_i - x_j|^2 \tag{2.47}$$

- we also consider the contribution $\mathbf{L}_i\mathbf{L}_j$ which in the continuum limit becomes:

$$\mathbf{L}_x\delta(x - x_i)\delta(x' - x_j)\mathbf{L}_{x'} \tag{2.48}$$

  and we also compute the sum $-\frac{1}{2}\eta_i\eta_j(\mathbf{L}_i^2 + \mathbf{L}_j^2)$ which in the continuum limit is:

$$-\frac{1}{2}\eta_i\eta_j\mathbf{L}_x\delta(x - x_i)\delta(x - x')\mathbf{L}_{x'} - \frac{1}{2}\eta_i\eta_j\mathbf{L}_x\delta(x - x_j)\delta(x - x')\mathbf{L}_{x'} = \\ = -\eta_i\eta_j\mathbf{L}_x\delta(x - x_i)\delta(x - x')\mathbf{L}_{x'} \tag{2.49}$$

  so considering (2.44), (2.48) and (2.49), the third term in (2.43) becomes:

$$\frac{1}{2}\int d^D x d^D x' \mathbf{L}_x\chi_{xx'}^{-1}\mathbf{L}_{x'}$$

$$\chi_{xx'}^{-1} = \frac{1}{\mathcal{N}a^D}\sum_{ij} J_{ij}[\delta(x - x_i)\delta(x' - x_j) - \delta(x - x_i)\delta(x - x')\eta_i\eta_j] \tag{2.50}$$

- we consider again the derivatives of the vector fields $\hat{n}$ so that the fourth term becomes:
$$\sum_{ij} J_{ij}\eta_i \mathbf{L}_j \hat{n}_i = \frac{1}{2}\sum_{ij} J_{ij}\eta_i \mathbf{L}_j(\partial_l\partial_k\hat{n})x_{ij}^l x_{ij}^k \sim \mathcal{O}(\Lambda R_j)^2 \tag{2.51}$$
and since $\Lambda R_j \ll 1$ this term is negligible.

So action (2.37) has the following expression [3]:

$$S_E[\hat{n},\mathbf{L}] = -i\Upsilon - i\int_0^\beta d\tau \sum_i (\hat{n}_i \times \partial_\tau \hat{n}_i \cdot \mathbf{L}_i) +$$

$$+\int_0^\beta d\tau \left(E_0^{classical} + \frac{1}{2}\int d^D x \left[\rho_s \sum_l |\partial_l \hat{n}|^2 + \int d^D x' (\mathbf{L}_x \chi_{xx'}^{-1} \mathbf{L}_{x'}) \right] \right). \tag{2.52}$$

We can complete the square and perform a Gaussian integration over $\mathbf{L}$. We also remember that $|\hat{n}(x)\times\partial_\tau\hat{n}(x)|^2 = |\partial_\tau\hat{n}(x)|^2$. We consider only Fourier components with $|q| \leq \Lambda$. Then semiclassical partiton function is [3]:

$$Z \sim \int_\Lambda \mathcal{D}\hat{n} e^{i\Upsilon[\hat{n}]} e^{-\frac{1}{2}\int_0^\beta d\tau \int_\Lambda d^D x (\chi_0 |\partial_\tau \hat{n}|^2 + \rho_s \sum_l |\partial_l \hat{n}|^2)}. \tag{2.53}$$

In expression (2.53) $\chi_0 = \rho_s/c^2$ where we have introduced the spin wave velocity. We can unify space and imaginary time in a relativistic notation $(x_1,...,x_D,c\tau) = (x_1,...,x_D,x_{D+1})$ so Z becomes [3]:

$$Z \sim \int_\Lambda \mathcal{D}\hat{n} e^{i\Upsilon[\hat{n}]} e^{-\int d^{D+1}x \mathcal{L}_{NL\sigma M}^{D+1}}. \tag{2.54}$$

$\mathcal{L}_{NL\sigma M}^{D+1}$ is the Lagrangian density of non linear sigma model in $D+1$ dimensions and $i\Upsilon[\hat{n}]$ is a topological term given by Berry phases.

2.7 Topological term: integer and half-integer spin

For one-dimensional quantum antiferromagnet the topological term $i\Upsilon[\hat{n}]$ due to Berry phases can be thought as $i2\pi s\mathcal{Q}$ [12] where $\mathcal{Q}$ is the winding number or Pontryagin index of a given spin configuration $\{\hat{n}(x)\}$. Therefore, as it has been anticipated in chapter 1, Berry phases are connected with non trivial topological properties. The winding number $\mathcal{Q}$ has the following expression [12]:

$$\mathcal{Q} = \frac{1}{8\pi}\int d^2x \varepsilon_{i,j}\hat{n}(\partial_i\hat{n}\times\partial_j\hat{n}). \tag{2.55}$$

We can require that at space-time infinity $\hat{n}$ becomes a constant vector $\hat{n_0}$ so at infinity the fields are all identified with $\hat{n_0}$, it means that the Euclidean space-time (on which the configuration $\hat{n}$ is defined) "closes" and it is topologically a S_2 sphere. Furthermore, since we have the constraint $\hat{n} = 1$, the manifold $\hat{n}$ is isomorphic to a sphere S_2 too. It means that $\hat{n}(x)$ is a smooth and differentiable mapping from S_2 to S_2, where the first S_2 indicates the Euclidean space-time and the second S_2 refers to the manifold $\hat{n}$ [12].
$\mathcal{Q}$ counts how many times the spin configuration $\hat{n}$ is wrapped around the sphere, as it is easy to understand if we note the resemblance between (2.55) and (2.25). In reference [12] $\mathcal{Q}$ is calculated for instanton and soliton configurations and in both cases it is equal to 1. However these two configurations are only some examples because in general $\mathcal{Q}$ is an integer which is not always 1.
The very important concept to underline is that smooth configurations $\hat{n}$ (or better their homotopy classes) can be classified according to their winding number $\mathcal{Q}$. Therefore we can discuss the behaviour of $e^{i2\pi s\mathcal{Q}}$ [12]:
- for integer spin it is 1 and it has no consequences;
- for half-integer spin it is a sign positive if $\mathcal{Q}$ is even and negative if $\mathcal{Q}$ is odd.

A detailed renormalisation group analysis [12] allows to obtain the dependence of the correlation lenght ξ on the bare coupling constant. What emerges is a different behaviour between integer and half-integer spin chains:
- for integer spin the correlation lenght is finite and the spectrum develops a gap, the sigma model is always disordered at strong coupling;
- for half-integer spin the topological term does not change while the sigma model coupling constant scales to strong coupling, but strong coupling means low spin so all half-integer spin chains have a behaviour which is qualitatively the same of the spin one-half case. In that case it was possible for the system to be gapless with an infinite correlation lenght.

Therefore a different behaviour distinguishes integer from half-integer spin chains which belong to different universality classes. This result is known as Haldane's conjecture [12].

2.8 Standard Spin Ladders

The study of spin ladders can begin by considering standard spin ladders. In the next chapter we will consider a slightly different case, where interaction along each chain is staggered.

To construct a standard spin ladder we can consider two antiferromagnetic Heisenberg chains which constitute the two legs of the rectangular ladder (they are identified by the index $a = 1, 2$). We also suppose that there is an exchange interaction between spins across the rungs. Therefore the Hamiltonian of the system is [13]:

$$H = J_{\parallel} \sum_{a=1,2} \sum_{n} S_{a,n} S_{a,n+1} + J_{\perp} \sum_{n} S_{1,n} S_{2,n} \tag{2.56}$$

where $J_{\parallel} > 0$ and $J_{\perp} > 0$. A representation of the system is present in Fig. 2.3.

The Hamiltonian of the system is characterized by the continuous symmetry $SU(2)$, which represents rotation in spin space. Therefore the Hamiltonian is completely rotation invariant. The system is also characterized by:

- invariance under traslation if there are periodic boundary condition;
- invariance under the interchange of the two chains.

  These properties are ensured by the fact that interaction is always the same along a chain and it is the same on both chains.

- Spin-flip symmetry.

  The important point is the antiferromagnetic order of spins if we want to have the minimum of the Hamiltonian, since $J_{\parallel} > 0$ and $J_{\perp} > 0$.

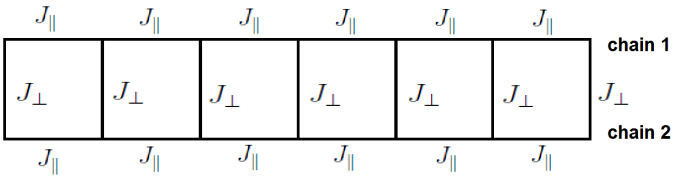

Figure 2.3: Representation of a standard spin ladder composed by two Heisenberg chains with seven sites on each chain.

2.9 Effective action: NLσM

The study of spin ladders can be generalized to the case of n_l legs of lenght N. Therefore the Hamiltonian of the system becomes [7]:

$$H = \sum_{a=1}^{n_l} \sum_{n=1}^{N} [J_{\parallel,a} S_{a,n} S_{a,n+1} + J_{\perp,a,a+1} S_{a,n} S_{a+1,n}] \tag{2.57}$$

where $J_{\parallel,a}$ and $J_{\perp,a,a+1}$ are such that antiferromagnetic order represents the classical minimum of the Hamiltonian.

Using path integral formulation (2.15), (2.16) and (2.17) and coherent states (2.9) and (2.10) the euclidean action can be written as (remember also (2.37)) [7]:

$$S_E[\hat{\Omega}] = -is \sum_{a,n} \omega[\hat{\Omega}_{a,n}(\tau)] + \int_0^\beta d\tau H(\tau). \tag{2.58}$$

Therefore the partition function is (remember also (2.21) and (2.22)):

$$Z = \int \mathcal{D}\hat{\Omega} e^{-S_E[\hat{\Omega}]} \tag{2.59}$$

$$Z = \int \mathcal{D}\hat{\Omega} \exp\left(is \sum_{a,n} \omega[\hat{\Omega}_{a,n}(\tau)] - \int_0^\beta d\tau H(\tau) \right). \tag{2.60}$$

We suppose that at quantum level we have short-range antiferromagnetic correlations so that coherent states can be described by Haldane map (2.38) specialized for this system [7]:

$$\hat{\Omega}_{a,n}(\tau) = (-1)^{a+n} \hat{\phi}(n,\tau) \left(1 - \frac{|\mathbf{l}_a(n,\tau)|^2}{s^2} \right)^{\frac{1}{2}} + \frac{|\mathbf{l}_a(n,\tau)|}{s}. \tag{2.61}$$

As we already know $\hat{\Omega}_{a,n}^2 = 1$, it implies that $\hat{\phi}(n)^2 = 1$ and $\hat{\phi}(n) \cdot \mathbf{l}_a(n) = 0$.

We assume that the field $\mathbf{l}_a(n)$ is small so that $\frac{|\mathbf{l}_a(n)|}{s} \ll 1$ and that the field $\hat{\phi}(n)$ is slowly varying. An important consequence of this assumption is that we will consider terms up to quadratic order in $\mathbf{l}_a(n,\tau)$, $\hat{\phi}(n,\tau)$ and its derivatives.

$\hat{\phi}$ does not depend on the index a which labels sites along the rungs, but it depends on the index n which labels sites along each leg. It means that the the field $\hat{\phi}$ does not change along a rung so staggered spin-spin correlations have a correlation lenght ξ which is greater than the width of the ladder $n_l a$.

Now we deal with the Hamiltonian (2.57), firstly we write it in terms of coherent states and secondly we use (2.61) to develop its expression [7]. We are interested in the continuum limit. The Hamiltonian becomes [7]:

$$H(\tau) = \sum_{a=1}^{n_l} \sum_{n=1}^{N} [J_{\parallel,a} s^2 \hat{\Omega}_{a,n}(\tau) \cdot \hat{\Omega}_{a,n+1}(\tau) + J_{\perp,a,a+1} s^2 \hat{\Omega}_{a,n}(\tau) \cdot \hat{\Omega}_{a+1,n}(\tau)]; \tag{2.62}$$

Now we compute both terms in (2.62) which are [7]:

$$\sum_{a=1}^{n_l} \sum_{n=1}^{N} J_{\parallel,a} s^2 \hat{\Omega}_{a,n}(\tau) \cdot \hat{\Omega}_{a,n+1}(\tau) \simeq$$

$$\simeq \int dx \left(\frac{s^2 \sum_{a=1}^{n_l} J_{\parallel,a}}{2} \hat{\phi}'^2(x,\tau) + 2 \sum_{a=1}^{n_l} \left(J_{\parallel,a} |\mathbf{l}_a(x,\tau)|^2 \right) \right); \tag{2.63}$$

$$\sum_{a=1}^{n_l} \sum_{n=1}^{N} J_{\perp,a,a+1} s^2 \hat{\Omega}_{a,n}(\tau) \cdot \hat{\Omega}_{a+1,n}(\tau) \simeq$$

$$\simeq \int dx \sum_{a=1}^{n_l} J_{\perp,a,a+1} \left(-1 + \frac{|\mathbf{l}_a(n,\tau)|^2}{2s^2} + \frac{|\mathbf{l}_{a+1}(n,\tau)|^2}{2s^2} + \frac{\mathbf{l}_a(n,\tau) \cdot \mathbf{l}_{a+1}(n,\tau)}{s^2} \right); \tag{2.64}$$

Therefore (2.62) can be written as [7]:

$$H(\tau) = \frac{1}{2} \int dx \left(s^2 \sum_a J_{\parallel,a} \hat{\phi}'^2(x,\tau) + \sum_{a,b} \mathbf{l}_a(x,\tau) M_{a,b} \mathbf{l}_b(x,\tau) \right) \tag{2.65}$$

where matrix $M_{a,b}$ is expressed in terms of $J_\parallel$ and $J_\perp$. In particular it is:
$4J_{\parallel,a} + J_{\perp,a,a+1} + J_{\perp,a,a-1}$ for $a = b$ and $J_{\perp,a,b}$ for $|a - b| = 1$ and $J_{\perp,1,0} = J_{\perp,n_l,n_l+1} = 0$.

Now we focus on the sum of Berry phases which can be computed as follows [3, 7]:

$$\delta\omega[\hat{\Omega}] = \int_0^\beta d\tau \hat{\Omega} \cdot (\dot{\hat{\Omega}} \times \delta\hat{\Omega}), \tag{2.66}$$

$$\delta\omega[\hat{\phi}] = \int_0^\beta d\tau \delta\hat{\phi} \cdot (\hat{\phi} \times \dot{\hat{\phi}}). \tag{2.67}$$

These expression are used to calculate the sum of Berry phases at leading order [7]:

$$s \sum_{a,n} \omega[\hat{\Omega}_{a,n}(\tau)] = s \sum_{a,n} (-1)^{a+n} \omega[\hat{\phi}(n,\tau)] + \sum_{a,n} \int_0^\beta d\tau (\hat{\phi}(n,\tau) \times \dot{\hat{\phi}}(n,\tau)) \cdot \mathbf{l}_a(n,\tau) =$$

$$= \Gamma[\hat{\phi}(n,\tau)] + \sum_{a,n} \int_0^\beta d\tau (\hat{\phi}(n,\tau) \times \dot{\hat{\phi}}(n,\tau)) \cdot \mathbf{l}_a(n,\tau). \tag{2.68}$$

We can complete the square and perform a Gaussian integration over $\mathbf{l}_a(n,\tau)$. We have that [7]:

$$Z = \int \mathcal{D}\hat{\phi} \exp\left(i\Gamma[\hat{\phi}] - \int_0^\beta d\tau \int dx \frac{\sum_{a,b} M^{-1}_{a,b}}{2} |\dot{\hat{\phi}}|^2 \right). \tag{2.69}$$

Coherently with paragraph 2.6 we find that the model is mapped in a non linear sigma model NLσM in (1+1) dimensions [7]:

$$Z = \int \mathcal{D}\hat{\phi} \exp\left(i\Gamma[\hat{\phi}] - \int_0^\beta d\tau \int dx \frac{1}{2g} [\frac{1}{v_s} \dot{\hat{\phi}}^2 + v_s \hat{\phi}'^2] \right), \tag{2.70}$$

where non linear sigma model NLσM parameters are [7]:

$$g^{-1} = s \left(\sum_{a,b,c} J_{\parallel,a} M^{-1}_{b,c} \right)^{\frac{1}{2}}, \tag{2.71}$$

$$v_s = s \left(\frac{\sum_a J_{\parallel,a}}{\sum_{b,c} M^{-1}_{b,c}} \right)^{\frac{1}{2}}. \tag{2.72}$$

2.10 Topological term: even odd number of legs

$\Gamma[\hat{\phi}]$ represents the topological terms and it corresponds to:

$$i\Gamma[\hat{\phi}] = is \sum_a (-1)^a \sum_n (-1)^n \omega[\hat{\phi}(n,\tau)]. \tag{2.73}$$

Since the field $\hat{\phi}(n,\tau)$ does not depend on a then $\sum_n (-1)^n \omega[\hat{\phi}(n,\tau)]$ is the same for each a. The factor $\sum_a (-1)^a$ is 0 for even n_l and -1 for odd n_l [7]. It means that in the first case we have [7]:

$$i\Gamma[\hat{\phi}] = 0 \tag{2.74}$$

and in the second case we have [7]:

$$i\Gamma[\hat{\phi}] = \sum_a ((-1)^a) \left(-\frac{is}{2} \int_0^\beta d\tau \int dx \hat{\phi} \cdot (\dot{\hat{\phi}} \times \hat{\phi}') \right) = 2\pi \sum_a ((-1)^a) \left(-\frac{is}{4\pi} \int_0^\beta d\tau \int dx \hat{\phi} \cdot (\dot{\hat{\phi}} \times \hat{\phi}') \right)$$

$$= \frac{i\theta}{4\pi}\left(-\int_0^\beta d\tau \int dx \hat{\phi}\cdot(\dot{\hat{\phi}}\times\hat{\phi}')\right). \tag{2.75}$$

To summarize the results we can say that: ladders which have an even number of legs are mapped into a (1+1) NLσM without topological term and they are therefore gapped, whereas ladders which have an odd number of legs are mapped into a (1+1) NLσM with topological term and they are therefore gapless for half-odd integer spin.

In the regime $J_\perp \ll J_\parallel$ the energy gap decreases with the number of legs $\Delta \sim \exp(-\pi s n_l)$, if $n_l \to \infty$ the difference between odd and even number of legs disappears [7].

In the regime $J_\perp \gg J_\parallel$ the energy gap can be computed by $\Delta = v_s g$ [7].

Chapter 3

Topological terms in staggered spin ladders

3.1 Analytical analysis

3.1.1 The model and its characteristics

In the previous chapter we discussed the case of standard spin ladders with n_l legs of lenght N. We remember that the topological term is different from zero for odd n_l, while it is zero for even n_l [7].
Now we want to focus on $n_l = 2$ ladders and to see if the introduction of a staggered interaction along both the chains can give a nonvanishing topological term even if $n_l = 2$. We consider these two possible cases:

- Case A: the ladder is characterized by a same staggered interaction along the two chains:

$$H = \sum_{a=1,2} \sum_{i=1}^{N} \left\{ J_{\parallel,a}(1 + (-1)^i \gamma) S_a(i) S_a(i+1) + J'_{\perp,a,a+1} S_a(i) S_{a+1}(i) \right\} \tag{3.1}$$

  We will show that the topological term is still zero in this case.

- Case B: the ladder is characterized by a staggered interaction in one chain which is shifted by one site with respect to that of the second chain:

$$H = \sum_{i=1}^{N} J_{\parallel,1}(1 + (-1)^{i-1} \gamma) S_1(i) S_1(i+1) + \sum_{i=1}^{N} J_{\parallel,2}(1 + (-1)^i \gamma) S_2(i) S_2(i+1) +$$

$$+ \sum_{a=1,2} \sum_{i=1}^{N} J'_{\perp,a,a+1} S_a(i) S_{a+1}(i) \tag{3.2}$$

A nonvanishing topological term is present in this case. A situation equivalent to this one can be achieved if we invert the two chains. We would obtain the same topological term except for a sign but the physical consequences are equal.

Both (3.1) and (3.2) are invariant under translation by an even number of sites with PBC. In (3.1) if we invert the chains nothing changes, because staggered interaction is the same in both chains. In (3.2) if we invert the chains and we translate by one site with PBC we obtain exactly the same system. But, as sais before, even if we only invert the two chains the physical content does not change.

In (3.1) and (3.2) $J_{\parallel,1}$, $J_{\parallel,2}$, $J'_{\perp,a,a+1}$ are such that antiferromagnetic order represents the classical minimum of the Hamiltonian.

We represent the configurations corresponding to these two cases in Fig. 3.1 below, in this figure we consider seven sites on each chain.

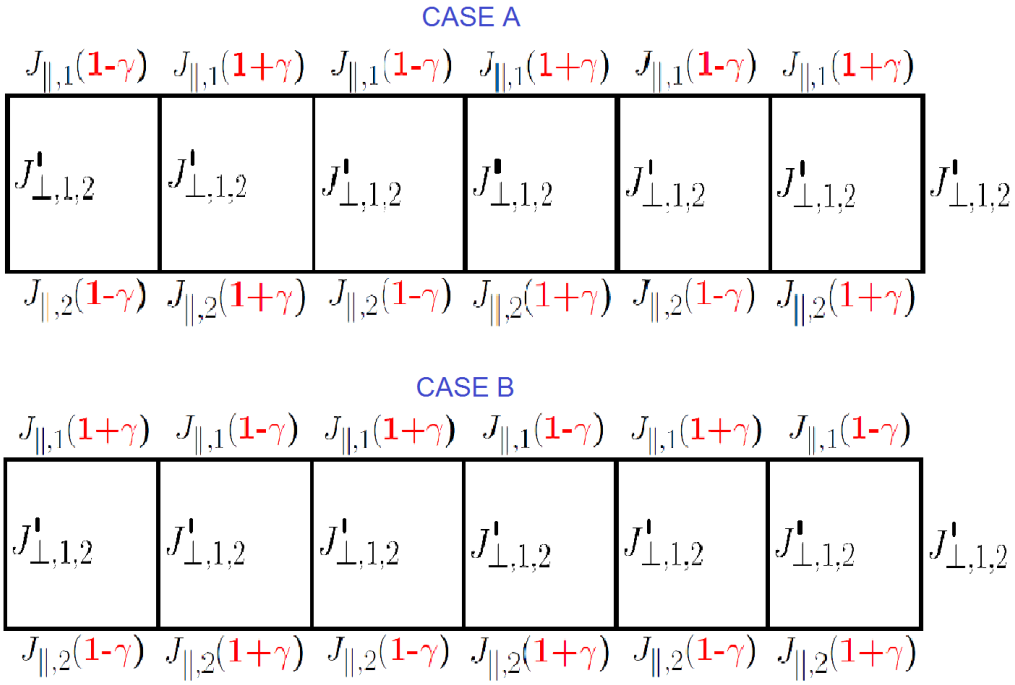

Figure 3.1: Representation of the ladders corresponding to the two Hamiltonians (3.1), (3.2), considering seven sites on each of them.

As in the previous chapter, we can consider the path integral formulation of the partition function (2.15), (2.16), (2.17) using coherent states (2.9), (2.10). In each of the two cases we have the following expression for the euclidean action [3, 7]:

$$S_E[\hat{\Omega}] = -is\sum_{a,i}\omega[\hat{\Omega}_{a,i}(\tau)] + \int_0^\beta d\tau H(\tau). \tag{3.3}$$

Therefore the partition function can be written in this way:

$$Z = \int \mathcal{D}\hat{\Omega} e^{-S_E[\hat{\Omega}]} \tag{3.4}$$

$$Z = \int \mathcal{D}\hat{\Omega} \exp\left(is\sum_{a,i}\omega[\hat{\Omega}_{a,i}(\tau)] - \int_0^\beta d\tau H(\tau)\right). \tag{3.5}$$

In the previous expression (3.5) we know that the first term is given by Berry phases and in the second term we replace operator $S_a(i)$ by the variables $s\hat{\Omega}_a(i,\tau)$. Then we can specialize the Haldane map (2.38) for these spin ladders, under the assumption that at quantum level we have short-range antiferromagnetic correlations. The map used is the same already seen in the previous chapter [7]:

$$\hat{\Omega}_{a,i}(\tau) = (-1)^{a+i}\hat{\phi}(i,\tau)\left(1 - \frac{|\mathbf{l}_a(i,\tau)|^2}{s^2}\right)^{\frac{1}{2}} + \frac{|\mathbf{l}_a(i,\tau)|}{s}. \tag{3.6}$$

As we do in standard spin ladders we suppose that $\frac{|\mathbf{l}_a(i,\tau)|}{s} \ll 1$ and that the field $\hat{\phi}(i,\tau)$ is slowly varying. It means that we consider terms up to quadratic order in $\mathbf{l}_a(i,\tau)$, $\hat{\phi}(i,\tau)$ and its derivatives. Furthermore $\hat{\phi}$ does not depend on the index a which labels sites along the rungs, it implies that it does not change along a rung. Finally, we know that $\hat{\Omega}_{a,i}^2 = 1$, so $\hat{\phi}(i,\tau)^2 = 1$ and $\hat{\phi}(i,\tau)\cdot\mathbf{l}_a(i,\tau) = 0$.

3.1.2 Case A

Effective action

We consider the first case, case A, which corresponds to an equal staggered interaction in the two chains of the ladder. We rewrite the Hamiltonian of this system:

$$H = \sum_{a=1,2}\sum_{i=1}^{N}\left\{J_{\parallel,a}(1+(-1)^i\gamma)S_a(i)S_a(i+1) + J'_{\perp,a,a+1}S_a(i)S_{a+1}(i)\right\}. \tag{3.7}$$

In order to achieve the path integral formulation of the partition function (3.4) and (3.5), we substitute $S_a(i)$, $S_a(i+1)$ and $S_{a+1}(i)$ with $s\hat{\Omega}_a(i,\tau)$, $s\hat{\Omega}_a(i+1,\tau)$ and $s\hat{\Omega}_{a+1}(i,\tau)$.

Therefore the Hamiltonian (3.7) becomes:

$$H(\tau) = \sum_{a,i} \left\{ J_{\parallel,a} s^2 (1 + (-1)^i \gamma) \hat{\Omega}_a(i,\tau) \hat{\Omega}_a(i+1,\tau) + J'_{\perp,a,a+1} s^2 \hat{\Omega}_a(i,\tau) \hat{\Omega}_{a+1}(i,\tau) \right\}. \tag{3.8}$$

Now we use the map (3.6) to express $\hat{\Omega}_a(i,\tau)$, $\hat{\Omega}_a(i+1,\tau)$ and $\hat{\Omega}_{a+1}(i,\tau)$ in the Hamiltonian (3.8), therefore we have to compute the following terms:

- the first term to be calculated is the sum of the interactions along each chain:

$$\sum_{a,i} J_{\parallel,a} s^2 (1 + (-1)^i \gamma) \hat{\Omega}_a(i,\tau) \hat{\Omega}_a(i+1,\tau); \tag{3.9}$$

- the second term to be calculated is the contribution due to the interaction between the two chains:

$$\sum_{a,i} J'_{\perp,a,a+1} s^2 \hat{\Omega}_a(i,\tau) \hat{\Omega}_{a+1}(i,\tau). \tag{3.10}$$

These terms are computed in Appendix A and we achieve these results:

- the sum of the interactions along each chain becomes:

$$\sum_{a,i} J_{\parallel,a} s^2 (1 + (-1)^i \gamma) \left(-1 + \frac{\hat{\phi'}^2(i,\tau)}{2} + 2 \frac{(\mathbf{l}_a(i,\tau))^2}{s^2} + (-1)^{a+i} \left(-2 \frac{\hat{\phi'}(i,\tau) \mathbf{l}_a(i,\tau)}{s} \right) \right); \tag{3.11}$$

- the contribution due to the interaction between the two chains becomes:

$$\sum_{a,i} J'_{\perp,a,a+1} s^2 \left(-1 + \frac{1}{2} \frac{|\mathbf{l}_a(i,\tau)|^2}{s^2} + \frac{1}{2} \frac{|\mathbf{l}_{a+1}(i,\tau)|^2}{s^2} + \frac{\mathbf{l}_a(i,\tau)}{s} \frac{\mathbf{l}_{a+1}(i,\tau)}{s} \right). \tag{3.12}$$

Continuum limit for the Hamiltonian

Now we consider the continuum limit of the Hamiltonian, sum of (3.11) and (3.12) and in this limit we can neglect constant and alternated terms. In order to better understand, we split (3.11) in two contributions and we compute their continuum limit separately. Therefore the first contribution of (3.11) is:

$$\sum_{a,i} J_{\parallel,a} s^2 \left(-1 + \frac{\hat{\phi'}^2(i,\tau)}{2} + 2 \frac{(\mathbf{l}_a(i,\tau))^2}{s^2} + (-1)^{a+i} \left(-2 \frac{\hat{\phi'}(i,\tau) \mathbf{l}_a(i,\tau)}{s} \right) \right) \rightarrow$$
$$\int dx \left(\frac{s^2 \sum_a J_{\parallel,a}}{2} \hat{\phi'}^2(x,\tau) + 2 \sum_a J_{\parallel,a} (\mathbf{l}_a(x,\tau))^2 \right). \tag{3.13}$$

The second contribution of (3.11) is:

$$\sum_{a,i} J_{\parallel,a} s^2 (-1)^i \gamma \left(-1 + \frac{\hat{\phi}'^2(i,\tau)}{2} + 2\frac{(\mathbf{l}_a(i,\tau))^2}{s^2} + (-1)^{a+i} \left(-2\frac{\hat{\phi}'(i,\tau)\mathbf{l}_a(i,\tau)}{s} \right) \right) \rightarrow$$

$$\int dx (-2s\gamma \sum_a (-1)^a J_{\parallel,a} \hat{\phi}'(x,\tau)\mathbf{l}_a(x,\tau)). \tag{3.14}$$

Then we also consider the continuum limit of (3.12):

$$\sum_{a,i} J'_{\perp,a,a+1} s^2 \left(-1 + \frac{1}{2}\frac{|\mathbf{l}_a(i,\tau)|^2}{s^2} + \frac{1}{2}\frac{|\mathbf{l}_{a+1}(i,\tau)|^2}{s^2} + \frac{\mathbf{l}_a(i,\tau)}{s}\frac{\mathbf{l}_{a+1}(i,\tau)}{s} \right) \rightarrow$$

$$\int dx \sum_a J'_{\perp,a,a+1} \left(\frac{1}{2}|\mathbf{l}_a(x,\tau)|^2 + \frac{1}{2}|\mathbf{l}_{a+1}(x,\tau)|^2 + \mathbf{l}_a(x,\tau)\mathbf{l}_{a+1}(x,\tau) \right). \tag{3.15}$$

We can write the sum of (3.13), (3.14) and (3.15) in a more compact way if we introduce the following matrix:

$$L_{a,b} = \begin{cases} 4J_{\parallel,a} + J'_{\perp,a,a+1} + J'_{\perp,a,a-1} & a = b \\ J'_{\perp,a,b} & |a-b| = 1 \end{cases} \tag{3.16}$$

where $J'_{\perp,a,b} = J'_{\perp,b,a}$ and $J'_{\perp,1,0} = 0$ and $J'_{\perp,n_l,n_l+1} = 0$, so we obtain the following expression for the Hamiltonian:

$$H(\tau) = \int dx \left[\frac{s^2 \sum_a J_{\parallel,a}}{2} \hat{\phi}'^2(x,\tau) + \sum_{a,b} \frac{\mathbf{l}_a(x,\tau) L_{a,b} \mathbf{l}_b(x,\tau)}{2} + (-2s\gamma \sum_a (-1)^a J_{\parallel,a} \hat{\phi}'(x,\tau)\mathbf{l}_a(x,\tau)) \right]. \tag{3.17}$$

Continuum limit of Berry phases contribution

The Berry phase term is:

$$is \sum_{i,a} \omega[\hat{\Omega}_a(i,\tau)] = is \sum_{i,a} (-1)^{a+i} \omega[\hat{\phi}(i,\tau)] + i \sum_{i,a} \int \mathbf{l}_a(i,\tau) \cdot (\hat{\phi}(i,\tau) \times \dot{\hat{\phi}}(i,\tau)) d\tau. \tag{3.18}$$

We want to know the continuum limit of (3.18) too. Therefore we consider the first term in (3.18) which in the continuum limit becomes as follows:

$$is \sum_{i,a} (-1)^{a+i} \omega[\hat{\phi}(i,\tau)] = is \sum_a (-1)^a \sum_i (-1)^i \omega[\hat{\phi}(i,\tau)] =$$

$$= is \sum_a (-1)^a \sum_i \left(\omega[\hat{\phi}(2i,\tau)] - \omega[\hat{\phi}(2i-1,\tau)] \right)$$

$$\rightarrow is\sum_a (-1)^a \left(-\frac{1}{2}\int \hat{\phi}'(x,\tau)\cdot(\hat{\phi}(x,\tau)\times\dot{\hat{\phi}}(x,\tau))d\tau dx\right) =$$

$$= \frac{-is}{2}\sum_a (-1)^a \int \hat{\phi}'(x,\tau)\cdot(\hat{\phi}(x,\tau)\times\dot{\hat{\phi}}(x,\tau))dxd\tau. \tag{3.19}$$

Then we focus on the second term in (3.18), whose continuum limit is:

$$i\sum_{i,a}\int \mathbf{l}_a(i,\tau)\cdot(\hat{\phi}(i,\tau)\times\dot{\hat{\phi}}(i,\tau))d\tau$$

$$\rightarrow i\sum_a \int \mathbf{l}_a(x,\tau)\cdot(\hat{\phi}(x,\tau)\times\dot{\hat{\phi}}(x,\tau))dxd\tau. \tag{3.20}$$

Therefore the Berry phase contribution becomes:

$$is\sum_{i,a}\omega[\hat{\Omega}_a(i,\tau)] =$$

$$\int dxd\tau\left[\frac{-is}{2}\sum_a (-1)^a\hat{\phi}'(x,\tau)\cdot(\hat{\phi}(x,\tau)\times\dot{\hat{\phi}}(x,\tau)) + i\sum_a \mathbf{l}_a(x,\tau)\cdot(\hat{\phi}(x,\tau)\times\dot{\hat{\phi}}(x,\tau))\right]. \tag{3.21}$$

Therefore in the partition function (3.5) we achieve:

$$-\int d\tau H(\tau) + is\sum_{i,a}\omega[\hat{\Omega}_a(i,\tau)] =$$

$$\int dxd\tau\left[-\frac{s^2\sum_a J_{\parallel,a}}{2}\hat{\phi'}^2(x,\tau) - \sum_{a,b}\frac{\mathbf{l}_a(x,\tau)L_{a,b}\mathbf{l}_b(x,\tau)}{2} + 2s\gamma\sum_a (-1)^a J_{\parallel,a}\hat{\phi}'(x,\tau)\mathbf{l}_a(x,\tau)\right] +$$

$$\int dxd\tau\left[-\frac{is}{2}\sum_a (-1)^a\hat{\phi}'(x,\tau)\cdot(\hat{\phi}(x,\tau)\times\dot{\hat{\phi}}(x,\tau)) + i\sum_a \mathbf{l}_a(x,\tau)\cdot(\hat{\phi}(x,\tau)\times\dot{\hat{\phi}}(x,\tau))\right]. \tag{3.22}$$

In the absence of staggering ($\gamma = 0$) this result would be:

$$-\int d\tau H(\tau) + is\sum_{i,a}\omega[\hat{\Omega}_a(i,\tau)] =$$

$$\int dxd\tau\left[-\frac{s^2\sum_a J_{\parallel,a}}{2}\hat{\phi'}^2(x,\tau) - \sum_{a,b}\frac{\mathbf{l}_a(x,\tau)L_{a,b}\mathbf{l}_b(x,\tau)}{2}\right] +$$

$$\int dxd\tau \left[-\frac{is}{2} \sum_a (-1)^a \hat{\phi}'(x,\tau) \cdot (\hat{\phi}(x,\tau) \times \dot{\hat{\phi}}(x,\tau)) + i \sum_a \mathbf{l}_a(x,\tau) \cdot (\hat{\phi}(x,\tau) \times \dot{\hat{\phi}}(x,\tau)) \right] \tag{3.23}$$

which is the same achieved in the previous chapter (2.65), (2.68) when we discussed standard spin ladders $\gamma = 0$ [7]. Therefore we check the consistency of our result (3.23) with what we already know (2.65), (2.68).

Gaussian integral

In Appendix B we show how to complete the square in $\mathbf{l}_a(x,\tau)$ in (3.22) so that we have a Gaussian integral in $\mathbf{l}_a(x,\tau)$ and $\mathbf{l}_a(x,\tau)$ degrees of freedom can be integrated out in the partition function (3.5).
Therefore the partition function (3.5) becomes:

$$Z = \int \mathcal{D}\hat{\phi} \exp\left(- \int dxd\tau \mathcal{L}(x,\tau) \right). \tag{3.24}$$

From (3.24) the Langrangian density is:

$$\mathcal{L}(x,\tau) = +\dot{\hat{\phi}}^2(x,\tau) \frac{\sum_{d,b} L^{-1}_{d,b}}{2} + \hat{\phi}'^2(x,\tau) \left(-4s^2\gamma^2 \sum_{d,b} (-1)^d J_{\parallel,d} \frac{L^{-1}_{d,b}}{2} (-1)^b J_{\parallel,b} + \frac{s^2 \sum_a J_{\parallel,a}}{2} \right)$$
$$+ \hat{\phi}'(x,\tau) \cdot (\hat{\phi}(x,\tau) \times \dot{\hat{\phi}}(x,\tau)) \left(\frac{is}{2} \sum_a (-1)^a \right). \tag{3.25}$$

Topological term

The Lagrangian density can be compared to that of NLσM plus a topological term:

$$\mathcal{L}(x,\tau) = \frac{1}{2g} \left(\frac{1}{v_s} \dot{\hat{\phi}}^2(x,\tau) + v_s \hat{\phi}'^2(x,\tau) \right) + \frac{i\theta}{4\pi} \hat{\phi}'(x,\tau) \cdot (\hat{\phi}(x,\tau) \times \dot{\hat{\phi}}(x,\tau)). \tag{3.26}$$

The two expressions (3.25) and (3.26) are equal if:

$$\theta = 2\pi s \sum_a (-1)^a. \tag{3.27}$$

Since we consider $a = 1, 2$ we do not have a topological term.

Furthermore if we want (3.25) and (3.26) to be equal we also have:

$$\frac{1}{2gv_s} = \frac{\sum_{d,b} L^{-1}_{d,b}}{2}, \tag{3.28}$$

$$\frac{v_s}{2g} = -4s^2\gamma^2 \sum_{d,b} (-1)^d J_{\parallel,d} \frac{L^{-1}_{d,b}}{2} (-1)^b J_{\parallel,b} + \frac{s^2 \sum_a J_{\parallel,a}}{2}, \tag{3.29}$$

$$\frac{1}{g} = \sqrt{\left(\sum_{d,b} L^{-1}_{d,b}\right)\left(-4s^2\gamma^2 \sum_{d,b} (-1)^d J_{\parallel,d} L^{-1}_{d,b} (-1)^b J_{\parallel,b} + s^2 \sum_a J_{\parallel,a}\right)}, \tag{3.30}$$

$$v_s = \sqrt{\frac{\left(-4s^2\gamma^2 \sum_{d,b} (-1)^d J_{\parallel,d} L^{-1}_{d,b} (-1)^b J_{\parallel,b} + s^2 \sum_a J_{\parallel,a}\right)}{\sum_{d,b} L^{-1}_{d,b}}}. \tag{3.31}$$

In the absence of staggering ($\gamma = 0$) these results would be:

$$\theta = 2\pi s \sum_a (-1)^a. \tag{3.32}$$

Since we consider $a = 1, 2$ we already know from paragraph 2.10 that we do not have a topological term.

Furthermore we would have:

$$\frac{1}{g} = s\sqrt{\sum_{a,d,b} J_{\parallel,a} L^{-1}_{d,b}}, \tag{3.33}$$

$$v_s = s\sqrt{\frac{\sum_a J_{\parallel,a}}{\sum_{d,b} L^{-1}_{d,b}}}. \tag{3.34}$$

which are the same achieved in the previous chapter (2.71), (2.72), (2.73), (2.74) when we discussed standard spin ladders $\gamma = 0$ [7]. Therefore we check the consistency of our results (3.32), (3.33), (3.34) with those already known (2.71), (2.72), (2.73), (2.74).

3.1.3 Case B

Effective action

We consider the second case, case B, which corresponds to a staggered interaction in the first chain shifted by one site with respect to that of the second chain. We rewrite the Hamiltonian of this system as:

$$H = \sum_{i=1}^{N} J_{\parallel,1}(1 + (-1)^{i-1}\gamma) S_1(i) S_1(i+1) + \sum_{i=1}^{N} J_{\parallel,2}(1 + (-1)^{i}\gamma) S_2(i) S_2(i+1) +$$

$$+ \sum_{a=1,2} \sum_{i=1}^{N} J'_{\perp,a,a+1} S_a(i) S_{a+1}(i). \tag{3.35}$$

In order to achieve the path integral formulation of the partition function (3.4) and (3.5), we substitute $S_a(i)$, $S_a(i+1)$ and $S_{a+1}(i)$ with $s\hat{\Omega}_a(i,\tau)$, $s\hat{\Omega}_a(i+1,\tau)$ and $s\hat{\Omega}_{a+1}(i,\tau)$. Therefore the Hamiltonian (3.35) becomes:

$$H = \sum_{i=1}^{N} J_{\parallel,1} s^2 (1+(-1)^{i-1}\gamma)\hat{\Omega}_1(i,\tau)\hat{\Omega}_1(i+1,\tau) + \sum_{i=1}^{N} J_{\parallel,2} s^2 (1+(-1)^{i}\gamma)\hat{\Omega}_2(i,\tau)\hat{\Omega}_2(i+1,\tau) +$$

$$+ \sum_{a=1,2}\sum_{i=1}^{N} J'_{\perp,a,a+1} s^2 \hat{\Omega}_a(i,\tau)\hat{\Omega}_{a+1}(i,\tau). \tag{3.36}$$

The first term of (3.36) is computed using the map (3.6) in Appendix A and it becomes:

$$\sum_{i=1}^{N} J_{\parallel,1} s^2 (1+(-1)^{i-1}\gamma)\hat{\Omega}_1(i,\tau)\hat{\Omega}_1(i+1,\tau) =$$

$$= \sum_{i=1}^{N} J_{\parallel,1} s^2 (1+(-1)^{i-1}\gamma)\left[-1 + \frac{\hat{\phi}'^2}{2}(i,\tau) + 2\frac{(\mathbf{l}_1(i,\tau))^2}{s^2} + (-1)^{1+i}\left(-2\frac{\hat{\phi}'(i,\tau)\mathbf{l}_1(i,\tau)}{s}\right)\right] =$$

$$= \sum_{i=1}^{N} J_{\parallel,1} s^2 (1+(-1)^{i-1}\gamma)\left[-1 + \frac{\hat{\phi}'^2}{2}(i,\tau) + 2\frac{(\mathbf{l}_1(i,\tau))^2}{s^2} + (-1)^{i}\left(+2\frac{\hat{\phi}'(i,\tau)\mathbf{l}_1(i,\tau)}{s}\right)\right]. \tag{3.37}$$

The second term of (3.36) is computed using the map (3.6) in Appendix A as before and it becomes:

$$\sum_{i=1}^{N} J_{\parallel,2} s^2 (1+(-1)^{i}\gamma)\hat{\Omega}_2(i,\tau)\hat{\Omega}_2(i+1,\tau) =$$

$$= \sum_{i=1}^{N} J_{\parallel,2} s^2 (1+(-1)^{i}\gamma)\left[-1 + \frac{\hat{\phi}'^2}{2}(i,\tau) + 2\frac{(\mathbf{l}_2(i,\tau))^2}{s^2} + (-1)^{2+i}\left(-2\frac{\hat{\phi}'(i,\tau)\mathbf{l}_2(i,\tau)}{s}\right)\right] =$$

$$= \sum_{i=1}^{N} J_{\parallel,2} s^2 (1+(-1)^{i}\gamma)\left[-1 + \frac{\hat{\phi}'^2}{2}(i,\tau) + 2\frac{(\mathbf{l}_2(i,\tau))^2}{s^2} + (-1)^{i}\left(-2\frac{\hat{\phi}'(i,\tau)\mathbf{l}_2(i,\tau)}{s}\right)\right]. \tag{3.38}$$

The third term of (3.36) is computed using the map (3.6) in Appendix A as before and it becomes:

$$\sum_{a=1,2}\sum_{i=1}^{N} J'_{\perp,a,a+1} s^2 \hat{\Omega}_a(i,\tau)\hat{\Omega}_{a+1}(i,\tau)$$

$$= \sum_i J'_{\perp,1,2} s^2 \left[-1 + \frac{|\mathbf{l}_1(i,\tau)|^2}{2s^2} + \frac{|\mathbf{l}_2(i,\tau)|^2}{2s^2} + \frac{\mathbf{l}_1(i,\tau)\mathbf{l}_2(i,\tau)}{s^2} \right]. \tag{3.39}$$

Therefore Hamiltonian (3.36), which is the sum of (3.37), (3.38) and (3.39), becomes:

$$H(\tau) = \sum_{i=1}^{N} J_{\parallel,1} s^2 (1+(-1)^{i-1}\gamma) \left[-1 + \frac{\hat{\phi}'^2}{2}(i,\tau) + 2\frac{(\mathbf{l}_1(i,\tau))^2}{s^2} + (-1)^i \left(+2\frac{\hat{\phi}'(i,\tau)\mathbf{l}_1(i,\tau)}{s} \right) \right] +$$

$$+ \sum_{i=1}^{N} J_{\parallel,2} s^2 (1+(-1)^i\gamma) \left[-1 + \frac{\hat{\phi}'^2}{2}(i,\tau) + 2\frac{(\mathbf{l}_2(i,\tau))^2}{s^2} + (-1)^i \left(-2\frac{\hat{\phi}'(i,\tau)\mathbf{l}_2(i,\tau)}{s} \right) \right] +$$

$$+ \sum_i J'_{\perp,1,2} s^2 \left[-1 + \frac{|\mathbf{l}_1(i,\tau)|^2}{2s^2} + \frac{|\mathbf{l}_2(i,\tau)|^2}{2s^2} + \frac{\mathbf{l}_1(i,\tau)\mathbf{l}_2(i,\tau)}{s^2} \right]. \tag{3.40}$$

We consider the continuum limit of Hamiltonian (3.40):

$$H(\tau) = \frac{J_{\parallel,1} s^s}{2} \int dx \hat{\phi}'^2(x,\tau) + 2J_{\parallel,1} \int dx (\mathbf{l}_1(x,\tau))^2 - 2J_{\parallel,1} s\gamma \int dx \hat{\phi}'(x,\tau)\mathbf{l}_1(x,\tau) +$$

$$+ \frac{J_{\parallel,2} s^s}{2} \int dx \hat{\phi}'^2(x,\tau) + 2J_{\parallel,2} \int dx (\mathbf{l}_2(x,\tau))^2 - 2J_{\parallel,2} s\gamma \int dx \hat{\phi}'(x,\tau)\mathbf{l}_2(x,\tau) +$$

$$+ \frac{J'_{\perp,1,2}}{2} \int dx \left[|\mathbf{l}_1(x,\tau)|^2 + |\mathbf{l}_2(x,\tau)|^2 + 2\mathbf{l}_1(x,\tau)\mathbf{l}_2(x,\tau) \right]. \tag{3.41}$$

In expression (3.41) constant and alternated terms can be neglected.

Therefore the Hamiltonian in the continuum limit is:

$$H(\tau) = \frac{\sum_{a=1,2} J_{\parallel,a} s^s}{2} \int dx \hat{\phi}'^2(x,\tau) - 2 \int dx \sum_{a=1,2} (J_{\parallel,a} s\gamma \hat{\phi}'(x,\tau)\mathbf{l}_a(x,\tau)) + \int dx \sum_{a,b} \frac{\mathbf{l}_a(x,\tau) L_{a,b} \mathbf{l}_b(x,\tau)}{2} \tag{3.42}$$

where we use matrix $L_{a,b}$ defined in (3.16).

In the partition function (3.5) there is also the Berry phase contribution, and now we focus on it:

$$is \sum_{a=1,2} \sum_i \omega[\hat{\Omega}_a(i,\tau)] =$$

$$= is \sum_{a=1,2} (-1)^a \sum_i (-1)^i \omega[\hat{\phi}(i,\tau)] + i \sum_{a=1,2} \sum_i \int d\tau \left(\hat{\phi}(i,\tau) \times \dot{\hat{\phi}}(i,\tau) \right) \cdot \mathbf{l}_a(i,\tau) =$$

$$= \sum_{a=1,2} (-1)^a \frac{-is}{2} \int dx \int d\tau \hat{\phi}'(x,\tau) \cdot \left(\hat{\phi}(x,\tau) \times \dot{\hat{\phi}}(x,\tau) \right) +$$

$$+ i \sum_{a=1,2} \int dx \int d\tau \left(\hat{\phi}(x,\tau) \times \dot{\hat{\phi}}(x,\tau) \right) \cdot \mathbf{l}_a(x,\tau) =$$

$$= 0 + i \sum_{a=1,2} \int dx \int d\tau \left(\hat{\phi}(x,\tau) \times \dot{\hat{\phi}}(x,\tau) \right) \cdot \mathbf{l}_a(x,\tau) \tag{3.43}$$

where the first term is zero because we consider $a = 1, 2$.

In the expression of the partition function (3.5), $-S_E[\hat{\Omega}]$ becomes as follows:

$$is \sum_{a=1,2} \sum_i \omega[\hat{\Omega}_a(i,\tau)] - \int d\tau H(\tau) =$$

$$= \int d\tau \int dx \left[i \sum_{a=1,2} \left(\hat{\phi}(x,\tau) \times \dot{\hat{\phi}}(x,\tau) \right) \cdot \mathbf{l}_a(x,\tau) \right.$$

$$\left. - \frac{\sum_{a=1,2} J_{\parallel,a} s^s}{2} \int dx \hat{\phi}'^2(x,\tau) + 2 \int dx \sum_{a=1,2} (J_{\parallel,a} s \gamma \hat{\phi}'(x,\tau) \mathbf{l}_a(x,\tau)) - \int dx \sum_{a,b} \frac{\mathbf{l}_a(x,\tau) L_{a,b} \mathbf{l}_b(x,\tau)}{2} \right]. \tag{3.44}$$

Gaussian integral

In Appendix B we show how to complete the square in $\mathbf{l}_a(x,\tau)$ in (3.44) so that we have a Gaussian integral in $\mathbf{l}_a(x,\tau)$ and $\mathbf{l}_a(x,\tau)$ degrees of freedom can be integrated out in the partition function (3.5).
Therefore the partition function (3.5) becomes:

$$Z = \int \mathcal{D}\hat{\phi} \exp\left(- \int dx d\tau \mathcal{L}(x,\tau) \right). \tag{3.45}$$

From (3.44) the Langrangian density is:

$$\mathcal{L}(x,\tau) = + \dot{\hat{\phi}}^2(x,\tau) \frac{\sum_{d,b} L^{-1}_{d,b}}{2} + \hat{\phi}'^2(x,\tau) \left(-4 s^2 \gamma^2 \sum_{d,b} J_{\parallel,d} \frac{L^{-1}_{d,b}}{2} J_{\parallel,b} + \frac{s^2 \sum_a J_{\parallel,a}}{2} \right)$$

$$-is\gamma\hat{\phi}'\left(\hat{\phi}\times\dot{\hat{\phi}}\right)\frac{+2J_{\parallel,1}\left(4J_{\parallel,2}+J'_{\perp,2,1}\right)+2J_{\parallel,2}\left(4J_{\parallel,1}+J'_{\perp,1,2}\right)-2J_{\parallel,1}J'_{\perp,2,1}-2J_{\parallel,2}J'_{\perp,1,2}}{16J_{\parallel,1}J_{\parallel,2}+4J_{\parallel,1}J'_{\perp,2,1}+4J_{\parallel,2}J'_{\perp,1,2}}. \tag{3.46}$$

Topological term

The Lagrangian density can also be written as the Lagrangian density of the NLσM plus a topological term:

$$\mathcal{L}(x,\tau)=\frac{1}{2g}\left(\frac{1}{v_s}\dot{\hat{\phi}}^2(x,\tau)+v_s\hat{\phi}'^2(x,\tau)\right)+\frac{i\theta}{4\pi}\hat{\phi}'(x,\tau)\cdot(\hat{\phi}(x,\tau)\times\dot{\hat{\phi}}(x,\tau)). \tag{3.47}$$

Therefore by comparing expression (3.46) with expression (3.47) we find:

$$\theta=-4\pi s\gamma\frac{+2J_{\parallel,1}\left(4J_{\parallel,2}+J'_{\perp,2,1}\right)+2J_{\parallel,2}\left(4J_{\parallel,1}+J'_{\perp,1,2}\right)-2J_{\parallel,1}J'_{\perp,2,1}-2J_{\parallel,2}J'_{\perp,1,2}}{16J_{\parallel,1}J_{\parallel,2}+4J_{\parallel,1}J'_{\perp,2,1}+4J_{\parallel,2}J'_{\perp,1,2}}, \tag{3.48}$$

$$\frac{1}{2gv_s}=\frac{\sum_{d,b}L^{-1}_{d,b}}{2}, \tag{3.49}$$

$$\frac{v_s}{2g}=-4s^2\gamma^2\sum_{d,b}J_{\parallel,d}\frac{L^{-1}_{d,b}}{2}J_{\parallel,b}+\frac{s^2\sum_a J_{\parallel,a}}{2}, \tag{3.50}$$

$$\frac{1}{g}=\sqrt{\left(\sum_{d,b}L^{-1}_{d,b}\right)\left(-4s^2\gamma^2\sum_{d,b}J_{\parallel,d}L^{-1}_{d,b}J_{\parallel,b}+s^2\sum_a J_{\parallel,a}\right)}, \tag{3.51}$$

$$v_s=\sqrt{\frac{\left(-4s^2\gamma^2\sum_{d,b}J_{\parallel,d}L^{-1}_{d,b}J_{\parallel,b}+s^2\sum_a J_{\parallel,a}\right)}{\sum_{d,b}L^{-1}_{d,b}}}. \tag{3.52}$$

In the expression (3.48) of θ we do not have the contribution $2\pi s\left(\sum_a(-1)^a\right)$ because we have already put $a=1,2$ in (3.43).
So, in order to sum up, we have that:

- when $\gamma=0$
$$\theta=2\pi s\left(\sum_a(-1)^a\right)=0;$$
- when we have an alternated staggered interaction as in this case
$$\theta=2\pi s\left(\sum_a(-1)^a\right)+$$

$$-4\pi s\gamma\frac{+2J_{\|,1}\left(4J_{\|,2}+J'_{\perp,2,1}\right)+2J_{\|,2}\left(4J_{\|,1}+J'_{\perp,1,2}\right)-2J_{\|,1}J'_{\perp,2,1}-2J_{\|,2}J'_{\perp,1,2}}{16J_{\|,1}J_{\|,2}+4J_{\|,1}J'_{\perp,2,1}+4J_{\|,2}J'_{\perp,1,2}}=$$

$$=-4\pi s\gamma\frac{+2J_{\|,1}\left(4J_{\|,2}+J'_{\perp,2,1}\right)+2J_{\|,2}\left(4J_{\|,1}+J'_{\perp,1,2}\right)-2J_{\|,1}J'_{\perp,2,1}-2J_{\|,2}J'_{\perp,1,2}}{16J_{\|,1}J_{\|,2}+4J_{\|,1}J'_{\perp,2,1}+4J_{\|,2}J'_{\perp,1,2}};$$

because $2\pi s\left(\sum_a(-1)^a\right)=0$ if $a=1,2$.

Furthermore (3.51) and (3.52) are consistent with (2.71) and (2.72) when $\gamma=0$.

3.2 Numerical analysis

Quantum many-body systems are a field of study that is attracting more and more an increasing interest. Phenomena as high-T_c superconductivity and topologically ordered phases fall into this research area and many efforts are made to describe them effectively. In order to understand the relevant interactions, which characterize their physics, simplified models are proposed. If we want to determine their properties only some lucky cases are exactly solvable while all others are described by numerical methods [25]. Therefore we are interested in the latter and we will describe them in the following paragraphs.

3.2.1 Density-matrix renormalization group algorithm

In 1992-1993 S. White introduced [35, 36] an improvement of the standard renormalization group approach used until then. Firstly we will explain what the standard approach is then we will focus on his innovative idea.

Standard RG algorithm

It is an algorithm which allows to achieve the ground state and some low-lying excited states for 1D lattice systems, such as for example the Heisenberg model or the Hubbard model. The steps of it are as follows [35, 36]:

- The 1D chain is usually broken into finite identical blocks. We can identify a block with $\mathcal{B}$ and the block Hamiltonian with H_B.
- We describe $\mathcal{B}$ by a list of the many-body states defined on the block. We call their number m and for each state we list all quantum numbers which are to be used. H_B concerns sites in block $\mathcal{B}$ and it is represented by an $m \times m$ matrix. In order to reconstract H (the Hamiltonian of the whole system) additional information are needed besides H_B and they are such to describe the interactions between blocks. Therefore, for example, in the Heisenberg model we need $m \times m$ matrix representations of S_i^Z, S_i^+, S_i^- for i equal to both left and right end sites of $\mathcal{B}$.
- At the beginning of the procedure one forms the Hamiltonian for two blocks joined together H_{BB} and $\mathcal{BB}$ has m^2 states.
- Then we diagonalize H_{BB}, obtaining the m lowest eigenvectors u^α.
- Matrix representations for S_l^Z,S_r^Z,... (l means the leftmost site of the right block and r means the rightmost site of the left block) for $\mathcal{BB}$ are formed from the corresponding matrices for $\mathcal{B}$. In order to write them in u^α basis, we can use matrix O which is such that $O(\alpha, i_1, i_2) = u^\alpha_{i_1,i_2}$.

- At this point we can consider the new block $\mathcal{B}'$, ($\mathcal{BB} \rightarrow \mathcal{B}'$), and the procedure starts again. The iteration is continued until the system is large enough to represent properties of the infinite system.

S. White understood that the main difficulty in this approach concerns the eigenstates of H_{BB} to be the states kept: since H_{BB} contains no connections to the rest of the lattice, its eigenstates have inappropriate features at the block ends [35, 36]. Therefore two alternatives to this standard approach were suggested:
- Combination of boundary conditions approach (CBC) is the first. In this case the lowest-lying eigenstates of several different block Hamiltonians are kept and these Hamiltonians differ only in the boundary conditions applied to the block. This approach is ill suited to interacting systems [35, 36].
- Superblock method is the second and it is the basis for the density matrix approach DMRG [35, 36]. We focus on it in the next paragraph below.

Density matrix RG algorithm

The superblock method is characterized by the fact that one diagonalizes a larger system (superblock) which is composed of three or more blocks and so it includes the two blocks $\mathcal{BB}$ which are used to form $\mathcal{B}'$. The wave functions of the superblock are projected onto $\mathcal{BB}$ and these projected states are kept [35, 36]. Here there is an important point:
· for a single-particle wave function this projection is single valued and trivial, furthermore in this case the accuracy increases rapidly with the number of extra blocks used [35, 36];
· for a many-particle wave function this projection is many valued. In fact a many-particle state usually "projects" onto a complete set of block states. However some of these states are more important than the others and the density matrix is used to tell us which states are the most important [35, 36].
In particular, if we keep the most probable eigenstates of the density matrix, we achieve the most accurate representation of the state of the system as a whole (the block plus the rest of the lattice).
We can suppose to have diagonalized a superblock and to have obtained a particular state $|\psi>$. If we now introduce $|i>$, $i = 1..., l$ and $|j>$, $j = 1, ..., J$, which are respectively a complete set of states of $\mathcal{BB}$ and the states of the rest of the superblock, then $|\psi>=\sum_{i,j}\psi_{i,j}|i>|j>$ [35, 36].
However we are interested to find for the system a set of states called u^α which are such that $|u^\alpha>=\sum_i u_i^\alpha|i>$ with $\alpha = 1, ..., m$ and such to be optimal in order to represent $|\psi>$. In other words, we wish to construct an accurate expansion of $|\psi>$ using $|u^\alpha>$ called $|\bar{\psi}>=\sum_{\alpha,j} a_{\alpha,j}|u^\alpha>|j>$ and to minimize $\| \, |\psi> - |\bar{\psi}> \|^2$ by varying over all $a_{\alpha,j}$ and all u^α ($<u^\alpha|u^\alpha>=\delta_{\alpha,\alpha'}$) [35, 36].
In order to find $a_{\alpha,j}$ and u^α through the minimization of $\| \, |\psi> - |\bar{\psi}> \|^2$ some steps are

necessary [35, 36]:

- whitout loss of generality we write $|\bar{\psi}>=\sum_\alpha a_\alpha|u^\alpha>|v^\alpha>$ with $v^\alpha=<j|v^\alpha>=N_\alpha a_{\alpha,j}$, N_α are such that $\sum_j |v_j^\alpha|^2=1$. We also replace $|\psi>=\sum_{i,j}\psi_{i,j}|i>|j>$ [35, 36].

- The difference $\| \, |\psi> - |\bar{\psi}> \|^2$ can be written in matrix notation. It is $\sum_{i,j}\left(\psi_{i,j}-\sum_{\alpha=1}^m a_\alpha u_i^\alpha v_j^\alpha\right)^2$. The solution to this minimization problem is known from linear algebra $\psi=UDV^T$, where U and D are $l\times l$ matrices and V is a $l\times J$ matrix. Linear algebra implies that u^α and v^α are the colums of U and V and a_α are the corresponding m largest magnitude diagonal elements of D. See [35] for details.

- Furthermore, since the reduced density matrix of the block is $\rho_{i,i'}=\sum_j \psi_{i,j}\psi_{i',j}=UD^2U^T$, the eigenvalues of ρ are equal to $w_\alpha=a_\alpha^2$. w_α represents the probability that the system is in the state u^α, so the optimal states u^α are those that correspond to the largest w_α, i.e. the largest eigenvalues of ρ [35, 36].
  In this case we suppose that the entire lattice is in a pure state, but the conceptual steps are the same even if it were mixed [35].

A density-matrix algorithm is defined by the form of the superblock, by the way in which blocks are enlarged and by the superblock eigenstates (target states) chosen to construct the block density matrix. By targeting only one state, the block states are more specilized for representing that state and fewer are necessary in order to obtain a certain accurancy. In general, if we deal with a cetain number of states m, we increase m in order to increase the accurancy [35, 36].

3.2.2 Tensor Network methods

Tensor Network (TN) methods have become increasingly used to simulate strongly correlated systems. Our introduction to them is based on reference [25]. They are characterized by a network of interconnected tensors which describes the wave function of the system. The "glue" among these pieces is played by the entanglement content of the wave function. Mathematically the amount and the structure of entanglement are linked to the chosen network patter and the number of parameters in the tensors [25].

Advantages of TN methods

- Each of the current numerical technique has its own limitation and that of TN concerns the amount and structure of entanglement, but indeed this is not a real limitation because Tensor Networks can simulate a wide range of models. In fact their flexibility implies that they allow us to study systems in different dimensions,

with different boundary conditions and different symmetries, composed by bosons, fermions or frustrated spins. Furthermore algorithms for infinte-size systems are developing in order to study them directly in the thermodynamic limit [25].

- The usual approach to describe quantum states concerns just the knowledge of the coefficients of the wave function in some given local basis, but it does not give any explicit information about the structure of the entanglement among its constituents. On the contrary Tensor Networks can capture the relevant entanglement properties of a system using, as said before, a network of interconnected tensor [25].
  We can consider TN states as quantum states given in some entanglement representation. Different entanglement representations are better suited for different types of states such as 1d, 2d, critical... . The effective lattice geometry, in which the states live, is very important because geometry and curvature can emerge naturally from the pattern of entanglement present in quantum states. This idea has been proposed in many works and TN is the correct approach to pursue this kind of connection [25].

- Representing a quantum state of a many-body system just by giving the coefficients of the wave function in some local basis is an inefficient representation. In fact if we have a system of N spins $\frac{1}{2}$ the dimension of the Hilber space is 2^N which is exponentially large in the number of particles.
  However, not all quantum states in the Hilbert space of a many-body system are equal because some of them are more relevant. In particular interactions between particles have usually a local character since they concern nearest or next-to-nearest nieghbors. One can demonstrate that low-energy eigenstates of gapped Hamiltonians with local interactions are characterized by the so-called area-law for the entanglement entropy. It means that the entanglement entropy of a region tends to scale as the size of the boundary of the region rather than as the volume. This feature selects the most relevant states in the Hilbert space and the manifold containing these states is just a tiny, exponentially small corner of the whole Hilbert space. TN approaches can target this corner directly, so they avoid the possibility of confusing it with the rest of Hilbert space [25].
  Furthermore, there is an other reason in order to avoid the use of the full immense Hilbert space: one can prove that after a time evolution $\mathrm{O}(\mathrm{poly}(N))$ the manifold of states that can be reached starting by a quantum state is exponentially small. In other words, the majority of the Hilbert space is reachable only after a time evolution $\mathrm{O}(\exp(N))$, it means that it is unreachable in practice. If you also consider that the initial state must be compatible with some local constraint, we find that all the quantum states, that you can always explore, are contained in a exponentially small manifold of the full Hilbert space [25].

- Finally Tensor Networks deal with tensor network diagrams, as we will explain, rather than with complicated equations. This new language is more visual and brings new intuitions, ideas and results [25].

Description of a TN

We consider a tensor as a multidimensional array of complex numbers and we define its rank as the number of indices the tensor has. Therefore a rank-0 tensor is a scalar, a rank-1 tensor is a vector and a rank-2 tensor is a matrix. An index contraction is the sum over all the possible values of the repeated indices of a set of tensors. The contraction of indices produces new tensors.
A Tensor Network is a set of tensors where some or all of its indices are contracted according to some pattern. The contraction of the indices of a tensor network is called the contraction of the tensor network. As it happens for tensors, the contraction of a tensor network with some open indices gives as a result another tensor or a scalar [25].
We can introduce a diagrammatic notation of tensors and of tensor networks in terms of tensor network diagrams. Tensors are represented by shapes and indices in tensors are represented by lines linked to the shapes, therefore a TN is represented by a set of shapes interconnected by lines. The shapes used for a scalar, a vector, a matrix and a rank-3 tensor are present in Fig. 3.2 below. It is taken from reference [25].
Contracted indices correspond to lines connecting tensors between each other and lines that do not go from one tensor to another correspond to open indices in the TN. Using TN diagrams some calculation are more intuitive and for example cyclic property of the trace is evident, see Fig. 3.3 below which represents the trace of the product of six matrices. It is taken from reference [25].

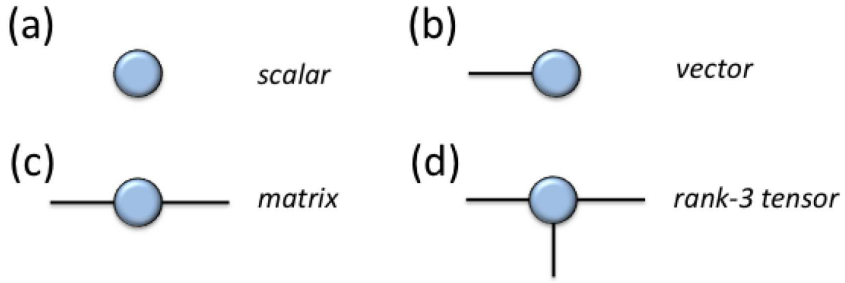

Figure 3.2: Graphic representation of a scalar (a), a vector (b), a matrix (c) and a rank-3 tensor (d) in the Tensor Network language. This picture is taken from [25].

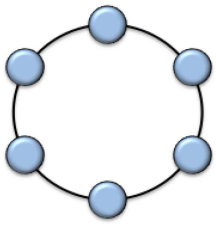

Figure 3.3: Graphic representation of the trace of the product of six matrices. This picture is taken from [25].

Since in TN methods one has to deal with many contractions, one tries to make them as efficiently as possible. But the total number of operations that must be done to achieve the final result of a TN contraction depends largely on the order in which indices in the TN are contracted. Therefore finding the optimal order of indices to be contracted in a TN is crucial. In particular, one must optimize over the different possible orderings of pairwise contractions and find the optimal case [25].

Tensor Network representation of a quantum many-body state

We can consider a quantum many-body system of N particles and we suppose that p different states can describe the degrees of freedom of each one of these particles. Therefore our system is composed by N p-level particles and it is described by the following wave function $|\psi>$ [25]:

$$|\psi>=\sum_{i_1,i_2,...,i_N} C_{i_1,i_2,...,i_N}|i_1>\otimes|i_2>\otimes...\otimes|i_N> \tag{3.53}$$

where $|i_r>$ is an individual basis for the states of each particle, $r=1,...,N$ and $i_r=1,...,p$. Therefore $C_{i_1,i_2,...,i_N}$ are p^N complex numbers and $\otimes$ denotes the tensor product of individual quantum states for each one of the particles in the many-body system.

We can consider the p^N numbers $C_{i_1,i_2,...,i_N}$, which describe the wave function $|\psi>$, as the coefficients of a tensor C where its indices are $i_1, i_2, ..., i_N$ and each of these indices can take up to p different values. Therefore C is a tensor of rank N with $\mathrm{O}(p^N)$ coefficients [25].

- We can specify the values of each of the p^N coefficients $C_{i_1,i_2,...,i_N}$, but their number is exponentially large in the system size so our description of the quantum state is very inefficient [25].

- On the contrary, we can achieve an accurate description of the expected entanglement properties of the state replacing the big tensor C by a TN of tensors with smaller rank. The final description of $|\psi>$ in terms of a TN usually depends on a polynomial number of parameters, this is an efficient description of the quantum state [25].
  The total number of these parameters is given by m_{tot} [25]:

$$m_{tot} = \sum_{t=1}^{N_{tensors}} m(t) \tag{3.54}$$

  where $m(t)$ is the number of parameters for the tensor t in the TN and $N_{tensors}$ is the number of tensors in the TN. A pratical TN is characteried by the fact that [25]:

  - $N_{tensors}$ must be O(poly(N)) or even O(poly(1));
  - $m(t) = \Pi_{a_t=1}^{rank(t)} D(a_t)$ for each tensor t, $a_t = 1, ..., rank(t)$ are its indices and $D(a_t)$ are the different possible values of the index a_t.

  If D_t is the maximum of all the number $D(a_t)$ for the tensor t and D is the maximum of all D_t considering all tensors, than m_{tot}=O(poly(N)poly(D)) [25].

The replacement of tensor C by a TN implies the appearance of extra degrees of freedom which are the links between tensors in the TN. These connecting indices represent the structure of the many-body entanglement in the quantum state $|\psi>$: the number of different values that each one of them can take is a quantitative measure of the amount of the correlation in the wave function. They are usually called bond or ancillary indices and their number of possible values are known as bond dimensions. The maximum of these values, that we have already called D, is the bond dimension of the tensor network [25].
Changing the bond dimension D modifies only the multiplicative factor of the area-law [25]. On the contrary, in order to modify the scaling with L (we can imagine to have a block of tensors of linear lenght L), a change of the geometric pattern of the TN is necessary [25]. It implies that the entanglement in the tensor network depends on both D (the "size" of bond indices) and the geometric pattern (the "way" these bond indices are connected). In other words, if we fix D different TN can have very different entanglement properties [25].

3.2.3 MPS (Matrix Product States) and DMRG

MPS are TN states that correspond to a one-dimensional array of tensors, in fact in an MPS there is one tensor per site in the many-body system. This family of TN states

is very popular beacuse it is behind some very important methods used to simulate one dimensional quantum many-body systems, for example the density matrix renormalization group algorithm. A 4-site MPS with open boundary condition and a 4-site MPS with periodic boundary condition are represented in Fig. 3.4. below [25].

Figure 3.4: This picture is taken from [25] and it represents a 4-site MPS with open boundary condition on the left and a 4-site MPS with periodic boundary condition on the right.

Here we describe some properties of MPS and a more detailed description is given in reference [25].

- In principle, all tensors in a finite-size MPS can be different and it implies that the MPS itself is not translational invariant. However translational invariance can be imposed and the thermodynamic limit of MPS can be taken choosing a fundamental unit cell of tensors that is repeated over the one dimensional lattice infinitely times. This unit cell can be composed by 1 site, i.e. 1 tensor, or 2 sites, i.e. 2 tensors, or 3 sites, i.e 3 tensors ... therefore in the first case the MPS is translational invariant over one-site shift, in the second case it is translational invariant over two-sites shift, in the third case it is translational invariant over three-sites shift [25] ...

- Given a quantum state $|\psi>$ in terms of an MPS characterized by open boundary conditions, there is an extremely convenient choice of tensors called canonical form of the MPS. It is define in the following way: if we have an MPS with open boundary condition, it is in the canonical form if, for each bond index β, the index corresponds to the labelling of Schmidt vectors in the Schmidt decomposition [24] of $|\psi>$ across that index, in other words [25]:

$$|\psi>=\sum_{\beta}^{D}\lambda_{\beta}|\phi_{\beta}^{L}>\otimes|\phi_{\beta}^{R}> \tag{3.55}$$

  where λ_β are Schmidt coefficients ordered into decreasing order and Schmidt vectors form orthonormal sets, it means $<\phi_{\beta}^{L}|\phi_{\beta'}^{L}>=<\phi_{\beta}^{R}|\phi_{\beta'}^{R}>=\delta_{\beta,\beta'}$.

– It is possible to rewrite expression (3.55) for a finite system of size N in the following way, see reference [25]:

$$|\psi>=\Sigma_i \sum_{\beta}^{D} \left(\Gamma^{[1]i_1}_{\beta_1}\lambda^{[1]}_{\beta_1}\Gamma^{[2]i_2}_{\beta_1\beta_2}\lambda^{[2]}_{\beta_2}...\Gamma^{[N]i_N}_{\beta_{N-1}}\right)|i_1>\otimes|i_2>\otimes...\otimes|i_N> \tag{3.56}$$

where Γ tensors correspond to changes of basis between Schmidt vectors and local basis $|i_1>$, $|i_2>$... .
Therefore (3.56) implies that the decomposition for the coefficient of the wave-function (3.53) is as follows [25]:

$$C_{i_1,i_2,...,i_N}=\left(\Gamma^{[1]i_1}_{\beta_1}\lambda^{[1]}_{\beta_1}\Gamma^{[2]i_2}_{\beta_1\beta_2}\lambda^{[2]}_{\beta_2}...\Gamma^{[N]i_N}_{\beta_{N-1}}\right). \tag{3.57}$$

– If the MPS is infinite and characterized by one-site translation invariance the canonical form corresponds to have just one tensor Γ and one vector λ describing the whole state [25].

In Fig. 3.5 there is the TN diagram for a finite MPS in canonical form and for an infinite MPS with 1-site unit cell in the canonical form, this picture is taken from reference [25].

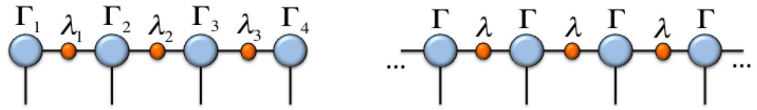

Figure 3.5: Canonical form [25] for a finite (left) and infinite (right) MPS.

MPS are very usefull to achieve grounds states and low-energy excitations of local Hamiltonians. This works well because, as said before, the relevant corner of the many-body Hilbert space can be target using the area-law for entanglement entropy. However there is still a basic question to ask: how do we fill in the coefficients of the tensors of MPS? This can be done in different ways which depend on the type of system and on the type of state that is target (ground state, excitation,...). Here we do not explain all these different scenarios, but we focus on a basic idea to find the ground state: the variational optimization.
According to reference [25], given an Hamiltonian H and a quantum state $|\psi>$ the variational principle implies that:

$$\frac{<\psi|H|\psi>}{<\psi|\psi>}\geq E_0 \tag{3.58}$$

where E_0 is the lowest eigenvalue of H. If $|\psi>$ is a tensor network that belongs to MPS, characterized by a fixed D, we can approach the ground state energy from above. This is achieved by minimizing the expectation value $<\psi|H|\psi> -\lambda <\psi|\psi>$ where λ is the Lagrangian multiplier.
In an ideal situation this minimization should be done simultaneosly over all the free parameters of the tensor network state (all the coefficients of all the tensors for all sites), but one usually proceeds tensor by tensor. It means that the minimization is computed with respect to one tensor and the others are kept fixed, then the tensor changes and this procedure is repeated for all tensors. This happens several times (sweeps) until the convergence in expectation values is obtained [25].
We can fixed all tensors of the tensor network except one called A, then the minimization respect to it implies that [25]:

$$\min_A <\psi|H|\psi> -\lambda <\psi|\psi> = \min_A \left(\vec{A}^\dagger H_{eff} \vec{A} - \lambda \vec{A}^\dagger N \vec{A}\right) \tag{3.59}$$

where coefficients of the tensor A are arranged as a vector, H_{eff} is an effective Hamiltonian and N is a normalization matrix which correspond to tensor networks for $<\psi|H|\psi>$ and $<\psi|\psi>$ without tensor A and A^* (this is the environment of tensors A and A^*). Minimization (3.59) can be done in the following way [25]:

$$\frac{\partial}{\partial A^\dagger}\left(\vec{A}^\dagger H_{eff} \vec{A} - \lambda \vec{A}^\dagger N \vec{A}\right) = 0 \tag{3.60}$$

this implies the eigenvalue problem [25]:

$$H_{eff}\vec{A} = \lambda N \vec{A}. \tag{3.61}$$

Once H_{eff} and N are known [25] this eigenvalue problem can be solved numerically. An important issue is the conditioning of the matrix N which may cause wrong results in the eigenvalues problem. More details can be found in [25].

If we perform this optimization for an MPS with open boundary contition we recover DMRG algorithm in the language of MPS [31] and this has been extended to periodic boundary condition too [27].

This is exactly our case: for our numerical analysis we use the Density Matrix Renormalization Group algorithm based on MPS tensor network.

3.2.4 Numerical results: critical point

To develop the numerical analysis we focus on case B (3.2) presented at the beginning of this chapter. In fact in this case we have a nonvanishing topological term (3.48) which should be added to the NLσM. We rewrite the Hamiltonian (3.2):

$$H = \sum_{i=1}^{N} J_{\parallel,1}(1 + (-1)^{i-1}\gamma)S_1(i)S_1(i+1) + \sum_{i=1}^{N} J_{\parallel,2}(1 + (-1)^{i}\gamma)S_2(i)S_2(i+1) + \\ + \sum_{a=1,2} \Sigma_{i=1}^{N} J'_{\perp,a,a+1} S_a(i)S_{a+1}(i). \tag{3.62}$$

Since the Lagrangian density is (3.47) then in the partition function (3.4), (3.5) we have the following contribution from the topological term:

$$e^{-\frac{i\theta}{4\pi}\int dx \int d\tau \left(\hat{\phi}'(x,\tau)\cdot(\hat{\phi}(x,\tau)\times\dot{\hat{\phi}}(x,\tau))\right)}. \tag{3.63}$$

The term $\frac{1}{4\pi}\int dx \int d\tau \left(\hat{\phi}'(x,\tau)\cdot(\hat{\phi}(x,\tau)\times\dot{\hat{\phi}}(x,\tau))\right)$ is the Pontragyn index or Winding number introduced in paragraph 2.7 (It can be defined with constant $\frac{1}{4\pi}$ or, as in paragraph 2.7, with constant $\frac{1}{8\pi}$ and the Levi-Civita tensor $\varepsilon_{i,j}$: thanks to the antisymmetry of $\varepsilon_{i,j}$ and $\times$ the two ways are equivalent). It is an integer, therefore if θ is π mod 2π then the exponential (3.63) is an alternated sign, which means that at $\theta = \pi$ mod 2π the energy gap closes. If $\theta = \pi$ and $J_{\parallel,1} = J_{\parallel,2} = J'_{\perp,1,2} = 1$ than, from (3.48) and Appendix B, we have:

$$\theta = -\frac{4\pi\gamma}{3} \tag{3.64}$$

then $\gamma_C = -0.75$. Numerically we would like to prove that the energy gap in (3.62) closes at this value of $\gamma_C = -0.75$.

One caveat is necessary: we will consider positive γ values in our analysis, but this is not a problem since both $\theta = \pi$ (negative γ) and $\theta = -\pi$ (positive γ) give, in the exponential (3.63), an alternated sign and for both the gap should close.

We also want to underline that our analytical forecast is consistent with that obtained in [18] by M.A.Martin-Delgrado, R.Shankar and G.Sierra. They studied the model (3.62) using a slighly different analytical procedure with respect to us and they already found the presence of a critical value of the topological term, such that the energy gap closes at that value. Their critical point corresponds to $\gamma_C = -0.75$, which is equal to our result. In particular they achieved the following expression for θ [18]:

$$\theta = 2\pi s n_l \left(1 + \gamma f_{n_l}\left(\frac{J'_{\perp,1,2}}{J_{\parallel,1}}\right)\right) \tag{3.65}$$

where they defined [18]:

$$f_{n_l} = \frac{1}{n_l^2}\left(\delta_{n_l,odd} + 2\Sigma_{m=1,\ldots,n_l-1}\frac{1}{\sin^2\left(\frac{m\pi}{2n_l}\right)} \times \frac{1}{1+\frac{J'_{\perp,1,2}}{J_{\parallel,1}}\cos^2\left(\frac{m\pi}{2n_l}\right)}\right) \tag{3.66}$$

If we look for γ_C when θ is π mod 2π and we replace $s = \frac{1}{2}$, $n_l = 2$ and $J'_{\perp,1,2} = J_{\parallel,1} = 1$ we find that their result is $\gamma_C = -0.75$.

We represent the ground state (subspace $S_{z,tot} = 0$), the first three excited states (which, because of the $SU(2)$ symmetry, are degenerate and belong to subspaces $S_{z,tot} = -1$, $S_{z,tot} = 0$, $S_{z,tot} = +1$) and the fourth excited state (subspace $S_{z,tot} = 0$) for PBC in Fig. 3.6 and for OBC in Fig. 3.7.
They are made considering 16 sites on each chain and γ varies from 0 to 1 with a 0.05 step.

We also represent:
- the scaling of the gap at $\gamma = 0.4$ and $\gamma = 0.35$ of the triplet with respect to the ground state for PBC in Fig. 3.8 and 3.9;
- the scaling of the gap at $\gamma = 0.4$ and $\gamma = 0.5$ of the triplet with respect to the ground state for OBC in Fig. 3.10 and 3.11;
For the scaling we consider chains with $N = 16, 18, 20, 22, 24, 26, 28, 30$ sites. In these cases we will report, after Fig. 3.8, 3.9, 3.10 and 3.11, the y-intercepts and the slopes of a linear fit of them, when the scaling is represented as a function of $\frac{1}{N}$.

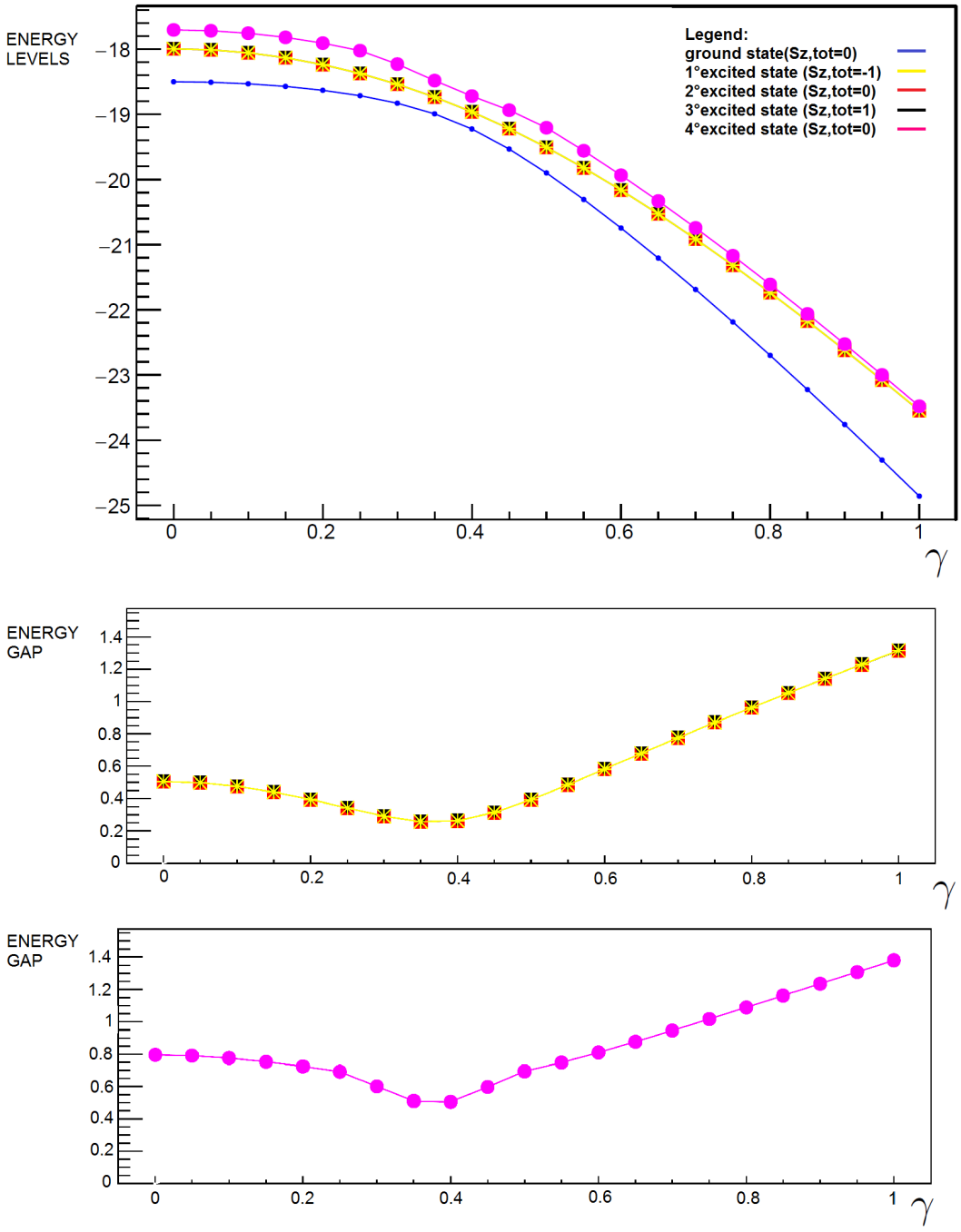

Figure 3.6: Representation of the energy levels (figure placed at the top) and their gaps with respect to the ground state (the two figures below) in the case of PBC. We use 16 sites on each chain and γ varies from 0 to 1 with a 0.05 step. See the legend for details.

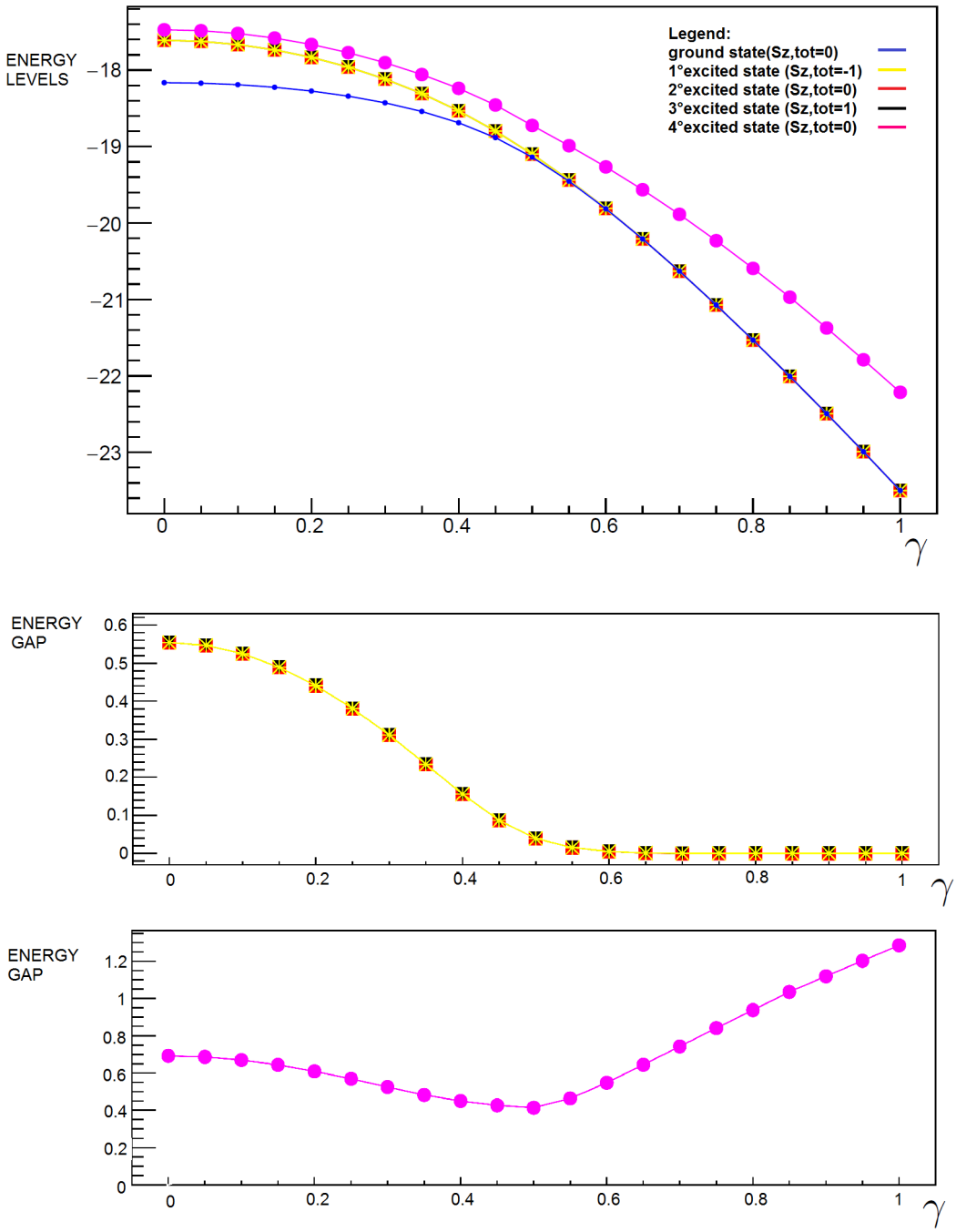

Figure 3.7: Representation of the energy levels (figure placed at the top) and their gaps with respect to the ground state (the two figures below) in the case of OBC. We use 16 sites on each chain and γ varies from 0 to 1 with a 0.05 step. See the legend for details.

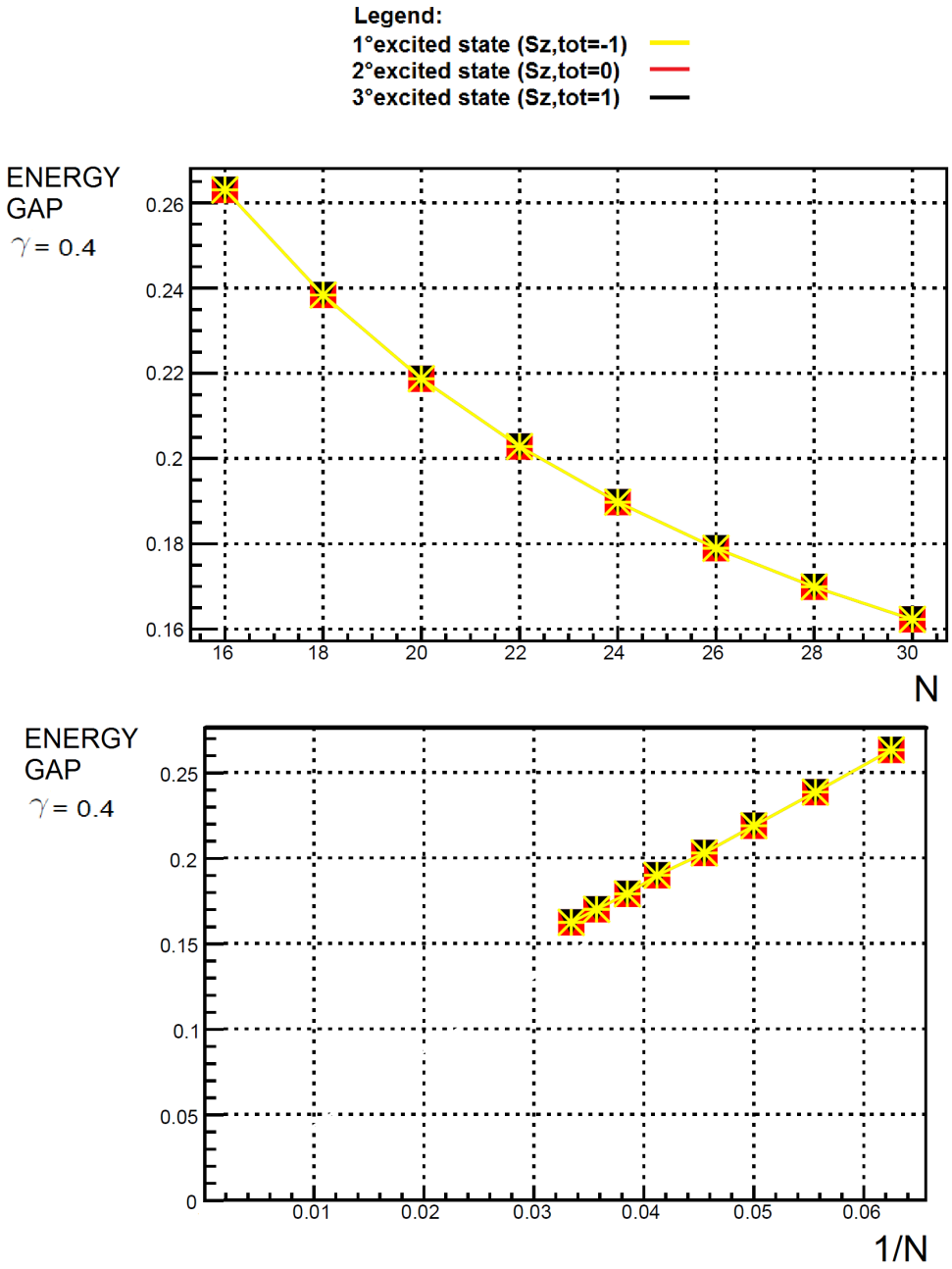

Figure 3.8: Representation of the scaling of the energy gap of each state of the triplet respect to the ground state. We use $N = 16, 18, 20, 22, 24, 26, 28, 30$ sites for each chain and $\gamma = 0.4$. PBC are used.

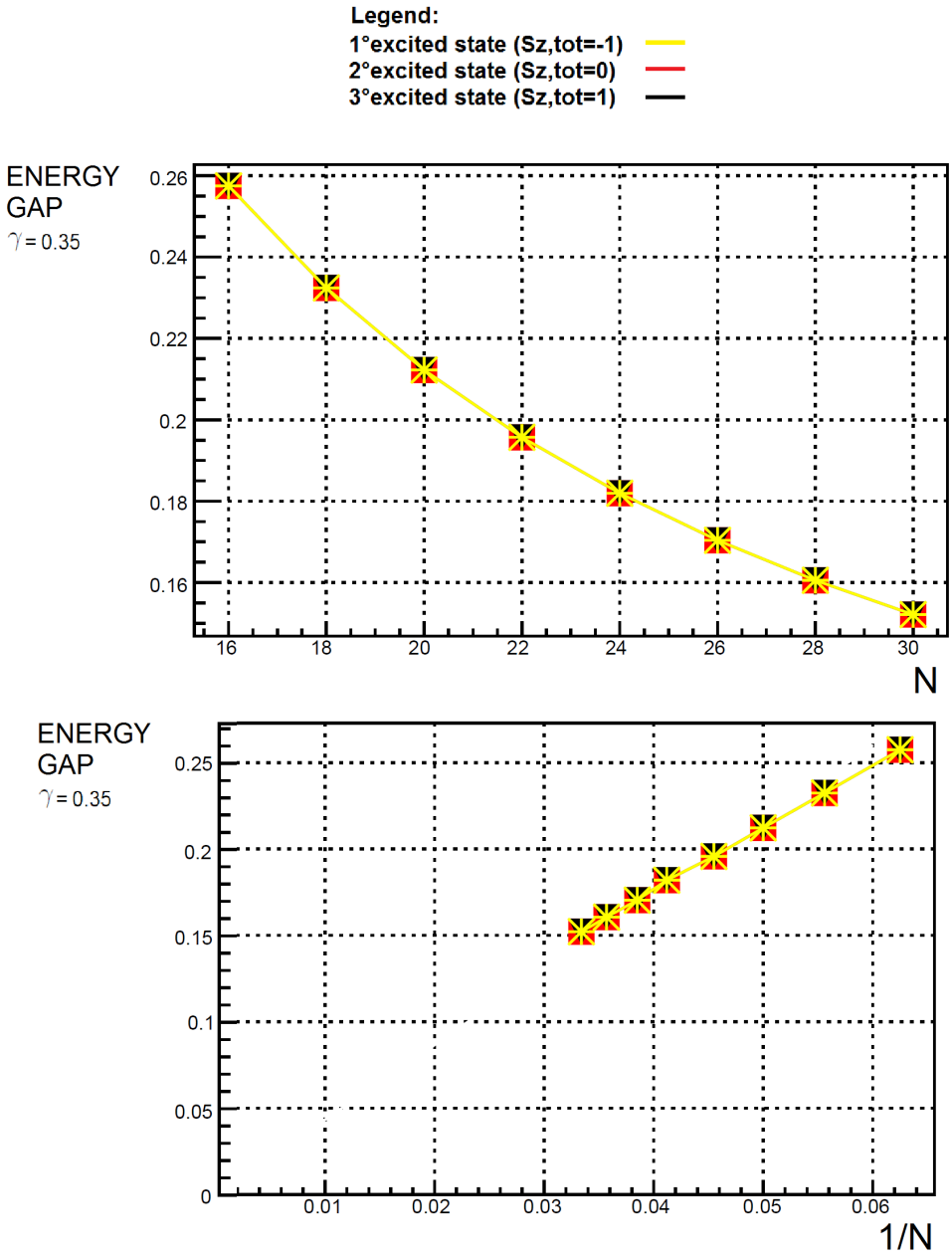

Figure 3.9: Representation of the scaling of the energy gap of each state of the triplet respect to the ground state. We use $N = 16, 18, 20, 22, 24, 26, 28, 30$ sites for each chain and $\gamma = 0.35$. PBC are used.

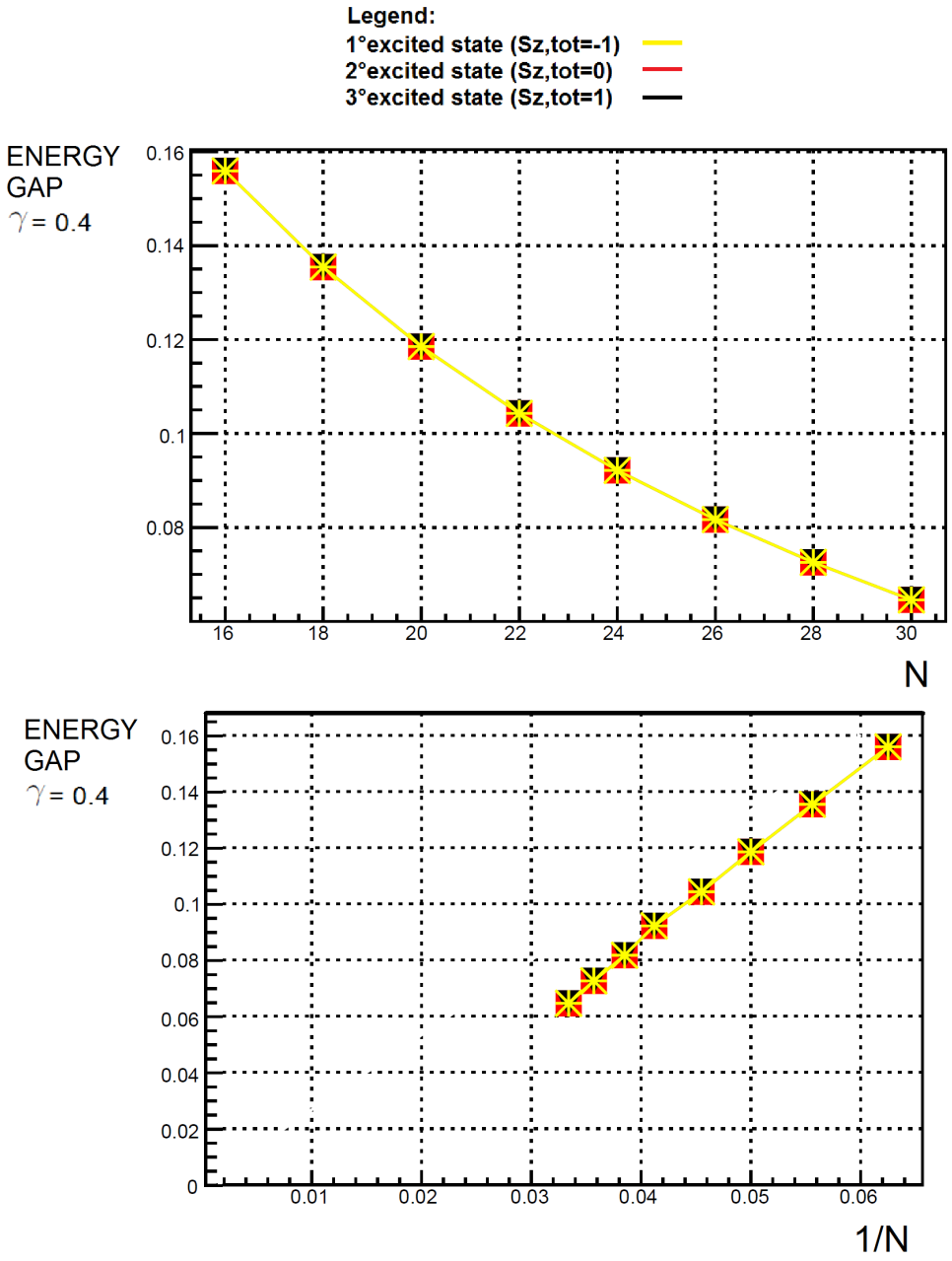

Figure 3.10: Representation of the scaling of the energy gap of each state of the triplet respect to the ground state. We use $N = 16, 18, 20, 22, 24, 26, 28, 30$ sites for each chain and $\gamma = 0.4$. OBC are used.

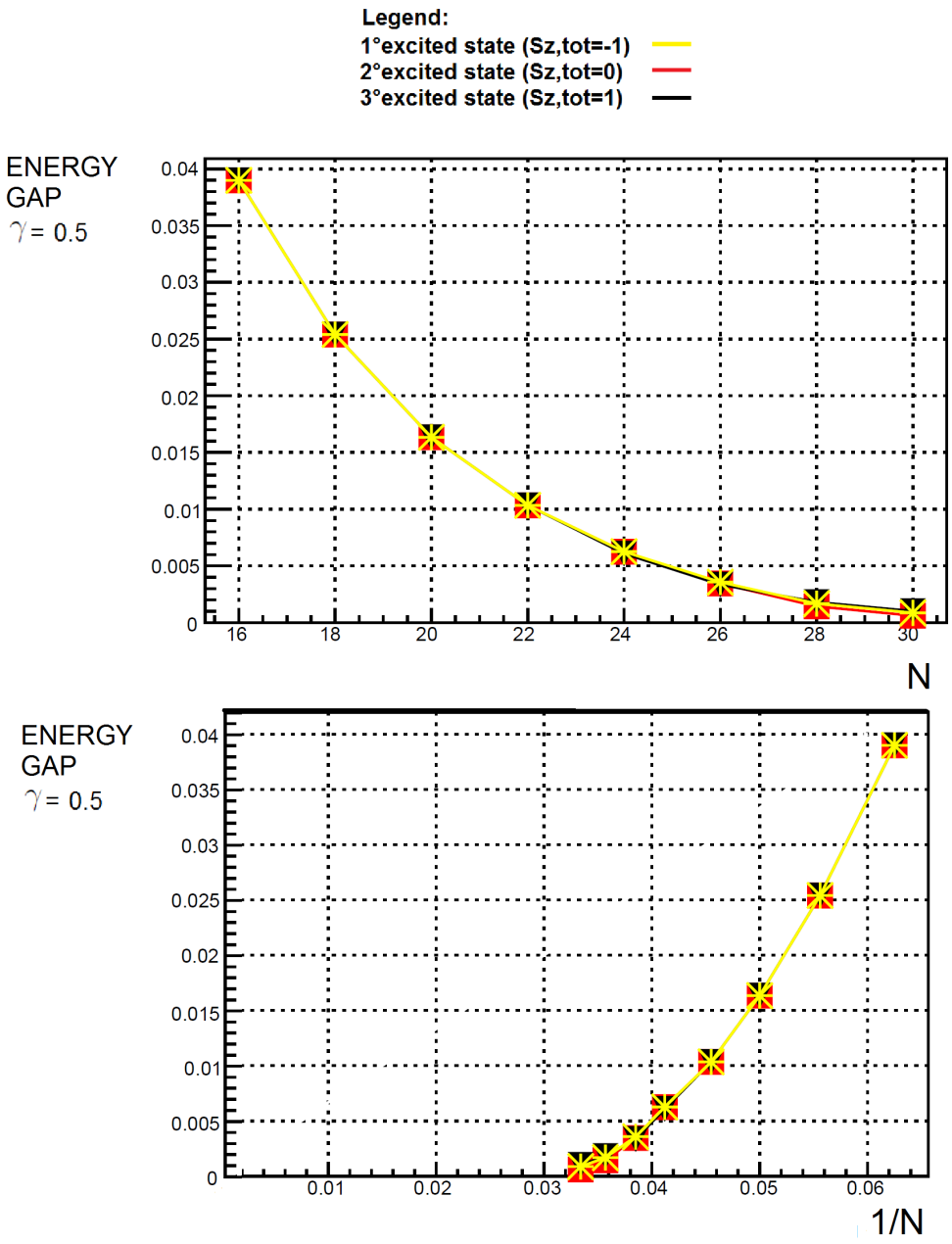

Figure 3.11: Representation of the scaling of the energy gap of each state of the triplet respect to the ground state. We use $N = 16, 18, 20, 22, 24, 26, 28, 30$ sites for each chain and $\gamma = 0.5$. OBC are used.

Numerical results

- The critical point γ_C seems to be near 0.35-0.4 for PBC and 0.4-0.5 for OBC rather than the expected theoretical value $\gamma_C = -0.75$, found by us at the beginning of this section 3.2.4 (which is based on calculations in section 3.1.3) and previously obtained also by M.A.Martin-Delgrado, R.Shankar, G.Sierra in [18].
- In Fig. 3.6 we notice that for $\gamma > \gamma_C$ a bulk gap opens, while in Fig. 3.7 the triplet for $\gamma > \gamma_C$ becomes degenerate with the ground state. In both cases a gap is present for $\gamma < \gamma_C$.
- If we consider PBC and
  - $\gamma = 0.4$, we report in Table 3.1 the results of a linear fit of the energy gap between each state of the triplet and the ground state as a function of $\frac{1}{N}$ (second picture in Fig. 3.8). The y-intercep represent the energy gap in the thermodynamic limit.
  - $\gamma = 0.35$, we report in Table 3.2 the results of a linear fit of the energy gap between each state of the triplet and the ground state as a function of $\frac{1}{N}$ (second picture in Fig. 3.9).
- If we consider OBC and
  - $\gamma = 0.4$, we report in Table 3.3 the results of a linear fit of the energy gap between each state of the triplet and the ground state as a function of $\frac{1}{N}$ (second picture in Fig. 3.10).
  - $\gamma = 0.5$, we report in Table 3.4 the results of a linear fit of the energy gap between each state of the triplet and the ground state as a function of $\frac{1}{N}$ (second picture in Fig. 3.11).

We will try to explain physically these results in paragraph 3.2.6.

state of the triplet	y-intercept	slope	Chi2
state with $S_{z,tot} = 0$	0.046 ± 0.001	3.46 ± 0.03	2.8×10^{-6}
state with $S_{z,tot} = +1$	0.046 ± 0.001	3.46 ± 0.03	2.8×10^{-6}
state with $S_{z,tot} = -1$	0.046 ± 0.001	3.46 ± 0.03	2.8×10^{-6}

Table 3.1: Results of a linear fit of the energy gap between each state of the triplet and the ground state as a function of $\frac{1}{N}$ for $\gamma = 0.4$ with PBC

state of the triplet	y-intercept	slope	Chi2
state with $S_{z,tot} = 0$	0.032 ± 0.001	3.61 ± 0.02	2.4×10^{-6}
state with $S_{z,tot} = +1$	0.032 ± 0.001	3.61 ± 0.02	2.4×10^{-6}
state with $S_{z,tot} = -1$	0.032 ± 0.001	3.61 ± 0.02	2.4×10^{-6}

Table 3.2: Results of a linear fit of the energy gap between each state of the triplet and the ground state as a function of $\frac{1}{N}$ for $\gamma = 0.35$ with PBC

state of the triplet	y-intercept	slope	Chi2
state with $S_{z,tot} = 0$	-0.039 ± 0.002	3.13 ± 0.04	7.3×10^{-6}
state with $S_{z,tot} = +1$	-0.039 ± 0.002	3.13 ± 0.04	7.3×10^{-6}
state with $S_{z,tot} = -1$	-0.039 ± 0.002	3.13 ± 0.04	7.3×10^{-6}

Table 3.3: Results of a linear fit of the energy gap between each state of the triplet and the ground state as a function of $\frac{1}{N}$ for $\gamma = 0.4$ with OBC

state of the triplet	y-intercept	slope	Chi2
state with $S_{z,tot} = 0$	-0.046 ± 0.005	1.3 ± 0.1	4.3×10^{-5}
state with $S_{z,tot} = +1$	-0.046 ± 0.005	1.3 ± 0.1	4.7×10^{-5}
state with $S_{z,tot} = -1$	-0.046 ± 0.005	1.3 ± 0.1	4.5×10^{-5}

Table 3.4: Results of a linear fit of the energy gap between each state of the triplet and the ground state as a function of $\frac{1}{N}$ for $\gamma = 0.5$ with OBC

3.2.5 Numerical results: NLOP

We try to characterize the phases of the model (3.62) using non-local order parameters, because they can tell us if there is some kind of topological order in our phases. In particular we specialize the cases (1.21) and (1.22), therefore we consider the following non-local order parameters:

$$C_P^{(x)}(r) = \left\langle \prod_{k=j}^{j+r-1} e^{i\pi(S^x_{k,1}+S^x_{k,2})} \right\rangle$$

$$C_P^{(y)}(r) = \left\langle \prod_{k=j}^{j+r-1} e^{i\pi(S^y_{k,1}+S^y_{k,2})} \right\rangle$$

$$C_P^{(z)}(r) = \left\langle \prod_{k=j}^{j+r-1} e^{i\pi(S^z_{k,1}+S^z_{k,2})} \right\rangle \tag{3.67}$$

and

$$C_S^{(x)}(r) = \left\langle 2S^x_j \prod_{k=j}^{j+r-1} e^{i\pi(S^x_{k,1}+S^x_{k,2})} 2S^x_{j+r} \right\rangle$$

$$C_S^{(y)}(r) = \left\langle 2S^y_j \prod_{k=j}^{j+r-1} e^{i\pi(S^y_{k,1}+S^y_{k,2})} 2S^y_{j+r} \right\rangle$$

$$C_S^{(z)}(r) = \left\langle 2S^z_j \prod_{k=j}^{j+r-1} e^{i\pi(S^z_{k,1}+S^z_{k,2})} 2S^z_{j+r} \right\rangle \tag{3.68}$$

First of all, subscript numbers 1 and 2 in all previous expressions refer to chain 1 and chain 2. Since in all exponentials we consider the sum of the spins on both chains, then we have a factor π rathen than 2π as in (1.21) and (1.22) for a single chain. In $C_S^{(\alpha)}(r)$, $\alpha = x, y, z$, we have a factor 2 both on the left and on the right sides to have a correct normalization.

In order to implement them numerically and try to get as close as possible to the thermodynamic limit, r is fixed to the maximum possible distance. This means $r = \frac{N}{2}$ for periodic boundary contitions and r is between $\frac{L}{4}$ and $\frac{3L}{4}$ for open boundary conditions (this choice is done in order to avoid edge effects).

For $C_P^{(\alpha)}$ we have considered three possible cases:

- Case a: the initial site (which is j in (3.67)) belongs to chain 1 and the final state (which is $j + r$ in (3.67)) belongs to chain 1; they are blue sites in Fig. 3.12, in this picture we have represented both periodic and open boundary conditions for

N=8 sites on each chain (16 in total in DMRG program). We consider all the exponentials from site j to site $j+r-1$ included and we place the identity on site $j+r$.

- Case b: the initial site (which is j in (3.67)) belongs to chain 2 and the final state (which is $j+r$ in (3.67)) belongs to chain 2; they are blue sites in Fig. 3.13, in this picture we have represented both periodic and open boundary conditions, for N=8 sites on each chain (16 in total in DMRG program). We consider all the exponentials from site j to site $j+r-1$ included and we place the identity on site $j+r$.

- Case c: the initial site (which is j in (3.67)) belongs to chain 1 and the final state (which is $j+r$ in (3.67)) belongs to chain 2; they are blue sites in Fig. 3.14, in this picture we have represented both periodic and open boundary conditions, for N=8 sites on each chain (16 in total in DMRG program). We consider all the exponentials from site j to site $j+r-1$ included and we place the identity on site $j+r$.

For $C_S^{(\alpha)}$ we have considered three possible cases:

- Case a: S_j^α, $\alpha = x, y, z$ in (3.68) belongs to chain 1 and S_{j+r}^α, $\alpha = x, y, z$ in (3.68) belongs to chain 1; they are blue sites in Fig. 3.12, in this picture we have represented both periodic and open boundary conditions, for N=8 sites on each chain (16 in DMRG program). We consider all the exponentials from site j to site $j+r-1$ included.

- Case b: S_j^α, $\alpha = x, y, z$ in (3.68) belongs to chain 2 and S_{j+r}^α, $\alpha = x, y, z$ in (3.68) belongs to chain 2; they are blue sites in Fig. 3.13, in this picture we have represented both periodic and open boundary conditions, for N=8 sites on each chain (16 in DMRG program). We consider all the exponentials from site j to site $j+r-1$ included.

- Case c: S_j^α, $\alpha = x, y, z$ in (3.68) belongs to chain 1 and S_{j+r}^α, $\alpha = x, y, z$ in (3.68) belongs to chain 2; they are blue sites in Fig. 3.14, in this picture we have represented both periodic and open boundary conditions, for N=8 sites on each chain (16 in DMRG program). We consider all the exponentials from site j to site $j+r-1$ included.

Even if we have not represented the staggered interaction (3.62) explicity, it is implied in all figures 3.12, 3.13, 3.14.

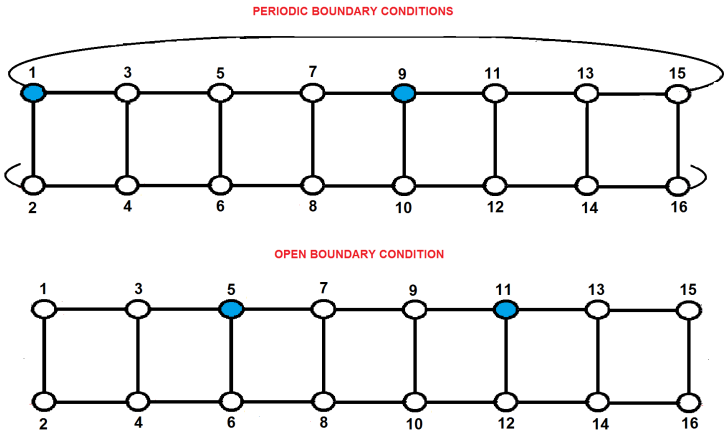

Figure 3.12: Case a: representation of the initial and final sites (blue sites) of NLOP with PBC and OBC. They are both placed on chain 1. Sites numbers are those used in DMRG program, because it is one dimensional.

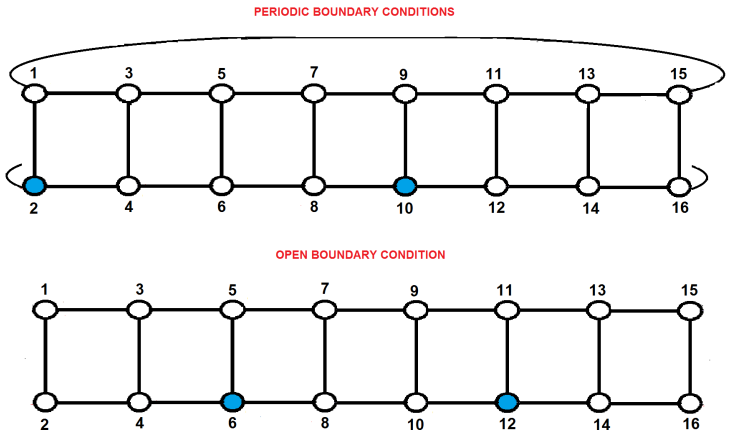

Figure 3.13: Case b: representation of the initial and final sites (blue sites) of NLOP with PBC and OBC. They are both placed on chain 2. Sites numbers are those used in DMRG program, because it is one dimensional.

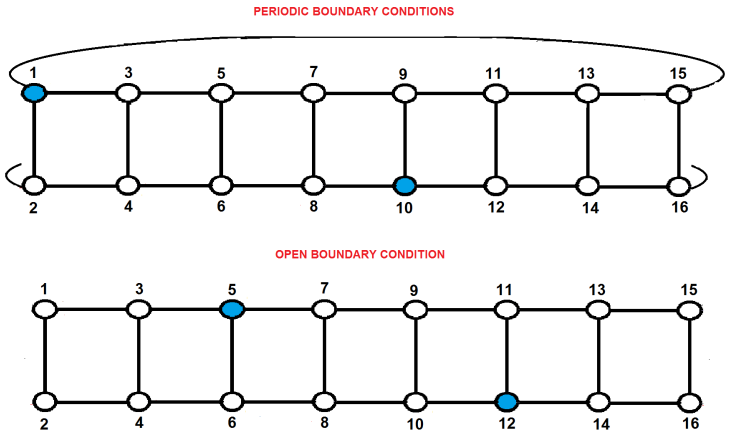

Figure 3.14: Case c: representation of the initial and final sites (blue sites) of NLOP with PBC and OBC. They are on chain 1 (the first) and on chain 2 (the second). Sites numbers are those used in DMRG program, because it is one dimensional.

In Fig. 3.15 and Fig. 3.16 we represent $C_P^{(\alpha)}$ (black) and $C_S^{(\alpha)}$ (red) for case a,b,c for PBC and on each chain $N = 30$ and $\alpha = x, y, z$. The parameter γ varies from 0 to 1 with a 0.05 step.

In Fig. 3.17 and Fig. 3.18 we represent $C_P^{(\alpha)}$ (black) and $C_S^{(\alpha)}$ (red) for case a,b,c for OBC and on each chain $N = 32$ and $\alpha = x, y, z$. The parameter γ varies from 0 to 1 with a 0.05 step.

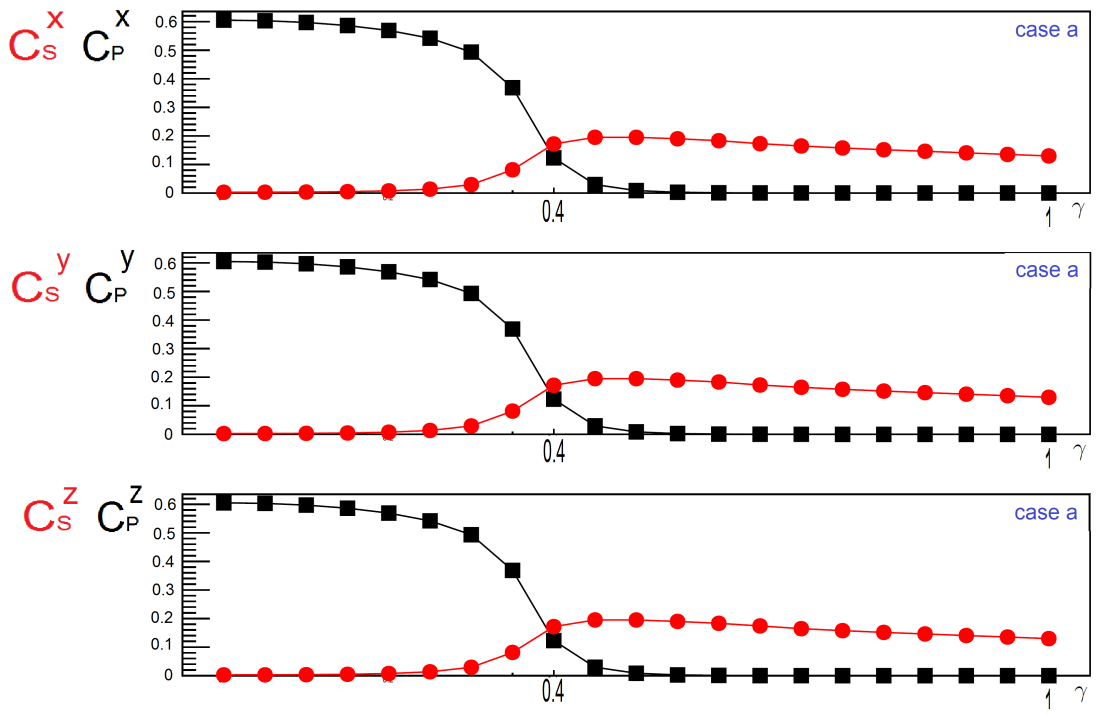

Figure 3.15: Representation of the x,y,z components of $C_P^{(\alpha)}$ (black) and $C_S^{(\alpha)}$ (red) when the first and the last sites are both on chain 1 (case a). We consider $N = 30$ on each chain and PBC. The parameter γ varies from 0 to 1 with a 0.05 step.

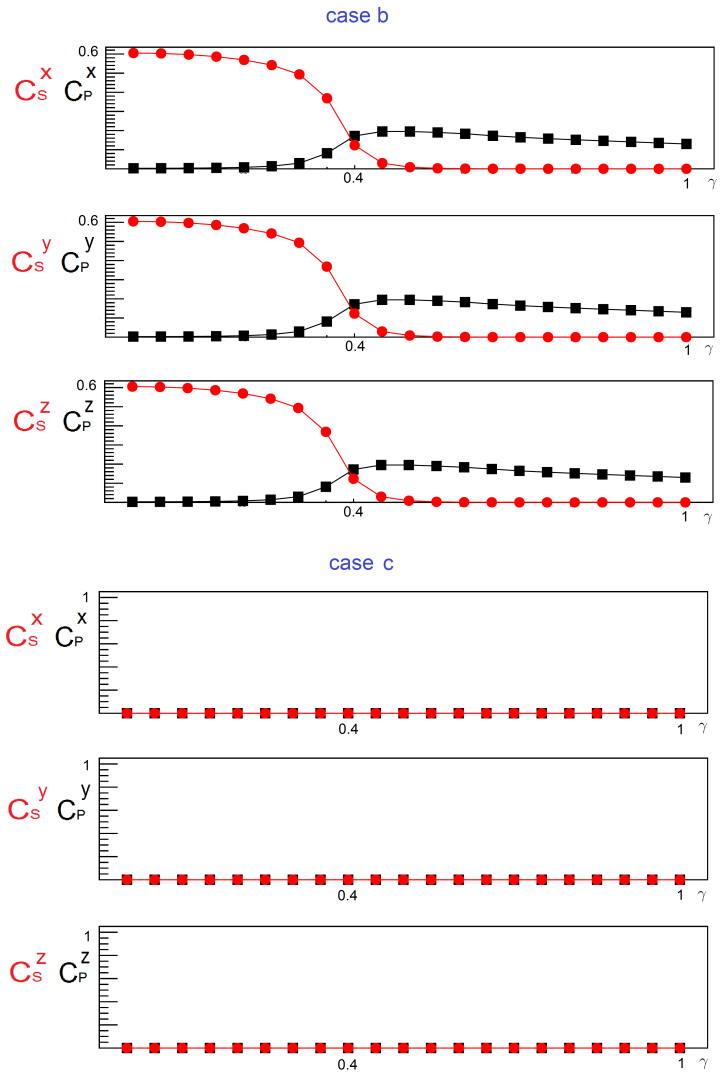

Figure 3.16: Representation of the x,y,z components of $C_P^{(\alpha)}$ (black) and $C_S^{(\alpha)}$ (red) when the first and the last sites are both on chain 2 (case b) above and when the first site is on chain 1 and the last site is on chain 2 (case c) below. We consider $N = 30$ on each chain and PBC. The parameter γ varies from 0 to 1 with a 0.05 step.

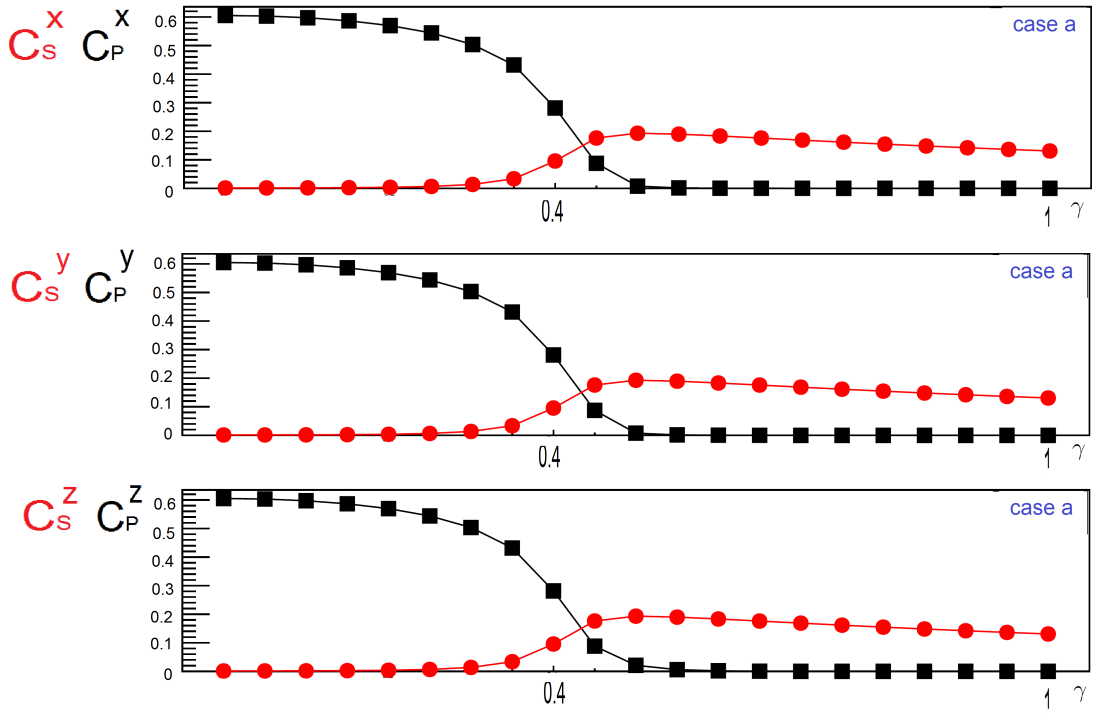

Figure 3.17: Representation of the x,y,z components of $C_P^{(\alpha)}$ (black) and $C_S^{(\alpha)}$ (red) when the first and the last sites are both on chain 1 (case a). We consider $N = 32$ on each chain and OBC. The parameter γ varies from 0 to 1 with a 0.05 step.

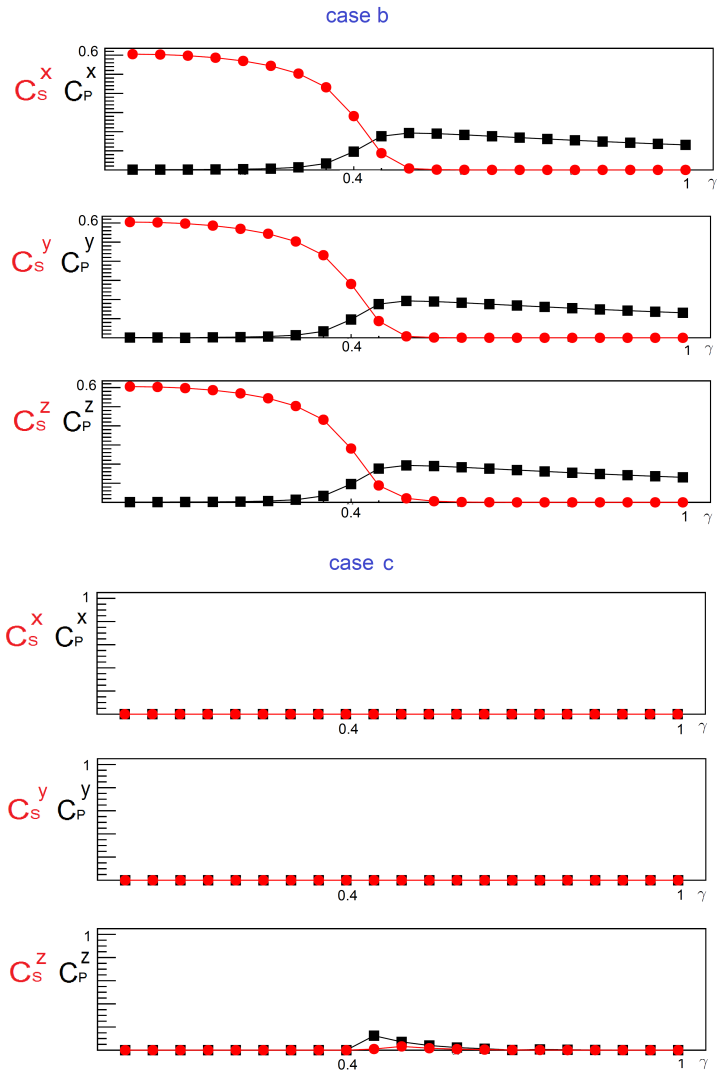

Figure 3.18: Representation of the x,y,z components of $C_P^{(\alpha)}$ (black) and $C_S^{(\alpha)}$ (red) when the first and the last sites are both on chain 2 (case b) above and when the first site is on chain 1 and the last site is on chain 2 (case c) below. We consider $N = 32$ on each chain and OBC. The parameter γ varies from 0 to 1 with a 0.05 step.

Numerical results

- In all cases the symmetry in x,y,z components is respected as we expect: these NLOP are computed with respect to the ground state which is invariant under $SU(2)$ so x,y,z components must be equivalent.

- Case a strictly adheres to formula (3.67) and (3.68). It is characterized by the fact that parity operator C_P^α is nonvanishing for $\gamma < \gamma_C$ and string operator C_S^α is nonvanishing for $\gamma > \gamma_C$. This happens for both PBC (Fig. 3.15) and OBC (Fig. 3.17).

- Case b is characterized by the fact that string operator C_S^α is nonvanishing for $\gamma < \gamma_C$ and parity operator C_P^α is nonvanishing for $\gamma > \gamma_C$. This happens for both PBC (Fig. 3.16) and OBC (Fig. 3.18).

- Case c has both C_P^α and C_S^α vanishing for all γ and for both PBC (Fig. 3.16) and OPC (Fig. 3.18).

The physical interpretation of these results and their link with those of energy gaps will be present in the next paragraph 3.2.6.

3.2.6 Numerical results: Interpretation and comments

- The critical point γ_C is placed near 0.35-0.4 for PBC and 0.4-0.5 for OBC rather than the expected theoretical prediction $\gamma_C = -0.75$, obtained by us and previously calculated also by M.A.Martin-Delgrado, R.Shankar, G.Sierra in [18]. This effect may be explained as a consequence of the finite size of the system in DMRG analysis. However, since the mismatch is quite important (it is about a factor 2), a more probable cause of this discrepancy is connected to the semiclassical approximation (large s) on which the Haldane map (3.6) is based. In fact a renormalization analysis, considering all quantum effects, would give more accurate results, that may lead to a big change in the value of γ_C.

- At the critical point the energy gap between each state of the triplet and the ground state closes. In the thermodynamic limit these gaps correspond to y-intercepts of a linear fit reported in Tables 3.1, 3.2, 3.3 and 3.4 and in fact these quantities are very close to zero, as we expect. However, we note that in Table 3.3 and in Table 3.4 we achieve negative values for y-intercets, but this effect is just due to the finite size of the system and it would disappear considering bigger and bigger sizes.

- By comparing Fig. 3.6 and Fig. 3.7 we note that for $\gamma < \gamma_C$ we have the same behavior for both PBC and OBC, in particular we see the presence of a gapped phase. For $\gamma > \gamma_C$ a bulk gap opens using PBC while the triplet becomes degenerate with the ground state using OBC. This implies that the two gapped phases, i. e. that for $\gamma < \gamma_C$ and that for $\gamma > \gamma_C$, are both insulating phases but with this important difference:

  - for $\gamma < \gamma_C$ the gapped phase is topologically trivial;
  - for $\gamma > \gamma_C$ the gapped phase is characterized by the presence of zero modes degenerate with the ground state. Furthermore, if we consider the case $\gamma = 1$ in Fig. 3.19, which is included in the range $\gamma > \gamma_C$, we note that the two spins at the ends of the chain can be combined into four different ways, in fact they are two $\frac{1}{2}$ spins and therefore they are force to be in the singlet state or in one state of the triplet. These four states are the ground state and the triplet states degenerate with it.
    Therefore, for these reasons, we suppose that these zero modes could be edge states, which, as we know from paragraph 1.4, are closely connected to topological invariant quantities. In fact, if they were actually edge modes, this would support the fact that the topological term θ gives rise to a topologically non trivial phase when the threshold value $\theta_C = \pi$ is exceeded. We will

discuss in the next chapter some ways to prove if this hypothesis is true.

- The conclusion, according to which the phase for $\gamma > \gamma_C$ would be topological, is coherent with the behavior of NLOP in Fig. 3.15, 3.16, 3.17. 3.18 for the reasons explained below.
  We consider the **Case a** in Fig. 3.15 and Fig. 3.17 as that of physical relevance.

  – In fact if we look at Case b and we consider the relation $e^{i\pi s_z} = 2is_z$ and the simmetry in x, y and z components, we see that:
  - the first and the last exponentials in the parity operator can be interpreted as spin operators so that this parity operator is equivalent to a string operator and viceversa.
  - The two edge spins in the string operator can be interpreted as exponential so that this string operator is equivalent to a parity operator and therefore we recover Case a.

  – Instead, if we look at Case c we note that the number of exponentials differs by one from Case a and this probably implies a compensation that yields a zero expectation value.

  Therefore we focus on **Case a**.

  – For $\gamma > \gamma_C$, consistently with what we have just said about energy levels, the phase seems to be topological and in fact it is characterized by a nonvanishing value of string operator C_S. String operator denotes a topologically non trivial phase [9, 20].

  – For $\gamma < \gamma_C$, consistently with what we have just said about energy levels, the phase seems to be trivial and in fact it is characterized by a nonvanishing value of parity operator C_P. Parity operator denotes a topologically trivial phase [9, 20].

  Our NLOP correspond to C_S and C_P defined for charge degrees of freedom in (1.21) and (1.22) so for $\gamma > \gamma_C$ the phase is an Haldane insulator and for $\gamma < \gamma_C$ the phase is a Mott insulator (Table 1.1).
  The transition MI-HI can be found in other models. For example even if it does not characterize the extended Hubbard model (1.136), as it is represented in Figure 1.6, it characterizes the Bose Hubbard model with nearest neighbor interaction [6].

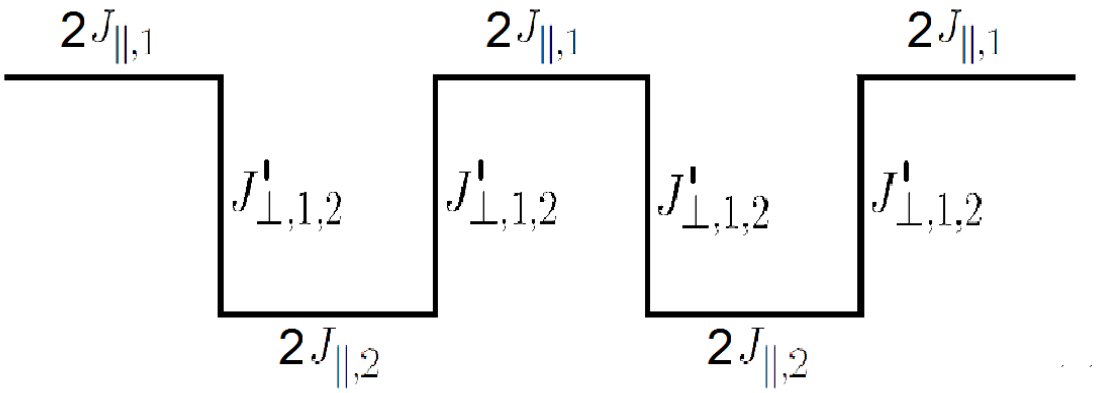

Figure 3.19: Representation of the ladder corresponding to the Hamiltonian (3.62) for $\gamma = 1$ and for six sites on each chain (in our numerical analysis $J_{\|,1} = J_{\|,2} = J'_{\perp,1,2} = 1$). Spins at the ends of the chian are forced to be in the singlet state or in one state of the triplet.

Chapter 4

Conclusions and Outlooks

In the previous chapter we concluded that our system is characterized by two gapped phases: a Mott insulator for $\gamma < \gamma_C$ and a Haldane insulator for $\gamma > \gamma_C$. The first one is topologically trivial, in fact it is characterized by a nonvanishing value of the parity operator C_P, whereas the second phase is topologically non trivial, in fact it is characterized by a nonvanishing value of the string operator C_S. Furthermore, in the topologically non trivial phase there are zero modes, which could be edge states. In order to verify if they are actually edge states, it would be interesting to study their wavefunction, in fact wavefunctions of edge states are localized at the edges of the system [2]. It would also be useful to ascertain that the correlation between the first spin and the last one is very strong. In fact if we have edge states, these two spins are force to be in the singlet state or in one state of the triplet, so they are strongly correlated to each other.

We also expect that the direct numerical computation of the winding number will give a vanishing value in the trivial phase and a nonvanishing integer value in topological phase. In order to calculate the winding number, one should know the explicit form of the dispersion relation [2], i.e. the dependence of the energy from the momentum. It is not possible to obtain this information within DMRG study, but it is conceivable to perform an exact diagonalization study in the momentum space, at least for not too large systems.

The analysis of the entanglement spectrum has been proposed as an other way to identify topological phases [26]. It is obtained by arbitrarily dividing the system into two parts, tracing out one half and diagonalizing the reduced density matrix of the other. In a trivial phase the eigenvalues of the reduced density matrix, i.e. the entanglement spectrum, can be non-degenerate, while in a topological phase the entanglement spectrum has at least a two-fold degeneracy [26]. For example the double degeneracy of the entanglement

spectrum characterizes the Haldane phase [26].
Therefore it would be interesting to analyze the entanglement spectrum in our staggered spin ladder too, in order to confirm the topological character of the phase for $\gamma > \gamma_C$.

In conclusion, we note that the numerical result for γ_C seems to be very close to half of our theoretical prediction. Furthermore, this is not the only case where the NLσM predicts the existence of critical points without locating them precisely: if we consider a staggered spin 1 chain there should be two critical points at $\gamma_C = \pm\frac{1}{2}$ [32], but numerically they are $\gamma_C = \pm\frac{1}{4}$ [37].
This effect may be due to numerical features or to the semiclassical approximation at the base of theoretical calculations, as said before in paragraph 3.2.6, but it may also be a physical effect. In the last case, for our ladder it may be explained as a consequence of the presence of two legs: the winding number of one chain is the same of the other one therefore they sum up and reduce by one half the value of θ_C which would become $\theta_C = \frac{\pi}{2}$. As a consequence the theoretical value of γ_C would be halved so fitting the numerical one.
This could be demonstrated by computing the value of θ_C for more then two legs and by comparing it with the corresponding numerical result, to see if it is always renormalized by the number of legs. This kind of research could open the study of topological behavior in two dimensional systems, which could be possible using a new Tensor Network approach known as PEPS [2].

Bibliography

[1] I.Affleck, T.Kennedy, E.H.Lieb and H.Tasaki, Valence bond ground states in isotropic quantum antiferromagnets, *Condensed Matter Physics and Exactly Soluble Models*, Springer, 1988.

[2] J.K.Asbóth, L.Oroszlány and A.P*ályi*, *A short Course on Topological Insulators*, Springer, 2015.

[3] A.Auerbach, *Interacting Electrons and Quantum Magnetism*, Springer, 2 edition, 1998.

[4] L.Barbiero, S.Fazzini and A.Montorsi, Non-local order parameters as a probe for phase transitions in the extended Fermi-Hubbard model, *Eur.Phys.J.Special Topics*226:2697-2704, 2017.

[5] L.Barbiero, A.Montorsi and M.Roncaglia, How hidden orders generate gaps in one-dimensional fermionic systems, *Phys.Rev.B*88:035109, 2013.

[6] E.G.Dalla Torre, E.Berg, E.Altman, Hidden Order in 1D Bose Insulators, *Phys.Rev.Lett.*97:260401, 2006.

[7] S.Dell'Aringa, E.Ercolessi, G.Morandi, P.Pieri, and M.Roncaglia, Effective actions for spin ladders, *Phys.Rev.Lett.*78:2457, 1997.

[8] F.Dolcini and A.Montorsi, Quantum phases of one-dimensional Hubbard models with three-and four-body couplings, *Phys.Rev.B*88:115115, 2013.

[9] S.Fazzini, Non-local orders in Hubbard-like low dimensional systems, *Doctoral Dissertion*, *Doctoral Program in Physics (*30^th *cycle)*.

[10] S.Fazzini, L.Barbiero and A.Montorsi, Low energy quantum regimes of 1D dipolar Hubbard model with correlated hopping, *J.Phys.: Conf.Ser.*841:012016, 2017.

[11] L.Fidkowski and A.Kitaev, Effects of Interactions on the topological classification of free fermion systems, *Phys.Rev.B*81:134509, 2010.

[12] E.Fradkin, *Field Theories of Condensed Matter Systems*, Addison-Wesley, 1 edition, 1991.

[13] A.O.Gogolin, A.A.Nerseyan, A.M.Tsvelik, *Bosonization and Strongly Correlated Systems*, Cambridge University Press, 2 edition, 1998.

[14] F.D.M.Haldane, *Continuum dynamics of the 1D Heisenberg antiferromagnet: Identification with the O(3) nonlinear sigma model Phys.Lett.A*93:464, 1983.

[15] F.D.M.Haldane, *Nonlinear Field Theory of Large-Spin Heisenberg Antiferromagnets: Semiclassically Quantized Solitons of the One-Dimensional Easy-Axis Néel State Phys.Rev.Lett.*50(15):1153, 1983.

[16] T.Kennedy and H.Tasaki, Hidden $z_2 \times z_2$ symmetry breaking in Haldane gap antiferromagnets, *Phys.Rev.B*45(1):304, 1992.

[17] J.M.Kosterlitz and D.J.Thouless, Ordering, metastability and phase transitions in two-dimensional systems, *J.Phys.C:Solid State Physics*6:1181, 1973.

[18] M.A.Martin-Delgrado, R.Shankar, G.Sierra, Phase Transitions in Staggered Spin Ladders, *Phys.Rev.Lett.*77:3443, 1996.

[19] N.D.Mermin and H.Wagner, Absence of ferromagnetism or antiferromagnetism in one-or two-dimensional isotropic heisenberg models, *Phys.Rev.Lett.*17(22):1133, 1966.

[20] A.Montorsi, F.Dolcini, R.Iotti and F.Rossi, Symmetry protected topological phases of 1D interacting fermions with spin-charge separation, *Phys.Rev.B*95:245108, 2017.

[21] A.Montorsi and M.Roncaglia, Nonlocal Order Parameters for 1D Hubbard Model, *Phys.Rev.Lett.*109:236404, 2012.

[22] G.Morandi, F.Napoli, and E.Ercolessi, *Statistical Mechanics: An Intermediate Course*, World Scientific, 2 edition, 2001.

[23] G.Mussardo, *Statistical Field Theory. An Introduction to Exactly Solved Models in Statistical Physics*, Oxford University Press, 1 edition, 2010.

[24] M.A.Nielsen and I.L.Chuang, *Quantum Computation and Quantum Information*, Oxford University Press, 1 edition, 2000.

[25] R.Orús, A Pratical Introduction to Tensor Networks: Matrix Product States and Projected Entangled Pair States, *Ann.Phys.*349:117-158, 2014.

[26] F.Pollmann, E.Berg, A.M.Turner and M.Oshikawa, Entanglement spectrum of a topological phase in one dimension, *Phys.Rev.B*81:064439, 2010.

[27] D. Porras, F.Verstraete and J.I.Cirac, DMRG and periodic boundary condition: a quantum information persepective, *Phys.Rev.Lett.*93:227205, 2004.

[28] S.Rao and D.Sen, An Introduction To Bosonization And Some Of its Applications, in S.Rao, editor, *Field Theories in Condensed Matter Physics. Texts and Readings in Physical Sciences*, Hindustan Book Agency, 2001.

[29] S.Sachdev, *Quantum Phase Transition*, Cambridge University Press, 2 edition, 2011.

[30] D.Sénéchal, An introduction to bosonization, In D.Sénéchal, A.M.S. Tremblay, and C.Bourbonnais, editors, *Theoretical Methods for Strongly Correlated Electrons*, Springer, 2004.

[31] U. Schollwöck, The density-matrix renormalization group in the age of matrix product states, *Ann.Phys.*326:96, 2011.

[32] G. Sierra, On the Application of the Non Linear Sigma Model to Spin Chains and Spin Ladders, *cond-mat/9610057*, 1996.

[33] The Class of Physics of the Royal Swedish Academy of Sciences, Topological Phase Transitions And Topological Phases Of Matter, *Scientific Background on the Nobel Prize in Physics*, 2016.

[34] X.-G.Wen, Symmetry-protected topological phases in noninteracting fermion systems, *Phys.Rev.B*85:085103, 2012.

[35] S.R. White, Density-matrix algorithms for quantum renormalization groups, *Phys.Rev.B*48:10345, 1993.

[36] S.R. White, Density Matrix Formulation for Quantum Renormalization Groups, *Phys.Rev.*69:2863, 1992.

[37] S. Yamamoto, Ground-State Properties of Antiferromagnetic Heisenberg Chains with Bond Alternation, *J.Phys.Soc.Jpn.*63:4327, 1994.

Appendix A

We want to compute $\hat{\Omega}_a(i,\tau)\hat{\Omega}_a(i+1,\tau)$ using the map (3.6).

$$\hat{\Omega}_a(i,\tau)\hat{\Omega}_a(i+1,\tau) = \left((-1)^{a+i}\hat{\phi}(i,\tau)\left(1-\frac{|\mathbf{l}_a(i,\tau)|^2}{s^2}\right)^{\frac{1}{2}}+\frac{\mathbf{l}_a(i,\tau)}{s}\right)$$

$$\left((-1)^{a+i+1}\hat{\phi}(i+1,\tau)\left(1-\frac{|\mathbf{l}_a(i+1,\tau)|^2}{s^2}\right)^{\frac{1}{2}}+\frac{\mathbf{l}_a(i+1,\tau)}{s}\right)$$

Since $|\mathbf{l}_a(i)/s| \ll 1$ we can consider the following approximation:

$$\simeq \left((-1)^{a+i}\hat{\phi}(i,\tau)\left(1-\frac{1}{2}\frac{|\mathbf{l}_a(i,\tau)|^2}{s^2}\right)+\frac{\mathbf{l}_a(i,\tau)}{s}\right)$$

$$\left((-1)^{a+i+1}\hat{\phi}(i+1,\tau)\left(1-\frac{1}{2}\frac{|\mathbf{l}_a(i+1,\tau)|^2}{s^2}\right)+\frac{\mathbf{l}_a(i+1,\tau)}{s}\right)=$$

$$=\left(-1\hat{\phi}(i,\tau)\hat{\phi}(i+1,\tau)\right)\left(1-\frac{1}{2}\frac{|\mathbf{l}_a(i,\tau)|^2}{s^2}-\frac{1}{2}\frac{|\mathbf{l}_a(i+1,\tau)|^2}{s^2}+\frac{1}{4}\frac{|\mathbf{l}_a(i,\tau)|^2}{s^2}\frac{|\mathbf{l}_a(i+1,\tau)|^2}{s^2}\right)+$$

$$+((-1)^{a+i}\hat{\phi}(i,\tau))\left(1-\frac{1}{2}\frac{|\mathbf{l}_a(i,\tau)|^2}{s^2}\right)\frac{\mathbf{l}_a(i+1,\tau)}{s}+$$

$$+((-1)^{a+i+1}\hat{\phi}(i+1,\tau))\left(1-\frac{1}{2}\frac{|\mathbf{l}_a(i+1,\tau)|^2}{s^2}\right)\frac{\mathbf{l}_a(i,\tau)}{s}+$$

$$+\frac{\mathbf{l}_a(i,\tau)\mathbf{l}_a(i+1,\tau)}{s^2}.$$

We know that $|\mathbf{l}_a(i)/s| \ll 1$ therefore we can ignore some terms and our previous expression becomes:

$$\simeq \left(-1\hat{\phi}(i,\tau)\hat{\phi}(i+1,\tau)\right)\left(1-\frac{1}{2}\frac{|\mathbf{l}_a(i,\tau)|^2}{s^2}-\frac{1}{2}\frac{|\mathbf{l}_a(i+1,\tau)|^2}{s^2}\right)+$$

$$+((-1)^{a+i}\hat{\phi}(i,\tau))(1)\frac{\mathbf{l}_a(i+1,\tau)}{s}+((-1)^{a+i+1}\hat{\phi}(i+1,\tau))(1)\frac{\mathbf{l}_a(i,\tau)}{s}+\frac{\mathbf{l}_a(i,\tau)\mathbf{l}_a(i+1,\tau)}{s^2}.$$

In order to better understand we focus on terms separately.

- We begin by considering $\hat{\phi}(i,\tau)\hat{\phi}(i+1,\tau)$ which becomes:
  $\hat{\phi}(i,\tau)\hat{\phi}(i+1,\tau)\simeq\hat{\phi}(i,\tau)(\hat{\phi}(i,\tau)+\hat{\phi}'(i,\tau)+\frac{1}{2}\hat{\phi}''(i,\tau))=\hat{\phi}(i,\tau)\hat{\phi}(i,\tau)+$
  $+\hat{\phi}(i,\tau)\hat{\phi}'(i,\tau)+\hat{\phi}(i,\tau)\frac{1}{2}\hat{\phi}''(i,\tau)=\left(1+\frac{\hat{\phi}(i,\tau)\hat{\phi}''(i,\tau)}{2}\right)=\left(1-\frac{\hat{\phi}'^2(i,\tau)}{2}\right)$

- Secondly we consider $\left(1-\frac{1}{2}\frac{|\mathbf{l}_a(i,\tau)|^2}{s^2}-\frac{1}{2}\frac{|\mathbf{l}_a(i+1,\tau)|^2}{s^2}\right)$ which becomes:
  $\left(1-\frac{1}{2}\frac{|\mathbf{l}_a(i,\tau)|^2}{s^2}-\frac{1}{2}\frac{|\mathbf{l}_a(i+1,\tau)|^2}{s^2}\right)\simeq\left(1-\frac{|\mathbf{l}_a(i,\tau)|^2}{s^2}\right)$

- Therefore by combining the previous results we achieve:
  $\left(1-\frac{\hat{\phi}'^2(i,\tau)}{2}\right)\left(1-\frac{|\mathbf{l}_a(i,\tau)|^2}{s^2}\right)=+1-\frac{\hat{\phi}'^2(i,\tau)}{2}-\frac{|\mathbf{l}_a(i,\tau)|^2}{s^2}$
  because $\frac{\hat{\phi}'^2(i,\tau)}{2}\frac{|\mathbf{l}_a(i,\tau)|^2}{s^2}=0$ because it is equal to $-\frac{\hat{\phi}(i,\tau)\hat{\phi}''(i,\tau)}{2}\frac{|\mathbf{l}_a(i,\tau)|^2}{s^2}=0$ because $\hat{\phi}(i,\tau)\mathbf{l}_a(i,\tau)=0$

- We also compute the following contribution $(-1)^{a+i}\hat{\phi}(i,\tau)\frac{\mathbf{l}_a(i+1,\tau)}{s}+(-1)^{a+i+1}\hat{\phi}(i+1,\tau)\frac{\mathbf{l}_a(i,\tau)}{s}$:
  $(-1)^{a+i}\hat{\phi}(i,\tau)\frac{\mathbf{l}_a(i+1,\tau)}{s}+(-1)^{a+i+1}\hat{\phi}(i+1,\tau)\frac{\mathbf{l}_a(i,\tau)}{s}=$
  $=(-1)^{a+i}\left(\hat{\phi}(i,\tau)\frac{\mathbf{l}_a(i+1,\tau)}{s}-\hat{\phi}(i+1,\tau)\frac{\mathbf{l}_a(i,\tau)}{s}\right)\simeq$
  $\simeq(-1)^{a+i}\left(\hat{\phi}(i,\tau)\left[\frac{\mathbf{l}_a(i,\tau)}{s}+\frac{\mathbf{l}'_a(i,\tau)}{s}\right]-\left[\hat{\phi}(i,\tau)+\hat{\phi}'(i,\tau)\right]\frac{\mathbf{l}_a(i,\tau)}{s}\right)=$
  $=(-1)^{a+i}\left(\hat{\phi}(i,\tau)\frac{\mathbf{l}'_a(i,\tau)}{s}-\hat{\phi}'(i,\tau)\frac{\mathbf{l}_a(i,\tau)}{s}\right)=(-1)^{a+i}\left(-2\frac{\hat{\phi}'(i,\tau)\mathbf{l}_a(i,\tau)}{s}\right)$

- The last term to be computed is $\frac{\mathbf{l}_a(i,\tau)\mathbf{l}_a(i+1,\tau)}{s^2}$:
  $\frac{\mathbf{l}_a(i,\tau)\mathbf{l}_a(i+1,\tau)}{s^2}\simeq\frac{(\mathbf{l}_a(i,\tau))^2}{s^2}$ because $\mathbf{l}_a(i,\tau)$ varies slowly with respect to i.

Therefore our expression becomes:

$$\left(-1+\frac{\hat{\phi}'^2(i,\tau)}{2}+\frac{|\mathbf{l}_a(i,\tau)|^2}{s^2}\right)+\left((-1)^{a+i}\left(-2\frac{\hat{\phi}'(i,\tau)\mathbf{l}_a(i,\tau)}{s}\right)+\frac{(\mathbf{l}_a(i,\tau))^2}{s^2}\right)=$$

$$=\left(-1+\frac{\hat{\phi}'^2(i,\tau)}{2}+2\frac{(\mathbf{l}_a(i,\tau))^2}{s^2}+(-1)^{a+i}\left(-2\frac{\hat{\phi}'(i,\tau)\mathbf{l}_a(i,\tau)}{s}\right)\right).$$

Now we focus on $\hat{\Omega}_a(i,\tau)\hat{\Omega}_{a+1}(i,\tau)$ and we calculate it using map (3.6).

$$\hat{\Omega}_a(i,\tau)\hat{\Omega}_{a+1}(i,\tau) = \left((-1)^{a+i}\hat{\phi}(i,\tau)\left(1-\frac{|\mathbf{l}_a(i,\tau)|^2}{s^2}\right)^{\frac{1}{2}}+\frac{\mathbf{l}_a(i,\tau)}{s}\right)$$

$$\left((-1)^{a+i+1}\hat{\phi}(i,\tau)\left(1-\frac{|\mathbf{l}_{a+1}(i,\tau)|^2}{s^2}\right)^{\frac{1}{2}}+\frac{\mathbf{l}_{a+1}(i,\tau)}{s}\right)$$

Since $|\mathbf{l}_a(i)/s| \ll 1$ we can consider the following approximation:

$$\simeq \left((-1)^{a+i}\hat{\phi}(i,\tau)\left(1-\frac{1}{2}\frac{|\mathbf{l}_a(i,\tau)|^2}{s^2}\right)+\frac{\mathbf{l}_a(i,\tau)}{s}\right)$$

$$\left((-1)^{a+i+1}\hat{\phi}(i,\tau)\left(1-\frac{1}{2}\frac{|\mathbf{l}_{a+1}(i,\tau)|^2}{s^2}\right)+\frac{\mathbf{l}_{a+1}(i,\tau)}{s}\right)=$$

$$=(-1)^{a+i}\hat{\phi}(i,\tau)(-1)^{a+i+1}\hat{\phi}(i,\tau)+$$

$$+(-1)^{a+i}\hat{\phi}(i,\tau)\left(-\frac{1}{2}\frac{|\mathbf{l}_a(i,\tau)|^2}{s^2}\right)(-1)^{a+i+1}\hat{\phi}(i,\tau)+$$

$$+(-1)^{a+i}\hat{\phi}(i,\tau)(-1)^{a+i+1}\hat{\phi}(i,\tau)\left(-\frac{1}{2}\frac{|\mathbf{l}_{a+1}(i,\tau)|^2}{s^2}\right)+$$

$$+(-1)^{a+i}\hat{\phi}(i,\tau)\left(-\frac{1}{2}\frac{|\mathbf{l}_a(i,\tau)|^2}{s^2}\right)(-1)^{a+i+1}\hat{\phi}(i,\tau)\left(-\frac{1}{2}\frac{|\mathbf{l}_{a+1}(i,\tau)|^2}{s^2}\right)+$$

$$+(-1)^{a+i}\hat{\phi}(i,\tau)\left(1-\frac{1}{2}\frac{|\mathbf{l}_a(i,\tau)|^2}{s^2}\right)\frac{\mathbf{l}_{a+1}(i,\tau)}{s}+$$

$$+(-1)^{a+i+1}\hat{\phi}(i,\tau)\left(1-\frac{1}{2}\frac{|\mathbf{l}_{a+1}(i,\tau)|^2}{s^2}\right)\frac{\mathbf{l}_a(i,\tau)}{s}+$$

$$+\frac{\mathbf{l}_a(i,\tau)}{s}\frac{\mathbf{l}_{a+1}(i,\tau)}{s}.$$

Since $|\mathbf{l}_a(i)/s| \ll 1$ we can ignore some terms then we have:

$$\simeq (-1)^{a+i}\hat{\phi}(i,\tau)(-1)^{a+i+1}\hat{\phi}(i,\tau)+$$

$$+(-1)^{a+i}\hat{\phi}(i,\tau)\left(-\frac{1}{2}\frac{|\mathbf{l}_a(i,\tau)|^2}{s^2}\right)(-1)^{a+i+1}\hat{\phi}(i,\tau)+$$

$$+(-1)^{a+i}\hat{\phi}(i,\tau)(-1)^{a+i+1}\hat{\phi}(i,\tau)\left(-\frac{1}{2}\frac{|\mathbf{l}_{a+1}(i,\tau)|^2}{s^2}\right)+$$

$$+(-1)^{a+i}\hat{\phi}(i,\tau)(1)\frac{\mathbf{l}_{a+1}(i,\tau)}{s}+$$
$$+(-1)^{a+i+1}\hat{\phi}(i,\tau)(1)\frac{\mathbf{l}_{a}(i,\tau)}{s}+$$
$$+\frac{\mathbf{l}_{a}(i,\tau)}{s}\frac{\mathbf{l}_{a+1}(i,\tau)}{s}.$$

- In this expression we have often $(-1)^{a+i}\hat{\phi}(i,\tau)(-1)^{a+i+1}\hat{\phi}(i,\tau)$ so firstly we are interested in its computation:
  $(-1)^{a+i}\hat{\phi}(i,\tau)(-1)^{a+i+1}\hat{\phi}(i,\tau) = (-1)^{2a+2i+1}\hat{\phi}^2(i,\tau) = -1\hat{\phi}^2(i,\tau) = -1.$
- We also note that $\hat{\phi}(i,\tau)\mathbf{l}_a(i,\tau) = 0$ and that $\hat{\phi}(i,\tau)\mathbf{l}_{a+1}(i,\tau) = 0$.

Therefore our expression becomes:

$$\left(-1+\frac{1}{2}\frac{|\mathbf{l}_a(i,\tau)|^2}{s^2}+\frac{1}{2}\frac{|\mathbf{l}_{a+1}(i,\tau)|^2}{s^2}+\frac{\mathbf{l}_{a}(i,\tau)}{s}\frac{\mathbf{l}_{a+1}(i,\tau)}{s}\right).$$

Appendix B

We show how to complete the following square:

$$-\frac{1}{2}\mathbf{l}_a L_{a,b}\mathbf{l}_b + \mathbf{b}_a\mathbf{l}_a$$

where:

- we have $\mathbf{b}_a = i\hat{\phi}\times\dot{\hat{\phi}} + 2s\gamma(-1)^a J_{\parallel,a}\hat{\phi}'$ for Hamiltonian (3.1), i. e. case A;
- we have $\mathbf{b}_a = i\hat{\phi}\times\dot{\hat{\phi}} + 2s\gamma J_{\parallel,a}\hat{\phi}'$ for Hamiltonian (3.2), i.e. case B;

Our previous expression becomes:

$$-\frac{1}{2}\mathbf{l}_a L_{a,b}\mathbf{l}_b + \mathbf{b}_a\mathbf{l}_a =$$

$$= -\frac{1}{2}(\mathbf{l}_a + \mathbf{x}_a)L_{a,b}(\mathbf{l}_b + \mathbf{x}_b) + \frac{1}{2}\mathbf{x}_a L_{a,b}\mathbf{x}_b$$

This equality holds if and only if $\mathbf{x}_a = -L^{-1}_{a,b}\mathbf{b}_b$.
The first term $-\frac{1}{2}(\mathbf{l}_a + \mathbf{x}_a)L_{a,b}(\mathbf{l}_b + \mathbf{x}_b)$ concerns the Gaussian integral in the partition function, while the second term $\frac{1}{2}\mathbf{x}_a L_{a,b}\mathbf{x}_b$ remains. Therefore we compute it:

$$\frac{1}{2}\mathbf{x}_a L_{a,c}\mathbf{x}_c = \frac{1}{2}\left(-L^{-1}_{a,b}\mathbf{b}_b\right)L_{a,c}\left(-L^{-1}_{c,d}\mathbf{b}_d\right) =$$

$$= \mathbf{b}_d\frac{L^{-1}_{d,b}}{2}\mathbf{b}_d = \sum_{d,b}\mathbf{b}_d\frac{L^{-1}_{d,b}}{2}\mathbf{b}_d =$$

$$= \mathbf{b}_1\frac{L^{-1}_{1,1}}{2}\mathbf{b}_1 + \mathbf{b}_2\frac{L^{-1}_{2,2}}{2}\mathbf{b}_2 + \mathbf{b}_1\frac{L^{-1}_{1,2}}{2}\mathbf{b}_2 + \mathbf{b}_2\frac{L^{-1}_{2,1}}{2}\mathbf{b}_1$$

- We know that matrix $L_{a,b}$ is as follows:

$$L_{a,b} = \begin{pmatrix} 4J_{\parallel,1} + J'_{\perp,1,2} & J'_{\perp,1,2} \\ J'_{\perp,2,1} & 4J_{\parallel,2} + J'_{\perp,2,1} \end{pmatrix}$$

- Then we compute matrix $L_{a,b}^{-1}$ because it is necessary to calculate $\frac{1}{2}\mathbf{x}_a L_{a,b}\mathbf{x}_b$:

$$L_{a,b}^{-1} = \begin{pmatrix} \frac{4J_{\parallel,2}+J'_{\perp,2,1}}{16J_{\parallel,1}J_{\parallel,2}+4J_{\parallel,1}J'_{\perp,2,1}+4J_{\parallel,2}J'_{\perp,1,2}} & \frac{-J'_{\perp,1,2}}{16J_{\parallel,1}J_{\parallel,2}+4J_{\parallel,1}J'_{\perp,2,1}+4J_{\parallel,2}J'_{\perp,1,2}} \\ \frac{-J'_{\perp,2,1}}{16J_{\parallel,1}J_{\parallel,2}+4J_{\parallel,1}J'_{\perp,2,1}+4J_{\parallel,2}J'_{\perp,1,2}} & \frac{4J_{\parallel,1}+J'_{\perp,1,2}}{16J_{\parallel,1}J_{\parallel,2}+4J_{\parallel,1}J'_{\perp,2,1}+4J_{\parallel,2}J'_{\perp,1,2}} \end{pmatrix}$$

Case A:

The term which is not concerned by the Gaussian integral is:

$$\mathbf{b}_1\frac{L_{1,1}^{-1}}{2}\mathbf{b}_1 + \mathbf{b}_2\frac{L_{2,2}^{-1}}{2}\mathbf{b}_2 + \mathbf{b}_1\frac{L_{1,2}^{-1}}{2}\mathbf{b}_2 + \mathbf{b}_2\frac{L_{2,1}^{-1}}{2}\mathbf{b}_1$$

Then we replace $\mathbf{b}_a = i\hat{\phi}\times\dot{\hat{\phi}} + 2s\gamma(-1)^a J_{\parallel,a}\hat{\phi}'$ in the previous expression:

$$= \left(i\hat{\phi}\times\dot{\hat{\phi}} + 2s\gamma(-1)J_{\parallel,1}\hat{\phi}'\right)\frac{1}{2}\frac{4J_{\parallel,2}+J'_{\perp,2,1}}{16J_{\parallel,1}J_{\parallel,2}+4J_{\parallel,1}J'_{\perp,2,1}+4J_{\parallel,2}J'_{\perp,1,2}}\left(i\hat{\phi}\times\dot{\hat{\phi}} + 2s\gamma(-1)J_{\parallel,1}\hat{\phi}'\right) +$$

$$+\left(i\hat{\phi}\times\dot{\hat{\phi}} + 2s\gamma J_{\parallel,2}\hat{\phi}'\right)\frac{1}{2}\frac{4J_{\parallel,1}+J'_{\perp,1,2}}{16J_{\parallel,1}J_{\parallel,2}+4J_{\parallel,1}J'_{\perp,2,1}+4J_{\parallel,2}J'_{\perp,1,2}}\left(i\hat{\phi}\times\dot{\hat{\phi}} + 2s\gamma J_{\parallel,2}\hat{\phi}'\right) +$$

$$+\left(i\hat{\phi}\times\dot{\hat{\phi}} + 2s\gamma(-1)J_{\parallel,1}\hat{\phi}'\right)\frac{1}{2}\frac{-J'_{\perp,1,2}}{16J_{\parallel,1}J_{\parallel,2}+4J_{\parallel,1}J'_{\perp,2,1}+4J_{\parallel,2}J'_{\perp,1,2}}\left(i\hat{\phi}\times\dot{\hat{\phi}} + 2s\gamma J_{\parallel,2}\hat{\phi}'\right) +$$

$$+\left(i\hat{\phi}\times\dot{\hat{\phi}} + 2s\gamma J_{\parallel,2}\hat{\phi}'\right)\frac{1}{2}\frac{-J'_{\perp,2,1}}{16J_{\parallel,1}J_{\parallel,2}+4J_{\parallel,1}J'_{\perp,2,1}+4J_{\parallel,2}J'_{\perp,1,2}}\left(i\hat{\phi}\times\dot{\hat{\phi}} + 2s\gamma(-1)J_{\parallel,1}\hat{\phi}'\right) =$$

$$= -\sum_{d,b}\frac{L_{d,b}^{-1}}{2}\dot{\hat{\phi}}^2 + 4s^2\gamma^2\hat{\phi}'^2\sum_{d,b}(-1)^d J_{\parallel,d}\frac{L_{d,b}^{-1}}{2}(-1)^b J_{\parallel,b} +$$

$$+is\gamma\hat{\phi}'\left(\hat{\phi}\times\dot{\hat{\phi}}\right)\frac{-2J_{\parallel,1}\left(4J_{\parallel,2}+J'_{\perp,2,1}\right)+2J_{\parallel,2}\left(4J_{\parallel,1}+J'_{\perp,1,2}\right)+2J_{\parallel,1}J'_{\perp,2,1}-2J_{\parallel,2}J'_{\perp,1,2}}{16J_{\parallel,1}J_{\parallel,2}+4J_{\parallel,1}J'_{\perp,2,1}+4J_{\parallel,2}J'_{\perp,1,2}} =$$

$$= -\sum_{d,b}\frac{L_{d,b}^{-1}}{2}\dot{\hat{\phi}}^2 + 4s^2\gamma^2\hat{\phi}'^2\sum_{d,b}(-1)^d J_{\parallel,d}\frac{L_{d,b}^{-1}}{2}(-1)^b J_{\parallel,b} + 0$$

We remember that $\left(\hat{\phi}\times\dot{\hat{\phi}}\right)^2 = \dot{\hat{\phi}}^2$ and that $J'_{\perp,2,1} = J'_{\perp,1,2}$.

Case B:

Ihe term which is not concerned by the Gaussian integral is:

$$\mathbf{b}_1\frac{L^{-1}_{1,1}}{2}\mathbf{b}_1+\mathbf{b}_2\frac{L^{-1}_{2,2}}{2}\mathbf{b}_2+\mathbf{b}_1\frac{L^{-1}_{1,2}}{2}\mathbf{b}_2+\mathbf{b}_2\frac{L^{-1}_{2,1}}{2}\mathbf{b}_1$$

Then we replace $\mathbf{b}_a=i\hat{\phi}\times\dot{\hat{\phi}}+2s\gamma J_{\parallel,a}\hat{\phi}'$ in the previous expression:

$$\begin{aligned}
&=\left(i\hat{\phi}\times\dot{\hat{\phi}}+2s\gamma J_{\parallel,1}\hat{\phi}'\right)\frac{1}{2}\frac{4J_{\parallel,2}+J'_{\perp,2,1}}{16J_{\parallel,1}J_{\parallel,2}+4J_{\parallel,1}J'_{\perp,2,1}+4J_{\parallel,2}J'_{\perp,1,2}}\left(i\hat{\phi}\times\dot{\hat{\phi}}+2s\gamma J_{\parallel,1}\hat{\phi}'\right)+\\
&+\left(i\hat{\phi}\times\dot{\hat{\phi}}+2s\gamma J_{\parallel,2}\hat{\phi}'\right)\frac{1}{2}\frac{4J_{\parallel,1}+J'_{\perp,1,2}}{16J_{\parallel,1}J_{\parallel,2}+4J_{\parallel,1}J'_{\perp,2,1}+4J_{\parallel,2}J'_{\perp,1,2}}\left(i\hat{\phi}\times\dot{\hat{\phi}}+2s\gamma J_{\parallel,2}\hat{\phi}'\right)+\\
&+\left(i\hat{\phi}\times\dot{\hat{\phi}}+2s\gamma J_{\parallel,1}\hat{\phi}'\right)\frac{1}{2}\frac{-J'_{\perp,1,2}}{16J_{\parallel,1}J_{\parallel,2}+4J_{\parallel,1}J'_{\perp,2,1}+4J_{\parallel,2}J'_{\perp,1,2}}\left(i\hat{\phi}\times\dot{\hat{\phi}}+2s\gamma J_{\parallel,2}\hat{\phi}'\right)+\\
&+\left(i\hat{\phi}\times\dot{\hat{\phi}}+2s\gamma J_{\parallel,2}\hat{\phi}'\right)\frac{1}{2}\frac{-J'_{\perp,2,1}}{16J_{\parallel,1}J_{\parallel,2}+4J_{\parallel,1}J'_{\perp,2,1}+4J_{\parallel,2}J'_{\perp,1,2}}\left(i\hat{\phi}\times\dot{\hat{\phi}}+2s\gamma J_{\parallel,1}\hat{\phi}'\right)=
\end{aligned}$$

$$=-\sum_{d,b}\frac{L^{-1}_{d,b}}{2}\dot{\hat{\phi}}^2+4s^2\gamma^2\hat{\phi}'^2\sum_{d,b}J_{\parallel,d}\frac{L^{-1}_{d,b}}{2}J_{\parallel,b}+$$

$$+is\gamma\hat{\phi}'\left(\hat{\phi}\times\dot{\hat{\phi}}\right)\frac{+2J_{\parallel,1}\left(4J_{\parallel,2}+J'_{\perp,2,1}\right)+2J_{\parallel,2}\left(4J_{\parallel,1}+J'_{\perp,1,2}\right)-2J_{\parallel,1}J'_{\perp,2,1}-2J_{\parallel,2}J'_{\perp,1,2}}{16J_{\parallel,1}J_{\parallel,2}+4J_{\parallel,1}J'_{\perp,2,1}+4J_{\parallel,2}J'_{\perp,1,2}}$$

We remember that $\left(\hat{\phi}\times\dot{\hat{\phi}}\right)^2=\dot{\hat{\phi}}^2$ and that $J'_{\perp,2,1}=J'_{\perp,1,2}$.

If $J_{\parallel,1}=J_{\parallel,2}=J'_{\perp,2,1}=1$ than we obtain that:

$$is\gamma\hat{\phi}'\left(\hat{\phi}\times\dot{\hat{\phi}}\right)\frac{16}{24}=is\gamma\hat{\phi}'\left(\hat{\phi}\times\dot{\hat{\phi}}\right)\frac{2}{3}$$